Population pharmacokinetic modeling to understand antineoplastic treatment

Dissertation

zur

Erlangung des Doktorgrades (Dr. rer. nat.)

der

Mathematisch-Naturwissenschaftlichen Fakultät

der

Rheinischen Friedrich-Wilhelms-Universität Bonn

vorgelegt von

Usman Arshad

aus Okara, Pakistan

Bonn, 2020

Angefertigt mit Genehmigung der Mathematisch-Naturwissenschaftlichen Fakultät der Rheinischen Friedrich-Wilhelms-Universität Bonn

1. Gutachter: Prof. Dr. Uwe Fuhr

2. Gutachter: Prof. Dr. Ulrich Jaehde

Tag der Promotion: 15.06.2020

Erscheinungsjahr: 2020

“Always begin with the end in mind”

Dr. Stepehen R. Covey

Dedicated to my family

Contents

Chapter 1

Introduction

Introduction

Pharmacometrics

The interdisciplinary research area of pharmacometrics deals with the quantitative description and interpretation of pharmacology [1]. Pharmacometrics makes use of mathematical, statistical and computational approaches by utilizing existing knowledge on physiology, disease and pharmacology to develop mathematical and statistical models that can be used to assist rationale selection of dosing regimen, prediction of clinical outcome and identification of the covariates as sources of variability [2]. Pharmacometric models can be useful in clinical practice for the individualization of drug treatment [3] [4] [5]. Nonlinear mixed effects (NLME) models are commonly implemented to describe pharmacokinetic/pharmacodynamic (PK/PD) profiles. The term mixed effects refer to the characteristics of the typical individual representative of a population (fixed effects) as well as the associated inter-individual variability (IIV), inter-occasion variability (IOV) and residual unexplained variability (RUV) collectively termed random effects [6].

NLME models are valuable to describe PK/PD relationships in a given population (population analysis) with sparse information, because they simultaneously fit data collected from multiple subjects. Estimation of PK/PD parameters such as drug clearance (CL) using NLME models is achieved by maximizing the likelihood of observing the data given the parameters [7], an approach called maximum likelihood estimation (MLE) which makes use of gradient-based numerical approximations such as first-order conditional estimation (FOCE) and second-order Laplacian methods. PK/PD data comprises of drug concentration (often plasma concentrations) measurements and pharmacodynamic endpoints or biomarkers. The primary objective behind the development of PK/PD models is to characterize the mathematical relationship between dose, concentration and effect. Development of PK/PD models can be accomplished in a sequential or simultaneous manner [8]. The former involves analysis of PK data followed by the incorporation of PD data, while the latter approach fits PK and PD data simultaneously. Depending on the study objective, a PK/PD model having the ability to reliably predict observed data is generally required. Being robust, flexible and the most

frequently used software in the field of pharmacometrics, NONMEM is used for the development and evaluation of PK/PD models part of this thesis [9].

Pharmacometrics to assist cancer chemotherapy

An important component of antineoplastic treatment involves cytotoxic chemotherapy using compounds that cause destruction of cancerous cells. Depending on tumor stage, type of cancer and patient status, chemotherapy can be useful to cure underlying disease, prolong patient survival and alleviate associated symptoms. During situations necessitating surgery or radiotherapy, prior chemotherapy is often used to reduce tumor burden, whereas post-surgery use of chemotherapeutic agents is helpful for the prevention of invasion of cancerous cells to other regions of the body. Hematological malignancies are more likely to be cured with chemotherapy [10] compared to solid tumors, which are seldom cured with the unaided use of these compounds. Adjuvant therapy has been shown to reduce relapse and death in a number of malignant diseases [11] [12]. Development of drug resistance is a major issue associated with the use of cytotoxic agents.

Decision making in appropriate dosing strategies is an associated challenge with cytotoxic chemotherapy. Successful remission of the tumors generally require higher drug doses to be administered, which is often restricted by the tolerability [13]. Rational dose selection is of paramount importance for cytotoxic agents with narrow therapeutic range. Identification of covariates during PK/PD analyses allows individualization of dosing regimens in order to get a better therapeutic outcome. Covariate models are developed to describe the relationship between PK/PD parameters and covariates which contain information regarding parameter(s) [14] [15] [16] [17] [18]. CL of a drug for example may be dependent on patient genotype for a drug metabolizing enzyme (covariate) where rapid metabolizers may require a relatively higher dose. Similarly, volume of distribution may vary with the variation in body mass and individuals with higher weight for instance may need a higher dose. Identification of appropriate covariate-parameter relationships may be useful to avoid exposure misspecifications by facilitating dose adjustments in patient subgroups.

Covariate based dose individualizations in oncology

Precision medicine involves dose adjustments based on individual patient characteristics. Suboptimal doses for anticancer agents with narrow therapeutic range may lead to serious complications. There is always a concern to identify, quantify, and manage IIV in order to adjust dosing regimens in patient subpopulations. Demographic and physiological covariates such as BSA and renal function may have an underlying relationship with PK/PD parameters which is identified during population analysis. Optimized dosing can therefore be achieved by minimizing the inter-patient variability in drug exposure/response with the consideration of significant covariate(s). A prominent example includes personalized dose adjustments based on patient's renal function for carboplatin [19]. Similarly, an improved treatment response with lower toxictity for 5-fluorouracil (5FU) treatment was observed when dose was linearly scaled according to individual's BSA [20]. Individualization based on patient genotype was also found valuable to minimize the risk of toxicity in case of irinotecan therapy [21]. A literature search [22] on personalized dosing based on covariate significance for anticancer drugs summarized that demographic covariates (especially body weight) are most commonly found to have a significant relationship with PK parameters, while parameters representative of renal function such as creatinine CL (CrCL), serum creatinine (SCr) and GFR are the other more prevalent covariates.

Mixture models: an alternative to covariate models

The population under study may possess heterogeneity in drug's PK and/or PD, which implies the presence of patient subgroups that respond to a particular drug in different manner. Differences can be observed in absorption or elimination of the compound, as well as the therapeutic outcome. Such differences can be best explained by inclusion of scientifically plausible covariate information. Situations may exist, where the relevant information on identity or individual value of a possible covariate is not available. A class of NLME models called mixture models is of particular value under such circumstances, as they are able to empirically describe the multimodal distributions of IIV [23]. Mixture modeling is a frequently used approach used for the partitioning of subjects to respective subpopulations [24] [25] [26].

Models describing biomarker turnover

Pharmacological effects are usually delayed relative to plasma drug concentrations. The observed delay may be due to multiple reasons such as delay in drug's distribution to its site of action, or turnover of physiological mediator(s) of drug effect such as enzymes [27]. It is generally not feasible to measure drug concentrations at the site of action, however the time course of drug effect can be empirically described by incorporation of hypothetical effect compartments [27]. Indirect response models are frequently used to describe the turnover of enzymes or biomarkers in the body, assuming that rate of formation of a biomarker follows zero-order kinetics, while rate of degradation follows a first-order process [28]. Drug response is frequently modeled based on the assumption that the drug inhibits/stimulates the rate of synthesis/degradation of a certain biomarker [28]. Drug effects are commonly incorporated as linear or sigmoidal functions driven by a measure of drug exposure such as concentrations in plasma or effect compartment.

Models describing myelosuppression during chemotherapy

Bone marrow suppression in response to cytotoxic chemotherapy makes patient more prone to develop infections due to leukopenia. Being the first line of defense, serious clinical implications are often associated with the decrease in neutrophils which comprise 60-70% of the total leukocyte count. Not only the extent, but also the duration of leukopenia is a potential challenge to administer desired dosing regimens. Most of the chemotherapeutic regimens are administered in cycles ranging from 21-28 days according to the time required for the reestablishment of a leukocyte count in the reference range. A semi-physiological model was developed by Friberg et al. to describe the suppression and reestablishment of leukocyte counts in rats administered with 5FU [29]. The model has been frequently employed to describe this undesired pharmacodynamic effect of chemotherapeutics since then. Being semi-mechanistic in nature, the model comprised of parameters related to drug and physiology, and considered the self-renewal of proliferating leukocytes, cellular maturation and a positive feedback describing the recovery period. The Friberg model provided clinically significant information by prediction of the time period required for leukocytes recovery in order to administer the subsequent dose, as an aggravation of toxicity may lead to life

threatening infections. The model was useful for individualized dosing in clinical practice [30] [31] as well as in preclinical and clinical drug development [32] [33] [34]. The model has been successfully applied to a number of anticancer drugs administered as monotherapy [32] [35] [36] [37] [38] [39] [40] [41] or a combination-based regimens [34] [42] [43] [44].

Investigated drugs

Mitotane

Mitotane (o,p'DDD) is the only anticancer drug used in the treatment for the rare disease of adrenocortical carcinoma (ACC). The drug causes impairment of steroidogenesis by inhibiting sterol-O-acyl transferase 1 [45]. Mitotane is highly lipophilic and has an oral bioavailability of 35-40% [46] [47]. Plasma mitotane concentrations >14 mg/L are efficacious [48] [49] [50], whereas concentrations greater than 20 mg/L are related to adverse effects, including CNS toxicity [51]. The drug is metabolized to o,p′-dichlorodiphenyl-ethene (o,p'-DDE) and –acetate (o,p'-DDA) [52] [53]. Mitotane is known to induce hepatic cytochrome P450 subfamily 3A4 (CYP3A4), leading to interactions with concomitant drugs [54]. The compound is primarily excreted in urine and bile, and has a long and variable elimination half-life of 18-159 days [55]. Early attainment of target concentrations avoiding a time delay is an associated challenge, whereas maintenance of plasma concentrations within the therapeutic range causes inconvenience as well. Maintenance doses of mitotane are currently being adjusted based on therapeutic drug monitoring (TDM). A pronounced delay in the attainment of target concentrations adds to the challenge. Model-based approaches to predict the desired exposure can therefore be useful.

5-Fluorouracil

Belonging to the class of fluoropyrimidines, 5FU is one of the frequently used chemotherapeutic agents for the treatment of solid malignancies including colorectal, breast, head and neck cancers [56]. 5FU is commonly used in combination with folinic acid, oxaliplatin and irinotecan for the treatment of colorectal and pancreatic cancer [57] [58] [59] [60]. Combination of 5FU and leucovorin (folinic acid) has been reported to cause lower toxicity, increased response rate and longer progression-free survival in

advanced colorectal cancer [61], whereas combined treatment with cisplatin is commonly recommended for oesophageal cancer [62]. 5FU undergoes enzymatic conversion, where the major fraction of the drug (80-90%) is converted to inactive metabolite 5-fluoro-5,6-dihydrouracil (5FUH2) by the hepatic enzyme dihydropyrimidine dehydrogenase (DPD), and only a small fraction is converted into cytotoxic nucleotides [63]. 5FU causes impairment of DNA synthesis by inhibiting thymidylate synthase (TS) [64]. Myelosuppression and mucositis are the dose limiting toxicities associated with 5FU based chemotherapeutic regimens [65]. Other associated toxicities include diarrhea, nausea, vomiting and encephalopathy [66]. Patients with deficiency of the metabolizing enzyme DPD are at higher risk of toxicity which may prove fatal [67]. PK profile of the drug is known to be variable and is influenced by dose, route and schedule of administration [68] [69] [70]. CL of the drug was related to patient's BSA [69] [71], gender [72] and age [71] [73]. Nonlinearity in its PK was observed due to saturable hepatic degradation [74]. Kidney and liver function [69] [72] were reported to influence the elimination of 5FU. The drug has a narrow therapeutic index and TDM is needed for the achievement of optimal exposure [75].

Methotrexate

Methotrexate belongs to the class of antifolates as it is known to inhibit both purine and pyrimidine biosynthesis [76] [63]. The drug has extensively been used in clinical practice for the treatment of solid and hematological malignancies, and autoimmune diseases like arthritis and psoriasis [77]. Clinically administered methotrexate dosing regimens are classified as low (<50 mg/m^2), intermediate (50-500 mg/m^2) and high (>500 mg/m^2) dose regimens [77] [78]. Considerable IIV in its pharmacokinetics and toxicity [79] [80] [81] poses challenges towards dose individualizations, and makes TDM essential for the identification of patients at higher risk of severe toxicities such as anemia, myelosuppression and acute renal failure. Numerous attempts have been made to study its pharmacokinetics using population analysis approach, where disagreements exist regarding the underlying covariate relationships. The drug has a wide variation in dosage regimens, where individual dose is calculated based on patient's body surface area (BSA), albeit the fraction of variability explained by BSA is of limited clinical relevance.

References

[1] E. I. Ette and P. J. Williams, *Pharmacometrics : the science of quantitative pharmacology*. John Wiley & Sons, 2007.

[2] E. Manolis, S. Rohou, R. Hemmings, T. Salmonson, M. Karlsson, and P. A. Milligan, "The role of modeling and simulation in development and registration of medicinal products: Output from the efpia/ema modeling and simulation workshop," *CPT Pharmacometrics Syst. Pharmacol.*, vol. 2, no. 2, Feb. 2013.

[3] K. Venkatakrishnan *et al.*, "Optimizing oncology therapeutics through quantitative translational and clinical pharmacology: challenges and opportunities.," *Clin. Pharmacol. Ther.*, vol. 97, no. 1, pp. 37–54, Jan. 2015.

[4] B. C. Bender, E. Schindler, and L. E. Friberg, "Population pharmacokinetic-pharmacodynamic modelling in oncology: a tool for predicting clinical response.," *Br. J. Clin. Pharmacol.*, vol. 79, no. 1, pp. 56–71, Jan. 2015.

[5] B. Ribba *et al.*, "A review of mixed-effects models of tumor growth and effects of anticancer drug treatment used in population analysis.," *CPT pharmacometrics Syst. Pharmacol.*, vol. 3, p. e113, 2014.

[6] D. R. Mould and R. N. Upton, "Basic concepts in population modeling, simulation, and model-based drug development," *CPT Pharmacometrics Syst. Pharmacol.*, vol. 1, no. 1, 2012.

[7] D. R. Mould and R. N. Upton, "Basic Concepts in Population Modeling, Simulation, and Model-Based Drug Development—Part 2: Introduction to Pharmacokinetic Modeling Methods," *CPT Pharmacometrics Syst. Pharmacol.*, vol. 2, no. 4, p. e38, 2013.

[8] L. Zhang, S. L. Beal, and L. B. Sheiner, "Simultaneous vs. Sequential Analysis for Population PK/PD Data I: Best-case Performance," *J. Pharmacokinet. Pharmacodyn.*, vol. 30, no. 6, pp. 387–404, Dec. 2003.

[9] R. J. Bauer, "NONMEM Tutorial Part I: Description of Commands and Options, With Simple Examples of Population Analysis," *CPT Pharmacometrics Syst. Pharmacol.*, Jun. 2019.

[10] K. Wheatley *et al.*, "A simple, robust, validated and highly predictive index for the determination of risk-directed therapy in acute myeloid leukaemia derived from

the MRC AML 10 trial. United Kingdom Medical Research Council's Adult and Childhood Leukaemia Working Parties.," *Br. J. Haematol.*, vol. 107, no. 1, pp. 69–79, Oct. 1999.

[11] B. M. Wolpin, J. A. Meyerhardt, H. J. Mamon, and R. J. Mayer, "Adjuvant treatment of colorectal cancer.," *CA. Cancer J. Clin.*, vol. 57, no. 3, pp. 168–85, 2007.

[12] R. Danesi and A. Di Paolo, "Chemoembolization is effective as second-line therapy in patients with colorectal carcinoma metastatic to the liver.," *Clin. Colorectal Cancer*, vol. 2, no. 3, pp. 180–1, Nov. 2002.

[13] L. Biganzoli and M. J. Piccart, "The bigger the better? ... or what we know and what we still need to learn about anthracycline dose per course, dose density and cumulative dose in the treatment of breast cancer.," *Ann. Oncol. Off. J. Eur. Soc. Med. Oncol.*, vol. 8, no. 12, pp. 1177–82, Dec. 1997.

[14] L. B. Sheiner, "Learning versus confirming in clinical drug development," *Clin. Pharmacol. Ther.*, vol. 61, no. 3, pp. 275–291, 1997.

[15] L. B. Sheiner and J.-L. Steimer, "Pharmacokinetic/Pharmacodynamic Modeling in Drug Development," *Annu. Rev. Pharmacol. Toxicol.*, vol. 40, no. 1, pp. 67–95, Apr. 2000.

[16] E. N. Jonsson and M. O. Karlsson, "Automated covariate model building within NONMEM," *Pharm. Res.*, vol. 15, no. 9, pp. 1463–1468, 1998.

[17] I. Matthews, C. Kirkpatrick, and N. Holford, "Quantitative justification for target concentration intervention - Parameter variability and predictive performance using population pharmacokinetic models for aminoglycosides," *Br. J. Clin. Pharmacol.*, vol. 58, no. 1, pp. 8–19, Jul. 2004.

[18] P. L. Bonate, *Pharmacokinetic-pharmacodynamic modeling and simulation*. Springer, 2011.

[19] A. H. Calvert *et al.*, "Carboplatin dosage: prospective evaluation of a simple formula based on renal function," *J. Clin. Oncol.*, vol. 7, no. 11, pp. 1748–1756, 1989.

[20] O. Capitain, A. Asevoaia, M. Boisdron-Celle, A. L. Poirier, A. Morel, and E. Gamelin, "Individual fluorouracil dose adjustment in FOLFOX based on pharmacokinetic follow-up compared with conventional body-area-surface dosing: A phase II,

proof-of-concept study," *Clin. Colorectal Cancer*, vol. 11, no. 4, pp. 263–267, Dec. 2012.

[21] D. M. Kweekel, H. Gelderblom, T. Van Der Straaten, N. F. Antonini, C. J. A. Punt, and H. J. Guchelaar, "UGT1A1*28 genotype and irinotecan dosage in patients with metastatic colorectal cancer: A Dutch Colorectal Cancer Group study," *Br. J. Cancer*, vol. 99, no. 2, pp. 275–282, Jul. 2008.

[22] A. S. Darwich, K. Ogungbenro, O. J. Hatley, and A. Rostami-Hodjegan, "Role of pharmacokinetic modeling and simulation in precision dosing of anticancer drugs," *Transl. Cancer Res.*, vol. 6, no. S10, pp. S1512–S1529, 2017.

[23] K. C. Carlsson, R. M. Savi, A. C. Hooker, and M. O. Karlsson, "Modeling subpopulations with the $MIXTURE subroutine in NONMEM: Finding the individual probability of belonging to a subpopulation for the use in model analysis and improved decision making," *AAPS J.*, vol. 11, no. 1, pp. 148–154, 2009.

[24] M. E. Spilker *et al.*, "Mixture model approach to tumor classification based on pharmacokinetic measures of tumor permeability," *J. Magn. Reson. Imaging*, vol. 22, no. 4, pp. 549–558, Oct. 2005.

[25] K. G. Kowalski, L. McFadyen, M. M. Hutmacher, B. Frame, and R. Miller, "A Two-Part Mixture Model for Longitudinal Adverse Event Severity Data," *J. Pharmacokinet. Pharmacodyn.*, vol. 30, no. 5, pp. 315–336, Oct. 2003.

[26] T. Tanigawa, R. Heinig, Y. Kuroki, and S. Higuchi, "Evaluation of interethnic differences in repinotan pharmacokinetics by using population approach.," *Drug Metab. Pharmacokinet.*, vol. 21, no. 1, pp. 61–69, 2006.

[27] N. Holford, "Clinical pharmacology = disease progression + drug action," *Br. J. Clin. Pharmacol.*, vol. 79, no. 1, pp. 18–27, 2015.

[28] N. L. Dayneka, V. Garg, and W. J. Jusko, "Comparison of four basic models of indirect pharmacodynamic responses.," *Pharmacodyn.*, vol. 21, no. 4, pp. 457–78, Aug. 1993.

[29] L. E. Friberg, A. Freijs, M. Sandstrom, and M. O. Karlsson, "Semiphysiological model for the time course of leukocytes after varying schedules of 5-fluorouracil in rats," *J. Pharmacol. Exp. Ther.*, vol. 295, no. 2, pp. 734–740, 2000.

[30] J. E. Wallin, L. E. Friberg, and M. O. Karlsson, "Model-Based Neutrophil-Guided

Dose Adaptation in Chemotherapy: Evaluation of Predicted Outcome with Different Types and Amounts of Information," *Basic Clin. Pharmacol. Toxicol.*, vol. 106, no. 3, pp. 234–242, 2010.

[31] J. E. Wallin, L. E. Friberg, and M. O. Karlsson, "A tool for neutrophil guided dose adaptation in chemotherapy," 2008.

[32] I. F. Trocòniz *et al.*, "Phase I dose-finding study and a pharmacokinetic/pharmacodynamic analysis of the neutropenic response of intravenous diflomotecan in patients with advanced malignant tumours.," *Cancer Chemother. Pharmacol.*, vol. 57, no. 6, pp. 727–35, Jun. 2006.

[33] A. S. Zandvliet, M. O. Karlsson, J. H. M. Schellens, W. Copalu, J. H. Beijnen, and A. D. R. Huitema, "Two-stage model-based clinical trial design to optimize phase I development of novel anticancer agents," *Invest. New Drugs*, vol. 28, no. 1, pp. 61–75, Jan. 2010.

[34] M. Sandström, H. Lindman, P. Nygren, E. Lidbrink, J. Bergh, and M. O. Karlsson, "Model describing the relationship between pharmacokinetics and hematologic toxicity of the epirubicin-docetaxel regimen in breast cancer patients.," *J. Clin. Oncol.*, vol. 23, no. 3, pp. 413–21, Jan. 2005.

[35] E. Soto *et al.*, "Semi-mechanistic population pharmacokinetic/pharmacodynamic model for neutropenia following therapy with the Plk-1 inhibitor BI 2536 and its application in clinical development.," *Cancer Chemother. Pharmacol.*, vol. 66, no. 4, pp. 785–95, Sep. 2010.

[36] F. Léger *et al.*, "Mechanism-based models for topotecan-induced neutropenia.," *Clin. Pharmacol. Ther.*, vol. 76, no. 6, pp. 567–78, Dec. 2004.

[37] C. van Kesteren *et al.*, "Semi-physiological model describing the hematological toxicity of the anti-cancer agent indisulam.," *Invest. New Drugs*, vol. 23, no. 3, pp. 225–34, Jun. 2005.

[38] J. E. Latz, M. O. Karlsson, J. J. Rusthoven, A. Ghosh, and R. D. Johnson, "A semimechanistic-physiologic population pharmacokinetic/pharmacodynamic model for neutropenia following pemetrexed therapy.," *Cancer Chemother. Pharmacol.*, vol. 57, no. 4, pp. 412–26, Apr. 2006.

[39] J. Hing, J. J. Perez-Ruixo, K. Stuyckens, A. Soto-Matos, L. Lopez-Lazaro, and P.

Zannikos, “Mechanism-based pharmacokinetic/pharmacodynamic meta-analysis of trabectedin (ET-743, Yondelis) induced neutropenia.,” *Clin. Pharmacol. Ther.*, vol. 83, no. 1, pp. 130–43, Jan. 2008.

[40] S. J. Kathman, D. H. Williams, J. P. Hodge, and M. Dar, “A Bayesian population PK-PD model of ispinesib-induced myelosuppression.,” *Clin. Pharmacol. Ther.*, vol. 81, no. 1, pp. 88–94, Jan. 2007.

[41] C. M. Ng, A. Patnaik, M. Beeram, C. C. Lin, and C. H. Takimoto, “Mechanism-based pharmacokinetic/pharmacodynamic model for troxacitabine-induced neutropenia in cancer patients.,” *Cancer Chemother. Pharmacol.*, vol. 67, no. 5, pp. 985–94, May 2011.

[42] A. S. Zandvliet, J. H. M. Schellens, C. Dittrich, J. Wanders, J. H. Beijnen, and A. D. R. Huitema, “Population pharmacokinetic and pharmacodynamic analysis to support treatment optimization of combination chemotherapy with indisulam and carboplatin.,” *Br. J. Clin. Pharmacol.*, vol. 66, no. 4, pp. 485–497, 2008.

[43] S. J. Kathman, D. H. Williams, J. P. Hodge, and M. Dar, “A Bayesian population PK-PD model for ispinesib/docetaxel combination-induced myelosuppression,” *Cancer Chemother. Pharmacol.*, vol. 63, no. 3, pp. 469–476, Feb. 2009.

[44] M. Joerger *et al.*, “Population pharmacokinetics and pharmacodynamics of paclitaxel and carboplatin in ovarian cancer patients: a study by the European organization for research and treatment of cancer-pharmacology and molecular mechanisms group and new drug development group.,” *Clin. Cancer Res.*, vol. 13, no. 21, pp. 6410–8, Nov. 2007.

[45] S. Sbiera *et al.*, “Mitotane Inhibits Sterol-O-Acyl Transferase 1 Triggering Lipid-Mediated Endoplasmic Reticulum Stress and Apoptosis in Adrenocortical Carcinoma Cells,” *Endocrinology*, vol. 156, no. 11, pp. 3895–3908, Nov. 2015.

[46] R. H. MOY, “Studies of the pharmacology of o,p’DDD in man.,” *J. Lab. Clin. Med.*, vol. 58, pp. 296–304, 1961.

[47] H. v. Slooten, A. P. van Seters, D. Smeenk, and A. J. Moolenaar, “O,p′-DDD (Mitotane) levels in plasma and tissues during chemotherapy and at autopsy,” *Cancer Chemother. Pharmacol.*, vol. 9, no. 2, pp. 85–88, Jan. 1982.

[48] F. Megerle *et al.*, “Mitotane Monotherapy in Patients With Advanced

Adrenocortical Carcinoma," *J. Clin. Endocrinol. Metab.*, vol. 103, no. 4, pp. 1686–1695, 2018.

[49] H. van Slooten, A. J. Moolenaar, A. P. van Seters, and D. Smeenk, "The treatment of adrenocortical carcinoma with o,p'-DDD: prognostic implications of serum level monitoring.," *Eur. J. Cancer Clin. Oncol.*, vol. 20, no. 1, pp. 47–53, Jan. 1984.

[50] H. Haak *et al.*, "Optimal treatment of adrenocortical carcinoma with mitotane: results in a consecutive series of 96 patients," *Br. J. Cancer*, vol. 69, no. 5, pp. 947–951, 1994.

[51] S. Mauclère-Denost *et al.*, "High-dose mitotane strategy in adrenocortical carcinoma: Prospective analysis of plasma mitotane measurement during the first 3 months of follow-up," *Eur. J. Endocrinol.*, vol. 166, no. 2, pp. 261–268, 2012.

[52] V. D. Reif, J. E. Sinsheimer, J. C. Ward, and D. E. Schteingart, "Aromatic hydroxylation and alkyl oxidation in metabolism of mitotane (o,p'-DDD) in humans.," *J. Pharm. Sci.*, vol. 63, no. 11, pp. 1730–6, 1974.

[53] J. E. Sinsheimer, J. Guilford, L. J. Bobrin, and D. E. Schteingart, "Identification of o,p'-Dichlorodiphenyl Acetic Acid as a Urinary Metabolite of 1-(o-Chlorophenyl)-1-(p-chlorophenyl)-2,2-dichloroethane," *J. Pharm. Sci.*, vol. 61, no. 2, pp. 314–316, 1972.

[54] N. P. van Erp, H.-J. Guchelaar, B. A. Ploeger, J. A. Romijn, J. d. Hartigh, and H. Gelderblom, "Mitotane has a strong and a durable inducing effect on CYP3A4 activity," *Eur. J. Endocrinol.*, vol. 164, no. 4, pp. 621–626, Apr. 2011.

[55] A. J. Moolenaar, H. van Slooten, A. P. van Seters, and D. Smeenk, "Blood levels of o,p'-DDD following administration in various vehicles after a single dose and during long-term treatment.," *Cancer Chemother. Pharmacol.*, vol. 7, no. 1, pp. 51–4, 1981.

[56] S. Christensen *et al.*, "5-Fluorouracil treatment induces characteristic T>G mutations in human cancer," *Nat. Commun.*, vol. 10, no. 1, Dec. 2019.

[57] L. Deyme, D. Barbolosi, and F. Gattacceca, "Population pharmacokinetics of FOLFIRINOX: a review of studies and parameters," *Cancer Chemother. Pharmacol.*, vol. 83, no. 1, pp. 27–42, 2018.

[58] A. de Gramont *et al.*, "Leucovorin and fluorouracil with or without oxaliplatin as

first-line treatment in advanced colorectal cancer," *J. Clin. Oncol.*, vol. 18, no. 16, pp. 2938–2947, 2000.

[59] V. Boige *et al.*, "Pharmacogenetic assessment of toxicity and outcome in patients with metastatic colorectal cancer treated with LV5FU2, FOLFOX, and FOLFIRI: FFCD 2000-05," *J. Clin. Oncol.*, vol. 28, no. 15, pp. 2556–2564, May 2010.

[60] D. A. Cameron, H. Gabra, and R. C. F. Leonard, "Continuous 5-fluorouracil in the treatment of breast cancer," *Br. J. Cancer*, vol. 70, no. 1, pp. 120–124, 1994.

[61] C. L. Hanna *et al.*, "High-dose folinic acid and 5-fluorouracil bolus and continuous infusion in advanced colorectal cancer: Poor response rate in unselected patients," *Br. J. Cancer*, vol. 72, no. 3, pp. 774–776, 1995.

[62] J. Tepper *et al.*, "Phase III Trial of Trimodality Therapy With Cisplatin, Fluorouracil, Radiotherapy, and Surgery Compared With Surgery Alone for Esophageal Cancer: CALGB 9781," *J. Clin. Oncol.*, vol. 26, no. 7, pp. 1086–1092, 2008.

[63] N. Hagner and M. Joerger, "Cancer Management and Research Dovepress Cancer chemotherapy: targeting folic acid synthesis," *Cancer Manag. Res.*, pp. 2–293, 2010.

[64] C. H. Köhne and G. J. Peters, "UFT: Mechanism of drug action," *Oncology*, vol. 14, no. 10 SUPPL. 9, pp. 13–18, 2000.

[65] M. Boisdron-Celle *et al.*, "Prevention of 5-fluorouracil-induced early severe toxicity by pre-therapeutic dihydropyrimidine dehydrogenase deficiency screening: Assessment of a multiparametric approach," *Semin. Oncol.*, vol. 44, no. 1, pp. 13–23, Feb. 2017.

[66] C. H. Takimoto *et al.*, "Severe neurotoxicity following 5-fluorouracil-based chemotherapy in a patient with dihydropyrimidine dehydrogenase deficiency.," *Clin. Cancer Res.*, vol. 2, no. 3, p. 481, Mar. 1996.

[67] A. B. P. Van Kuilenburg *et al.*, "Lethal outcome of a patient with a complete dihydropyrimidine dehydrogenase (DPD) deficiency after administration of 5-fluorouracil: Frequency of the common IVS14+1G>A mutation causing DPD deficiency," *Clin. Cancer Res.*, vol. 7, no. 5, pp. 1149–1153, 2001.

[68] C. Kosmas *et al.*, "Cardiotoxicity of fluoropyrimidines in different schedules of

administration: a prospective study," *J. Cancer Res. Clin. Oncol.*, vol. 134, no. 1, pp. 75–82, Nov. 2007.

[69] C. Terret *et al.*, "Dose and time dependencies of 5-fluorouracil pharmacokinetics," *Clin. Pharmacol. Ther.*, vol. 68, no. 3, pp. 270–279, Sep. 2000.

[70] J. J. Lee, J. H. Beumer, and E. Chu, "Therapeutic drug monitoring of 5-fluorouracil," *Cancer Chemother. Pharmacol.*, vol. 78, no. 3, pp. 447–464, 2016.

[71] R. E. Port, B. Daniel, R. W. Ding, and R. Herrmann, "Relative importance of dose, body surface area, sex, and age for 5-fluorouracil clearance.," *Oncology*, vol. 48, no. 4, pp. 277–81, 1991.

[72] F. Mueller *et al.*, "Gender-specific elimination of continuous-infusional 5-fluorouracil in patients with gastrointestinal malignancies: results from a prospective population pharmacokinetic study," *Cancer Chemother. Pharmacol.*, vol. 71, no. 2, pp. 361–370, 2013.

[73] M.-C. Etienne *et al.*, "Co-variables influencing 5-fluorouracil clearance during continuous venous infusion. A NONMEM analysis," *Eur. J. Cancer*, vol. 34, no. 1, pp. 92–97, Jan. 1998.

[74] O. Bouché, P. Laurent-Puig, M. Boisdron-Celle, V. Guérin-Meyer, and O. Capitain, "5-fluorouracile : MSI, pharmacocinétique, DPD, TYMS et MTHFR," *Médecine Personnal. en cancérologie Dig.*, pp. 75–92, 2013.

[75] M. Wilhelm *et al.*, "Prospective, Multicenter Study of 5-Fluorouracil Therapeutic Drug Monitoring in Metastatic Colorectal Cancer Treated in Routine Clinical Practice," *Clin. Colorectal Cancer*, vol. 15, no. 4, pp. 381–388, 2016.

[76] H. Nicole and Markus Joerger, "Cancer chemotherapy: targeting folic acid synthesis," 2010. [Online]. Available: https://www.ncbi.nlm.nih.gov/pmc/articles/PMC3033035/. [Accessed: 24-Dec-2019].

[77] S. L. Goss *et al.*, "Methotrexate Dose in Patients With Early Rheumatoid Arthritis Impacts Methotrexate Polyglutamate Pharmacokinetics, Adalimumab Pharmacokinetics, and Efficacy: Pharmacokinetic and Exposure-response Analysis of the CONCERTO Trial," *Clin. Ther.*, vol. 40, no. 2, pp. 309–319, 2018.

[78] K. H. Hui, H. M. Chu, P. S. Fong, W. T. F. Cheng, and T. N. Lam, "Population

Pharmacokinetic Study and Individual Dose Adjustments of High-Dose Methotrexate in Chinese Pediatric Patients With Acute Lymphoblastic Leukemia or Osteosarcoma," *J. Clin. Pharmacol.*, vol. 59, no. 4, pp. 566–577, 2019.

[79] K. Schmiegelow, "Advances in individual prediction of methotrexate toxicity: a review," *Br. J. Haematol.*, vol. 146, no. 5, pp. 489–503, 2009.

[80] W. E. Evans, M. V Relling, J. M. Boyett, and C. H. Pui, "Does pharmacokinetic variability influence the efficacy of high-dose methotrexate for the treatment of children with acute lymphoblastic leukemia: what can we learn from small studies?," *Leuk. Res.*, vol. 21, no. 5, pp. 435–7, 1997.

[81] L. R. Treviño *et al.*, "Germline Genetic Variation in an Organic Anion Transporter Polypeptide Associated With Methotrexate Pharmacokinetics and Clinical Effects," *J. Clin. Oncol.*, vol. 27, no. 35, pp. 5972–5978, 2009.

Chapter 2

Aims and objectives

Aims and objectives

Overall aims and objectives

The research work presented in this thesis was primarily aimed to develop, evaluate, and subsequently use PK/PD models with adequate predictive ability for an improved antineoplastic treatment outcome. Novel approaches for the evaluation of mixture models were aimed to be developed. It was desired to understand the PK/PD behavior of the drugs in a better way. We focused towards the refinement of dosing schedules in routine clinical practice by precise interpretation of plasma drug concentrations using model-based approaches. Plasma drug exposure was predicted by developing population pharmacokinetic models, whereas simultaneous modelling of pharmacokinetic and pharmacodynamic data was further intended for the prediction of desired/undesired clinical outcome. Project specific aims and objectives are described below.

Evaluation of mixture models

The first project (chapter 3) aimed to contribute towards the development of a novel methodology for better evaluation of mixture models. The focus was to adapt the standard model diagnostic procedure termed visual predictive check (VPC) for mixture models. This class of NLME models has frequently been implemented in pharmacometrics research, but little attention has been paid to develop appropriate diagnostic procedures for their evaluation. The approach was initially planned to be implemented and assessed by generating some simulated data. Subsequently, it was desired to evaluate the available models and pharmacokinetic data of antineoplastic agents.

Mitotane pharmacokinetics

The second project presented in chapter 4 of this thesis was intended to investigate the pharmacokinetics of mitotane by developing a population pharmacokinetic model with the data collected from a large cohort of adrenocortical carcinoma patients. Incorporation of enzyme autoinduction was aimed as the drug was previously reported to be a strong inducer of cytochrome P450 subfamily CYP3A4. Moreover, it was desired to identify the covariates of influence regarding mitotane pharmacokinetics. Evaluation

of clinically practiced dosing regimens for the attainment of therapeutic concentrations using model based simulations was further intended.

5FU pharmacokinetics and pharmacodynamics

The third project (chapter 5) was designed to understand and predict the progression of myelotoxicity driven by 5FU exposure in colorectal cancer patients. It was planned to simultaneously model the pharmacokinetic and pharmacodynamic (adverse event) data, thus filling the gap in existing knowledge regarding quantitative pharmacology of 5FU. The project was further aimed to be characterize the impact of covariates on 5FU pharmacology, mainly patient demographic and genetic profiles. Model based prediction of toxicity related to different clinically applied 5FU based regimens was meant to be part of the present analysis.

Methotrexate pharmacokinetics

The fourth project (chapter 6) addressed some clinical aspects related to methotrexate pharmacokinetics. Plasma concentration and covariate data was available from the TDM database maintained at University Hospital Cologne. It was desired to develop a pharmacokinetic model using the data collected from a large cohort of patients with solid and hematological malignancies. Identification of the covariate relationships mainly patient demographics and clinical laboratory values were part of the study. Subsequently, assessment of ongoing clinical practice of dosing methotrexate based on BSA compared to flat dosing was desired.

Chapter 3

Development of visual predictive checks accounting for multimodal parameter distributions in mixture models.

Usman Arshad[1,2], Estelle Chasseloup[1], Rikard Nordgren[1], Mats O. Karlsson[1]

Journal of Pharmacokinetics and Pharmacodynamics 2019. 46(3):241-250

1. Department of Pharmaceutical Biosciences, Uppsala University, Uppsala, Sweden.
2. Department I of Pharmacology, University Hospital Cologne, Germany.

Abstract

The assumption of interindividual variability being unimodally distributed in nonlinear mixed effects models does not hold when the population under study displays multimodal parameter distributions. Mixture models allow the identification of parameters characteristic to a subpopulation by describing these multimodalities. Visual predictive check (VPC) is a standard simulation based diagnostic tool, but not yet adapted to account for multimodal parameter distributions. Mixture model analysis provides the probability for an individual to belong to a subpopulation (IP_{mix}) and the most likely subpopulation for an individual to belong to (MIXEST). Using simulated data examples, two implementation strategies were followed to split the data into subpopulations for the development of mixture model specific VPCs. The first strategy splits the observed and simulated data according to the MIXEST assignment. A shortcoming of the MIXEST-based allocation strategy was a biased allocation towards the dominating subpopulation. This shortcoming was avoided by splitting observed and simulated data according to the IP_{mix} assignment. For illustration purpose, the approaches were also applied to an irinotecan mixture model demonstrating 36% lower clearance of irinotecan metabolite (SN-38) in individuals with UGT1A1 homo/heterozygote vs wild-type genotype. VPCs with segregated subpopulations were helpful in identifying model misspecifications which were not evident with standard VPCs. The new tool provides an enhanced power of evaluation of mixture models.

Keywords: Visual predictive checks, mixture models, multimodal parameter distributions, pharmacokinetics, pharmacodynamics.

Introduction

Evaluation of the applicability of a model for a specific purpose is a major consideration during pharmacometric analysis. Diagnostic tools have been developed and used extensively for evaluation of pharmacokinetic (PK) / pharmacodynamics (PD) models [1]. The simulation based diagnostic tool known as visual predictive check (VPC) has gathered much focus because of the (i) advantage to retain the original data profile, (ii) ability to describe the central trend and dispersion in the data, and (iii) simplicity for interpretations [2, 3, 4, 5]. A VPC is a graphical and statistical comparison of observed and predicted data by deriving the distribution of observations and predictions against the independent variable such as time [3]. Depending on the underlying data, the objective of the study and the intended use of the model, different VPCs such as stratified VPCs (predictive performance across stratification variable such as a covariate), prediction corrected VPCs (to identify random effect misspecification by removing the variability coming from independent variables such as doses) and covariate VPCs (to evaluate the predictive performance of the model across the covariate range) may be used [3, 4].

The nonlinear mixed effect modeling approach quantifies the intrinsic variability associated with pharmacokinetic / pharmacodynamic profiles across the studied population [6]. The underlying assumption of interindividual variability (IIV) being unimodally distributed is not true when the studied population exhibits heterogeneity leading to multimodal parameter distributions [7]. Heterogeneous pharmacological behavior may result in clinically significant differences in drug exposure/toxicity. A classic example involves acetylation polymorphism in case of isoniazid where clearance (CL) was observed to be bimodally distributed and a higher prevalence of peripheral neuropathy and hepatotoxicity was observed in slow metabolizers due to elevated plasma concentrations [8]. Situations may arise where a polymorphism is associated with the exposure/response to a drug, but the covariate capable of describing such behavior is not available. The mixture modeling (also referred as clustering) approach is a useful tool under such circumstances [9]. A number of studies have been reported to utilize mixture modeling. A major proportion of these studies aimed to describe the bimodal distribution of CL as reported in case of serotonin receptor antagonist repinotan, antianginal drug perhexiline and beta-lactam antibiotic ceftizoxime [10, 11,

12]. A bivariate absorption describing the subpopulations with and without absorption lag was presented by Piotrovsky *et al.* [13]. An analysis was performed to segregate the patients with and without adverse effects with the help of adverse event data by Kowalski *et al.* [14]. Mixture modeling was also applied to model the probability of cure in cancer survival analysis where the proportion of fatal and cured cases was estimated [15, 16, 17]. Similarly, a mixture model classifying the mammary tumors in rats as benign or malignant was published by Spilker *et al.* [18].

Despite the utility of mixture models to describe data arising from a population with underlying heterogeneity, there are limitations in assessing mixture models since the common simulation based assessment tools do not account for the multimodality in parameter distributions. Attempts have been made to develop posterior predictive checks [19] for mixture models [8]. However, VPCs are not yet adapted to mixture models and may fail to adequately evaluate the predictive performance of a mixture model. The aim of the current project was to design VPCs accounting for multimodal parameter distributions and thereby allow (i) the diagnosis of the mixture component aspects of the model, and (ii) more powerful assessment of other model aspects by reducing between-subpopulation variability from the graphs.

Methods

Theoretical overview of parameter estimation using mixture models

The underlying assumption behind the mixture modeling approach is to partition the population into subpopulations according to a probability model [8]. With the implementation of mixture models using the $MIXTURE subroutine in NONMEM, pharmacokinetic parameters characteristic to a subpopulation can be obtained [20].

$$CL_1 = \theta_1 \cdot e^{\eta_1} \qquad \dots clearance\ for\ subpopulation\ 1$$
$$CL_2 = \theta_2 \cdot e^{\eta_2} \qquad \dots clearance\ for\ subpopulation\ 2$$

Whereas, the corresponding subpopulation probabilities are estimated as,

$$P_{mix1} = \theta_3 \qquad \dots probability\ for\ subpopulation\ 1$$
$$P_{mix2} = 1 - \theta_3 \qquad \dots probability\ for\ subpopulation\ 2$$

A P_{mix1} estimate of 0.6 corresponds to a 60/40% mixture proportion. The individual likelihood to belong to a subpopulation 1 (IL_{mix1}) can be derived from the individual objective function value (IOFV). The individual probability for belonging to a subpopulation (IP_{mix}) is then computed from the individual likelihood (IL_{mix}) and population probability estimates [7].

$$IL_{mix1} = e^{(IOFV/2)}$$

$$IP_{mix1} = \frac{IL_{mix1} \cdot P_{mix1}}{IL_{mix1} \cdot P_{mix1} + IL_{mix2} \cdot P_{mix2}}$$

Where, IL_{mix2} is the corresponding likelihood estimate for the individual to belong to subpopulation 2. The empirical subpopulation assignment that the subject's data is described by the corresponding submodel is given the name MIXEST within NONMEM.

Mixture model output

Analysis with mixture models provided two individual-level metrics of subpopulation association (i) the most likely subpopulation for an individual to belong to, and (ii) the probability for an individual to belong to each subpopulation [7]. The former metric (MIXEST) is discrete in nature and can be retrieved from output table files. The latter metric termed IP_{mix} can be retrieved from the *.phm file which is a standard output of models with mixture components. IP_{mix} is considered to be more informative than the MIXEST variable because of its continuous nature.

Mixture specific VPCs

Two strategies were adapted for allocation of subjects to the subpopulations in order to develop mixture model specific VPCs with separate panels for each allocated subpopulation. The first strategy utilized the MIXEST information to stratify the observed and simulated data. Thus, the original and simulated individuals were separated according to their most likely subpopulation. A tendency for subjects to be allocated to the dominating subpopulation (similar to the shrinkage phenomenon in individual, empirical Bayes, parameter estimation) is expected with the MIXEST-based allocation strategy. This shortcoming was avoided through the second strategy to randomly partition the observed and simulated data according to the IP_{mix} value. Partitioning with the former approach was called MIXEST mixture while the latter was

termed randomized mixture. In order to retrieve the IP_{mix} information for the original and simulated data, an evaluation step is required. This was accomplished by directing NONMEM to perform an evaluation step given the final model parameters by setting MAXEVAL=0 for each simulated data set. Naturally, MIXEST can also be computed from the IP_{mix} value, therefore further processing to derive VPC statistics for graphical display was facilitated by the use of single output file (*.phm). A discrepancy in the individual subpopulation allocation frequency between original and simulated data would be indicative of model misspecification and hence provide an additional evaluation aspect specific for mixture models. Therefore, percentage of individuals in each subpopulation for both the original (ORIGID) and the simulated data (SIMID) and the population estimate for the mixture probability (PMIX) are displayed in the VPC plots.

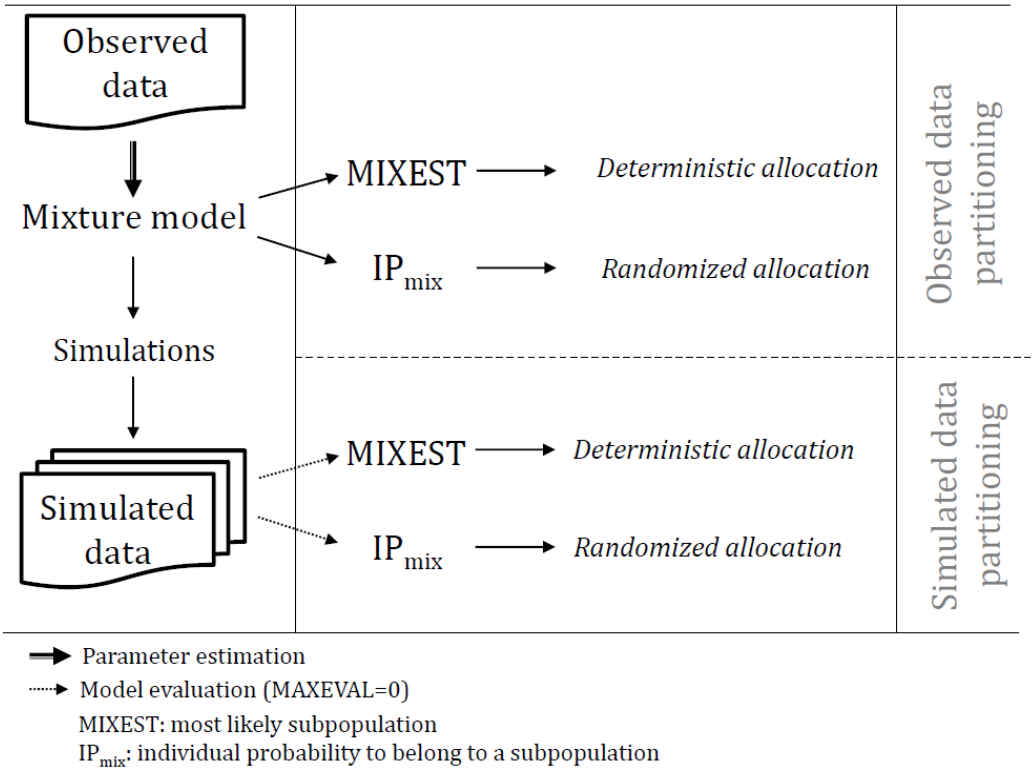

Fig. 1: Illustration of proposed methodology

Implementation of mixture VPCs

A PsN functionality was developed to direct NONMEM runs and post-processing NONMEM output according to the two strategies (MIXEST and randomized) in order to generate the mixture model VPCs. VPCs were implemented using a ggplot2 based package in R [21, 22, 23].

Linear PK data

Data was simulated from a one-compartment PK model (ka = 1 h^{-1}, CL = 20/80 L/h, V_d = 100 L; interindividual variances = 0.09; proportional residual variance = 0.04). A total of 1000 virtual subjects were simulated with 70/30% mixture proportions. Six samples were taken at time points 0.5, 1, 2, 4, 8 and 12 hours following a virtual dose of 100 mg. A bivariate covariate resulting in a 4 fold difference in CL between subgroups was modeled by the inclusion of a mixture component. In order to compare the mixture model with a model without any mixture component stochastic simulation and estimation (SSE) was performed with PsN version 4.8.0 [24]. The simulated data were analyzed by fitting a covariate-free non-mixture model, a covariate model and a mixture model using NONMEM version 7.4.2 [20]. VPCs were constructed for the mixture model using both the MIXEST and the randomized allocation. Performance of the allocation strategies was evaluated by decreasing the difference in drug CL (20/60 L/h) and increasing size of the dominant subpopulation (85/15% mixture proportions).

Parallel linear and nonlinear PK data

Pharmacokinetic data and NONMEM code were extracted from a publically available illustrative PK model example [25]. Thirty-six subjects were part of the analysis with a rich sampling over a period of 672 h (22 observations per individual). Individuals received 4 doses of 50 mg at 0, 168, 336 and 504 h. The pharmacokinetic profile was described by a two-compartment model with two distinct physiological elimination pathways (linear and nonlinear). The pharmacokinetic parameters included V_{max} = 1.2 mg/h, K_m = 10 mg/L, CL_{linear} = 0.03/0.12 L/h, V_1 = 3 L, V_2 = 2 L and Q = 0.075 L/h. The parameters for drug disposition (CL_{linear}, V_{max}, V_1 and V_2) were scaled with the body weight of each individual. A bivariate covariate describing a 4 folds difference in the linear CL pathway with a 40/60% mixture proportions was introduced before

simulation. SSE was performed to simulate the data given the model parameters followed by estimation with a mixture model. Mixture specific VPCs were developed to assess the predictive performance of the model.

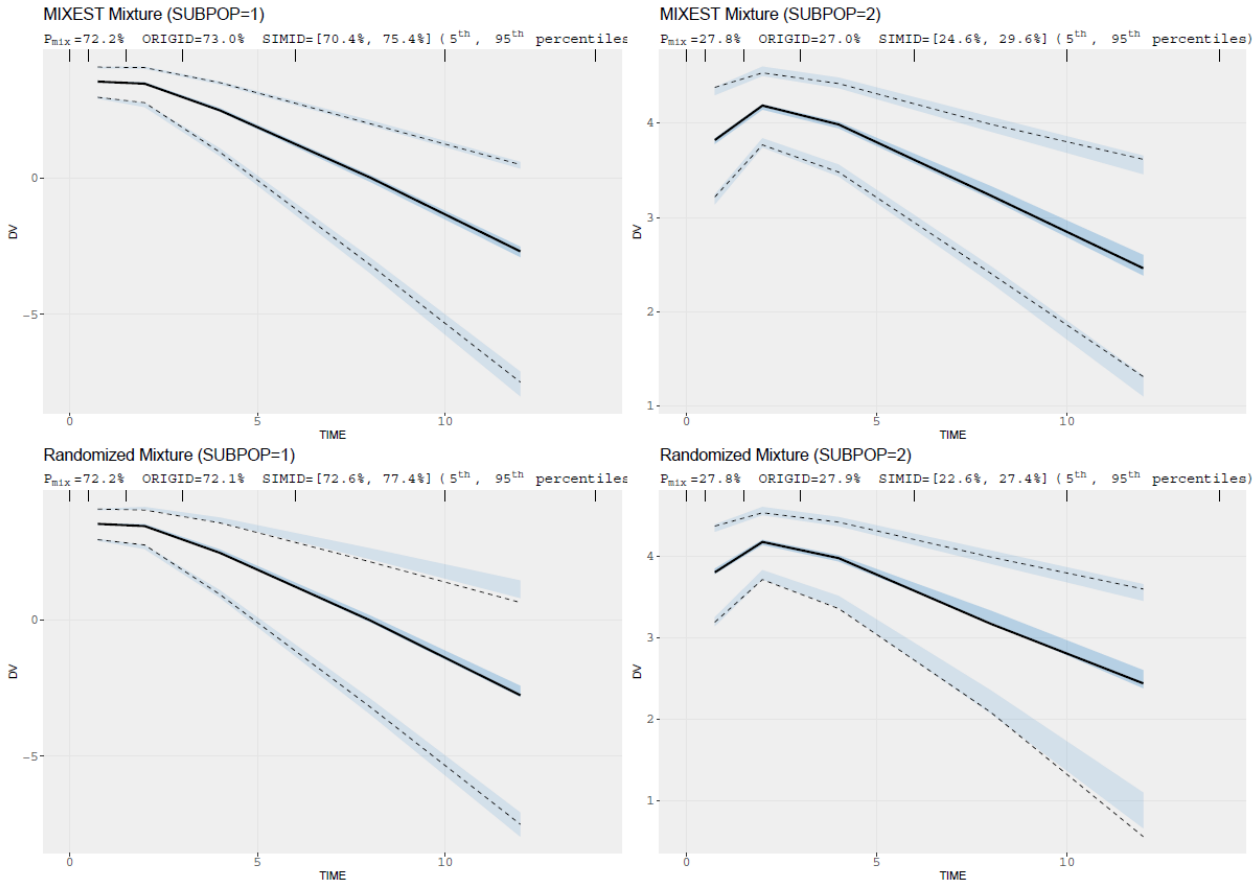

Fig. 2: Mixture VPCs for linear PK data: Upper panel displays MIXEST based VPCs while lower panel displays IP_{mix} based VPCs. One-compartment mixture model with 70/30% mixture proportions having 4 folds CL difference. (SUBPOP=subpopulation number, P_{mix}=estimated population proportion, ORIGID,SIMID= individuals (%) allocated to respective subpopulations in original and simulated data respectively)

Irinotecan PK data

Irinotecan PK profile was described by a combined model from previously published studies [26, 27]. Data comprised of 109 patients with various malignant solid tumors who received an intravenous infusion of 100-350 mg/m^2 for a period of 0.75-2.25 h. A total number of 1930 plasma concentration measurements of active metabolite SN-38 were available for the analysis. The model (Fig. 5) comprised of a three-compartment

model for the parent drug, a two-compartment model for the active metabolite (SN-38) and a two-compartment model for the inactive glucuronide conjugate of SN-38 (SN-38G). The drug was characterized by linear PK properties and the disposition parameters were scaled with body surface area. IIV was associated with all the parameters and the residual unexplained variability was modeled by an additive model. Based on the established influence of genetic polymorphism upon SN-38 CL, a mixture model was developed as the patient genotype information was unavailable. Traditional and mixture specific VPCs were developed for the irinotecan mixture model for comparative evaluation of the recently developed methodology.

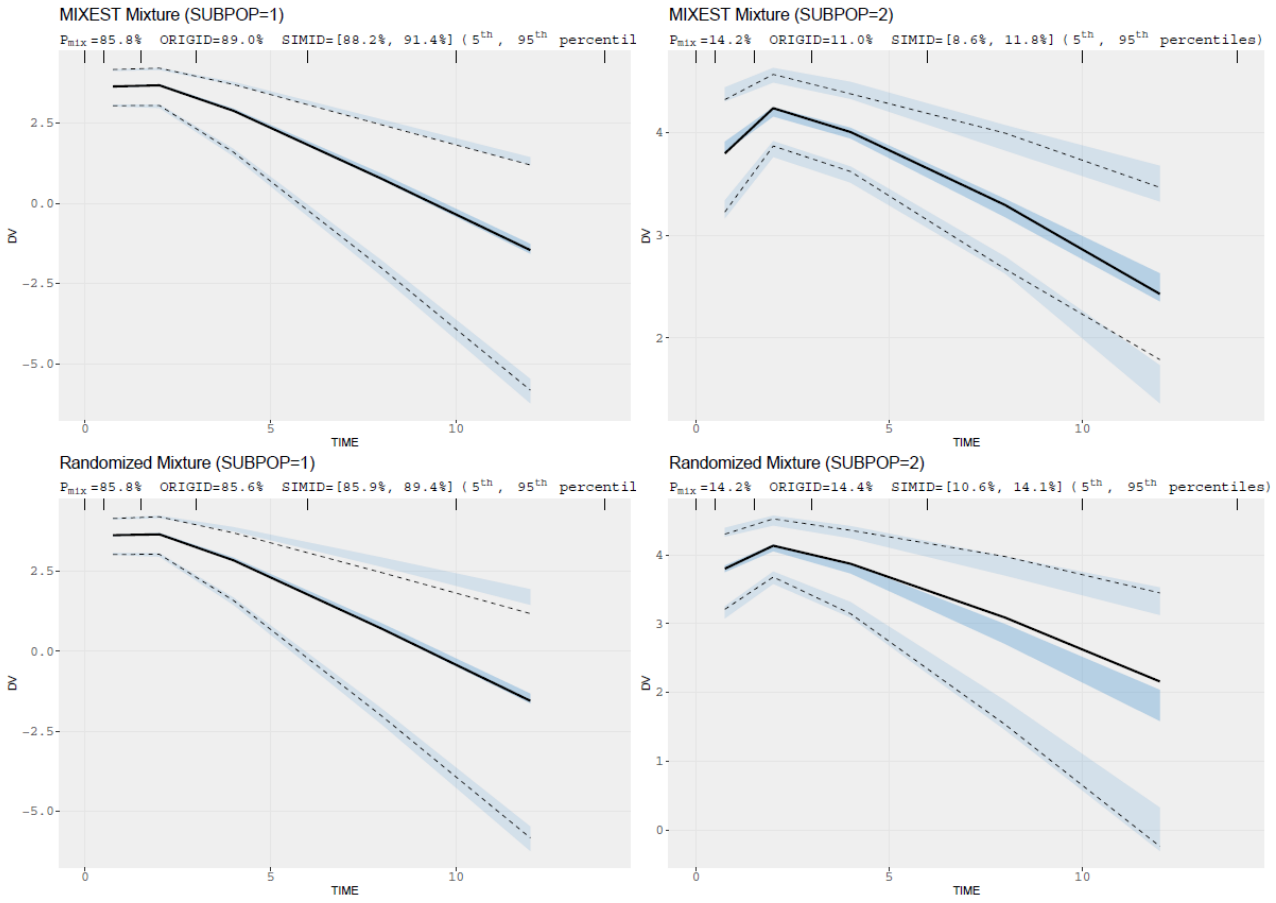

Fig. 3: Mixture VPCs for linear PK data: One-compartment mixture model with 85/15% mixture proportions having 3 folds CL difference.

Results

Allocation of individuals to subpopulations according to MIXEST and IP_{mix} information is elaborated in Fig. 1.

VPCs for linear PK data

SSE results showed that the mixture model with a P_{mix} estimate of 72.2% provided an improved goodness-of-fit (OFV= -664) over the covariate free, non-mixture model (OFV= -642).The inclusion of covariate information provided the best fit (OFV= -774), as expected. Fig. 2 presents the mixture specific VPCs for the simulated PK data with linear kinetics. Both the MIXEST and the randomized mixtures were adequate to evaluate the predictive performance of the model. However, for a population with a comparatively lower difference in drug CL (20/60 L/h) and a greater proportion of dominant subpopulation (P_{mix} estimate of 85.8%) an allocation bias towards the dominant subpopulation was observed with the MIXEST based method (Fig. 3).

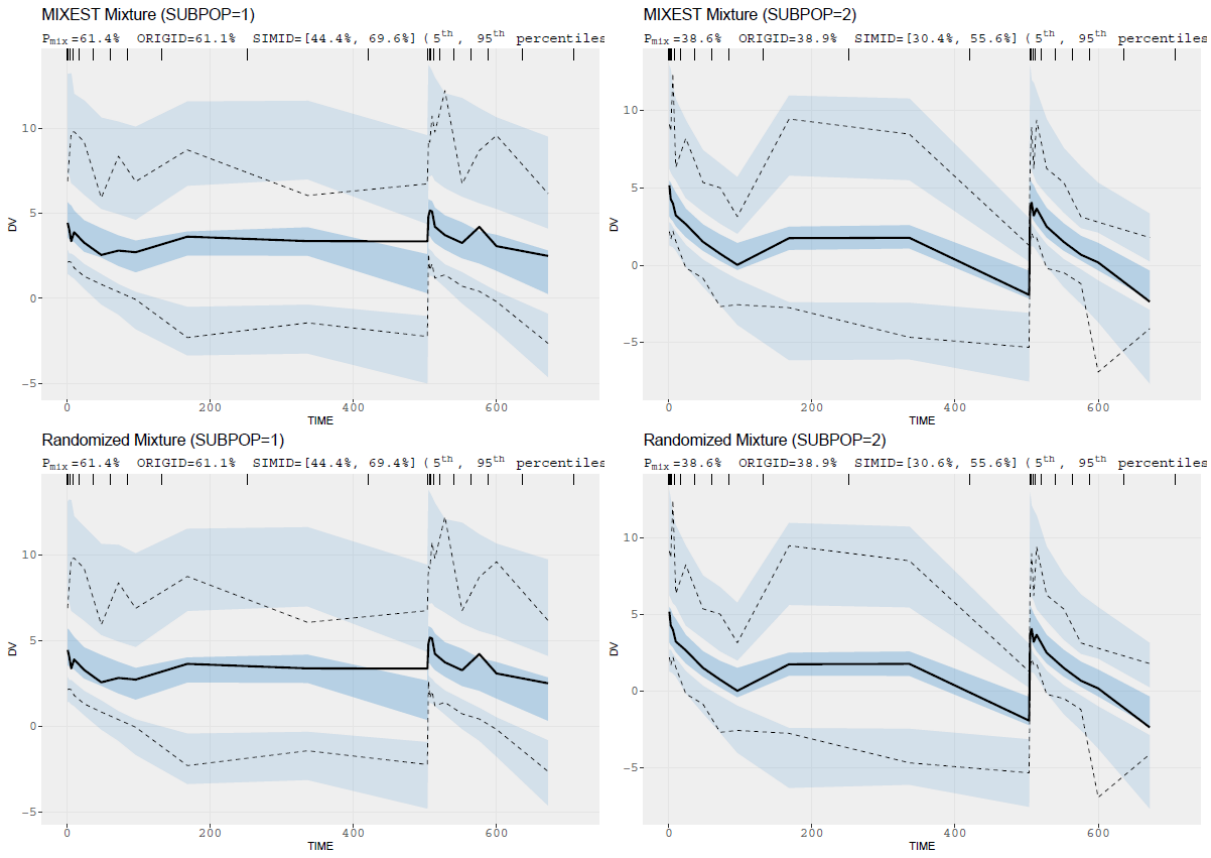

Fig. 4: Mixture VPCs for parallel linear and nonlinear PK data: two-compartment model with mixed elimination kinetics having a mixture proportion of 60/40%with four folds CL difference (mixture component on linear CL model)

VPCs for parallel linear and nonlinear PK data

Mixture VPCs for a mixture model describing parallel linear and nonlinear CL pathways are presented in Fig. 4. P_{mix} was estimated to 61.4%. No allocation bias was observed in this case as the 4 folds difference in CL for the linear pathway was sufficient to separate the subpopulations with 40/60% proportions.

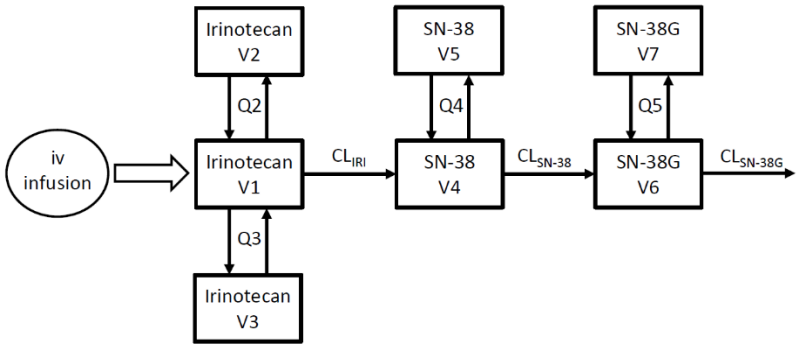

Fig. 5: Schematic representation of the irinotecan mixture model having 36% lower CL of SN-38 in patients with UGT1A1 hetero/homozygote vs wild-type genotype.

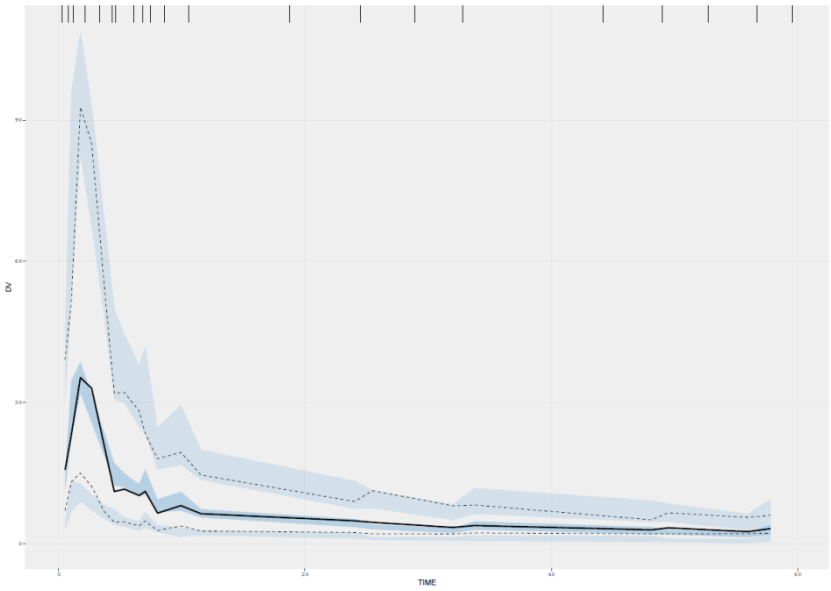

Fig. 6: Traditional VPC for irinotecan mixture model

VPCs for irinotecan PK data

The irinotecan mixture model (Fig. 5) provided a P_{mix} estimate of 70.3% and an approximately 36% lower CL of SN-38 in patients with UGT1A1 hetero/homozygote (*1/*28, *28/*28) vs wild-type (*1/*1) genotype. The traditional VPC (Fig. 6) did not show any model misspecification implying that the model was adequate to describe the pharmacokinetics of the population under study. However, a model misspecification was captured with the implementation of recent approaches. It was evident from mixture VPCs (Fig. 7) that the mixture model was under-predictive for slow metabolizers while over-predictive for fast metabolizers.

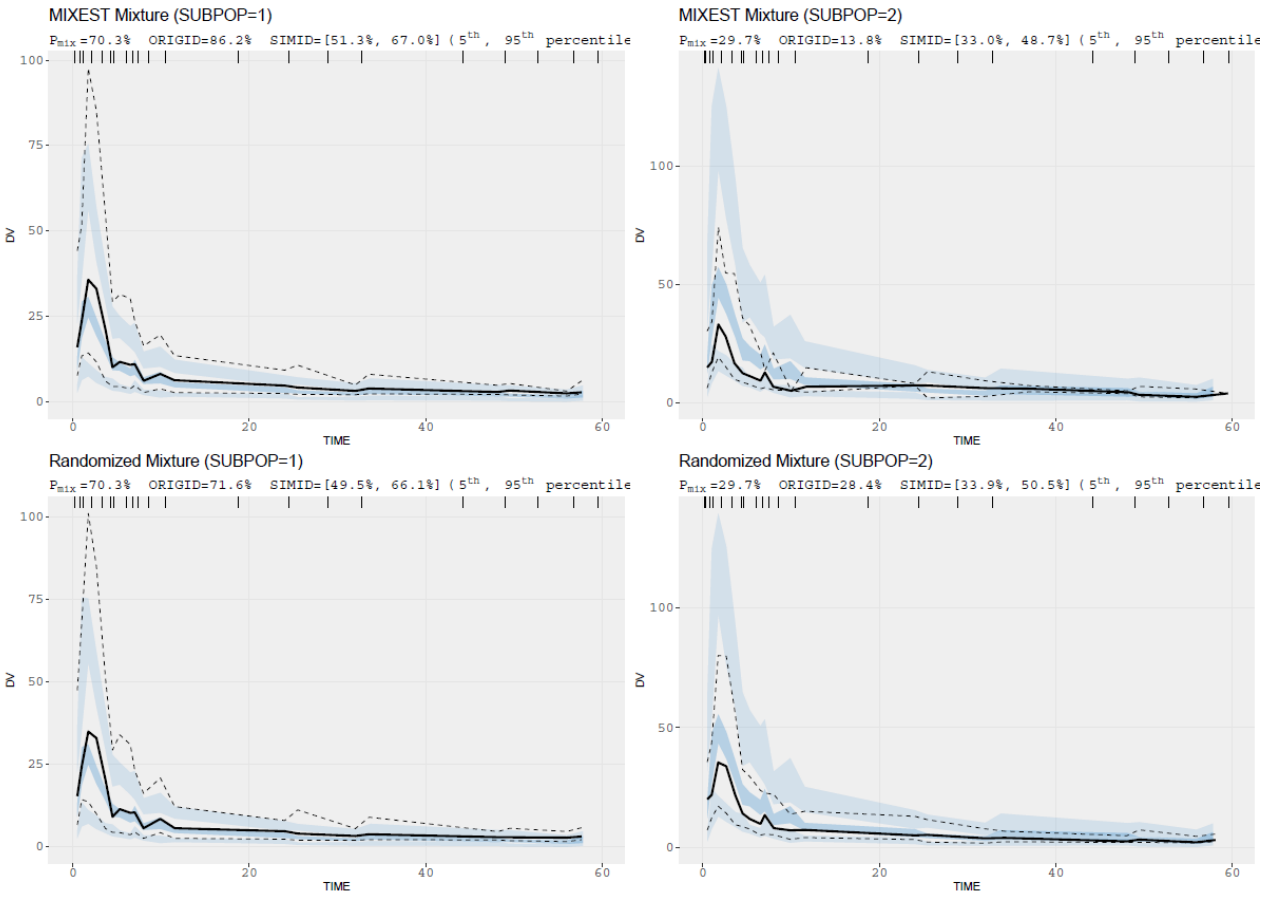

Fig. 7: Mixture VPCs for irinotecan mixture model; left panel: VPCs for slow metabolizers; right panel: VPCs for fast metabolizer

Discussion

A major objective during population analysis is to identify, or otherwise manage, the sources of variability in order to assist decision making. Sources for variability characterized in PK/PD models result in predictable differences in exposure/responses between patient groups and provide a tool to tailor the treatment individually. Identifying not only the magnitude, but also the shape of the unexplained variability can be important. Mixture models are suitable for appropriately characterizing multimodality associated with parameter distributions. VPC is considered to be one of the most informative tools, able to simultaneously diagnose the fixed and random effects [3, 4]. Therefore, mixture VPCs were designed to overcome the limitations of the classical VPCs for the evaluation of mixture models.

Evaluation with the two VPC implementation strategies for simulated data (Fig. 2) illustrates how mixture VPCs can be useful to split the data into subpopulations thereby enhancing the power of evaluation by decreasing the remaining variability within a subpopulation. Both the MIXEST and the IP_{mix} based allocation strategies were adequate to cluster the simulated data for a drug exhibiting linear PK with sufficiently differentiable CL (20/80 L/h). Apart from the visual evaluation, information provided in the display is of significant importance. The population probability estimate (P_{mix}) is representative of the agreement of the model with prevalence of subpopulations in existing literature. Uncertainty or bias associated with P_{mix} can be reflective of model misspecification or insufficient information available in the data. The number of individuals allocated to the respective subgroups should be in accordance with the P_{mix} estimate. Allocation bias in the original and the simulated data can be evaluated from the values assigned to ORIGID and SIMID. No discrepancy between MIXEST and IP_{mix} based allocation of individuals in this illustrative example implies that the data was informative enough to separate the individuals according to their likelihood/probability estimates.

As multimodal parameter distributions stem from a failure to incorporate a multimodally distributed covariate in the model, it is good practice to consider existing covariate data before the decision to proceed with mixture models. Model comparison using SSE results confirm that the covariate model provides a preference over the

mixture model, while a mixture model in turn is a better characterization of the data compared to the standard, unimodal, distribution.

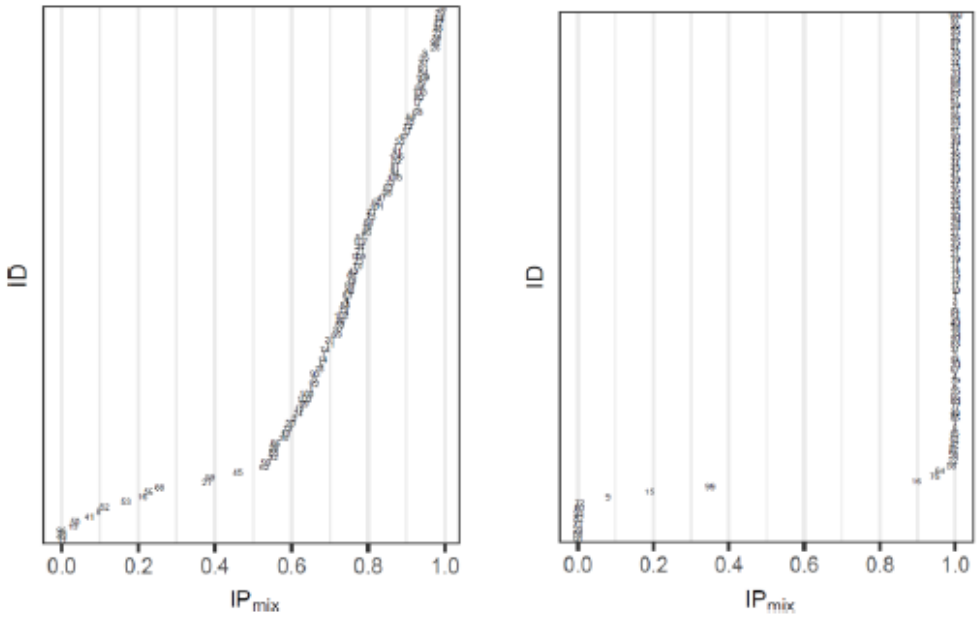

Fig. 8: Distribution of individuals in a population; left panel: a less separated mixture; right panel: a clearly separated mixture

Under circumstances where the individual data is less informative, the MIXEST estimate may exhibit shrinkage towards the dominant subpopulation in contrast to IP_{mix}. Kaila *et al*. [28] used Monte Carlo simulations to examine factors that might impact the ability to correctly classify a subject in a bimodal group. Using a one-compartment model with subjects assigned to one of two CL groups, the authors found that misclassification of individuals was dependent on (i) the magnitude of the difference between the mean CL estimates for the subgroups, (ii) IIV in CL, (iii) proportion of subjects in each subpopulation and (iv) sample size. One should be careful to inspect multimodalities in all the parameter estimates and not only the parameter of physiological interest. A probability partitioning may exist across more than one parameter. There may be a 30/70% partitioning for CL, but a 10/90% partitioning for the volume of distribution. Analysis of such data with a model containing a single mixture component may also lead to uncertainty in probability estimates leading to misclassification or biased allocation.

Fig. 3 demonstrates a biased allocation where the fraction of the dominant subpopulation was larger (85/15%) and the difference in CL was comparatively lower (20/60 L/h). An allocation bias of 3.2% towards the larger subpopulation can be observed with the MIXEST mixture. The less informative individuals with IP_{mix} estimate around 0.5 can be identified with the help of a diagnostic plot displaying the distribution of individuals in a mixture (Fig. 8). The plot presents a less separated (left) and a clearly separated (right) mixture population. We hereby demonstrate that a randomized allocation based upon IP_{mix} information takes into account the uncertainty for an individual to belong to a subpopulation where the data from an individual is less informative.

Fig. 4 displays VPCs for a population with mixed elimination kinetics. The phenomenon is often observed for therapeutic monoclonal antibodies. The linear CL pathway is possibly mediated by antibody Fc-receptors interaction, while the nonlinear CL pathway reflects binding to its pharmacologic target. A higher allocation bias (16%) using MIXEST method was observed with the evaluation of irinotecan mixture model. Moreover, a clear model misspecification was observable from mixture VPCs (Fig. 7) which was otherwise not evident from the classical VPC (Fig. 6). Irinotecan mixture VPCs were supportive of the argument that by reducing the between subpopulation variability in the VPC an enhanced power of evaluation can be achieved. Mixture VPCs were suggestive of further structural model modifications to adequately describe the subpopulation profiles but the respective analysis was beyond the scope of current project.

VPCs like other simulation-based diagnostics test a model's ability to generate data that mimics the observed data. Systematic differences between simulated and real data indicate the deficiency of the model to predict the observed data. An important aspect regarding such procedures is that post-processing of both the observed and simulated data is done in similar way, whether the post-processing occurs through model-based or model-independent methods. Indeed, model-based post-processing is considered advantageous to learn about the model misspecifications [29, 30]. Capturing misspecification in a feature of the model does not necessarily mean that the model is completely inadequate. We are frequently making use of the models with deficiencies. However, we rely on good diagnostics for the evaluation of model's deviation in order to

proceed further. Such decisions are contextual in nature. Although, considerable amount of cases can be seen where mixture modeling approach was used to report results [31-40], but the class of mixture models did not gather much attention to develop diagnostics. Recommended diagnostics for the assessment of non-linear mixed effects models such as VPC, conditional weighted residuals (CWRES), normalized prediction distribution errors (NPDE) are relatively new [1] and less applicable to mixture models. A recent procedure was presented by Lavielle *et al* [41] but does not address mixture models either. Implementation of recent methodology would assist both model developers and users to better assess the mixture aspects than what is being practiced currently.

The proposed methodologies are implemented in PsN and VPCs can be generated with the addition of the option –mix to the vpc command. For comparative evaluation purpose, a traditional VPC plot was also included in the PsN output.

Conclusions

A graphical and statistical comparison of observations and predictions derived from the multimodal distributions in mixture models is presented. Partitioning of observed and predicted data between subpopulations can be done in two ways depending on the underlying information (MIXEST or IP_{mix}). Randomized allocation based upon individual IP_{mix} information provides a preference over MIXEST based discrete allocation as a lower allocation bias is associated with the former case. Mixture VPCs can be a useful diagnostic tool for the development and evaluation of mixture models in the future.

References

1. Nguyen THT, Mouksassi M-S, Holford N et al (2017) Model evaluation of continuous data pharmacometric models: Metrics and graphics. CPT: Pharmacometrics & Syst Pharmacol 6:87-109
2. Holford N (2005) The visual predictive check – superiority to standard diagnostic (Rorschach) plots. PAGE 14. Abstr 738. Available from: www.page-meeting.org/?abstract=738
3. Karlsson MO, Holford N (2008) A tutorial on visual predictive checks. PAGE 17. Abstr 1434. Available from: http://www.page-meeting.org/?abstract=1434.
4. Bergstrand M, Hooker AC, Wallin JE, Karlsson MO (2011) Prediction-corrected visual predictive checks for diagnosing nonlinear mixed effects models. AAPS J 13:143-151
5. Jamsen KM, Patel K, Nieforth K, Kirkpatrick CMJ (2018) A regression approach to visual predictive checks for population pharmacometric models. CPT: Pharmacometrics & Syst Pharmacol 7: 678-686
6. Mould DR, Upton RN (2012) Basic concepts in population modeling, simulation, and model-based drug development. CPT: Pharmacometrics & Syst Pharmacol 1:1-14
7. Carlsson KC, Savic RM, Hooker AC, Karlsson MO (2009) Modeling subpopulations with the $mixture subroutine in nonmem: finding the individual probability of belonging to a subpopulation for the use in model analysis and improved decision making. AAPS J 11:148–154
8. Peretti E, Karlaganis G, Lauterburg GH (1987) Acetylation of acetylhydrazine, the toxic metabolite of isoniazid in humans. Inhibition by concomitant administration of isoniazid J Pharmacol Exp Ther 243:686-689
9. Frame B (2007) Mixture modeling in NONMEM V. In: Ette EI, Williams PJ (eds) Pharmacometrics: The Science of Quantitative Pharmacology. John Willey & Sons, Inc., Hoboken, New Jersey, pp 723-757.
10. Tanigawa T, Heinig R, Kuroki Y, Higuchi S (2006) Evaluation of interethnic differences in repinotan pharmacokinetics by using population approach. Drug Metab Pharmacokinet 21:61–69
11. Hussein R, Charles BG, Morris RG, Rasiah RL (2001) Population pharmacokinetics of perhexiline from very sparse, routine monitoring data. Ther Drug Monit 23:636–643

12. Facca, B. Frame B, Triesenberg S (1998) Population pharmacokinetics of ceftizoxime administered by continuous infusion in clinically ill adult patients. Antimicrob Agents Chemother 42:1783–1787
13. Piotrovsky V, Van Peer A, Van Osselaer N, Armstrong M, Aerssens J (2003) Galantamine population pharmacokinetics in patients with Alzheimer's disease: modeling and simulations. J. Clin Pharmacol 43:514 – 523
14. Kowalski KG, McFadyen L, Hutmacher MM, Frame B, Miller R (2003) A two-part mixture model for longitudinal adverse event severity data. J. Pharmacokinet Pharmacodyn 30:315-336
15. De Angelis R, Capocaccia R, Hakulinen T, Soderman B, Verdecchia A (1999) Mixture models for cancer survival analysis: application to population based data with covariates. Statist Med 18:441-454
16. Phillips N, Coldman A, McBride ML (2002) Estimating cancer prevalence using mixture models for cancer survival. Stat Med 21:1257-1270
17. Gordon NH (1996) Cure mixture models in breast cancer survival studies. In: Jewell NP, Kimber AC, Lee MLT, Whitmore GA. (eds) Lifetime Data: Models in Reliability and Survival Analysis. Springer, Boston, MA, pp 339-346
18. Spilker ME, Seng AKY. Yao A et al (2005) Mixture model approach to tumor classification based on pharmacokinetic measures of tumor permeability. J Magn Reson Imaging 22:549- 558
19. Yano Y, Beal SL, Sheiner LB (2001) Evaluating pharmacokinetic/pharmacodynamics models using the posterior predicitive check. J Pharmacokinet Pharmacodyn 28:171–192
20. Beal S., Sheiner LB., Boeckmann A, Bauer RJ (2009) NONMEM User's Guides (1989-2009). Icon Development Solutions, Ellicott City, MD, USA
21. Wickham H (2016) ggplot2: Elegant graphics for data analysis. Springer International Publishing
22. Keizer R (2017) vpc: R package version 1.0.0. Available from: https://CRAN.R-project.org/package=vpc
23. R Core Team. R: A language and environment for statistical computing. R Foundation for Statistical Computing, Vienna, Austria. Available from: https://www.R-project.org/

24. Lindbom L, Pihlgren P, Jonsson EN (2004) PsN-Toolkit -a collection of computer intensive statistical methods for non-linear mixed effect modeling using NONMEM. Comput Methods Programs Biomed 79:241-257
25. Gastonguay M. Metrum Research Group. Available from: https://metrumrg.com/course/mi212-advanced-topics-population-pk-pd-modeling-simulation
26. Xie R, Mathijssen RH, Sparreboom A, Verweij J, Karlsson MO (2002) Clinical pharmacokinetics of irinotecan and its metabolites in relation with diarrhea. Clin Pharmacol Ther 72:265-275
27. Jiménez BJ and Ruixo JJP (2013) Influencia de los polimorfismos genéticos en UGT1A1, UGT1A7 y UGT1A9 sobre la farmacocinética de irinotecán, SN-38 y SN-38G. Farm Hosp 37:111-127
28. Kaila N, Straka RJ, Brundage RC (2006) Mixture models and subpopulation classification: a pharmacokinetic simulation study and application to metoprolol CYP2D6 phenotype. J of Pharmacokin and Pharmacodyn 34: 141-156
29. Brendel K, Comets E, Laffont C, Laveille C, Mentré F (2006) Metrics for external model evaluation with an application to the population pharmacokinetics of gliclazide. Pharm Res. 23:2036-2049
30. Ibrahim MMA, Nordgren R, Kjellsson MC, Karlsson MO (2018) Model-based residual post-processing for residual model identification. AAPS J 20:81
31. Tamaki Y, Maema K, Kakara M, Fukae M, Kinoshita R, Kashihara Y, Muraki S, Hirota T, Ieiri I (2018) Characterization of changes in HbA1c in patients with and without secondary failure after metformin treatments by a population pharmacodynamic analysis using mixture models. Drug Metab Pharmacokinet 33:264-269
32. Schoemaker R, Wade JR, Stockis A (2016) Brivaracetam population pharmacokinetics and exposure-response modeling in adult subjects with partial-onset seizures. J Clin Pharmacol 56:1591-1602
33. Woloch C, Di Paolo A, Marouani H, Bocci G, Ciccolini J, Lacarelle B, Danesi R, Iliadis A (2012) Population pharmacokinetic analysis of 5-FU and 5-FDHU in colorectal cancer patients: search for biomarkers associated with gastro-intestinal toxicity. Curr Top Med Chem 12:1713-1719
34. Woillard JB, de Winter BC, Kamar N, Marquet P, Rostaing L, Rousseau A (2011) Population pharmacokinetic model and Bayesian estimator for two tacrolimus

formulations--twice daily Prograf and once daily Advagraf. Br J Clin Pharmacol 71:391-402

35. Lohy Das JP, Kyaw MP, Nyunt MH, Chit K, Aye KH, Aye MM, Karlsson MO, Bergstrand M, Tarning J (2018) Population pharmacokinetic and pharmacodynamic properties of artesunate in patients with artemisinin sensitive and resistant infections in Southern Myanmar. Malar J 17:126.
36. Schalkwijk S, Ter Heine R, et al (2018) A mechanism-based population pharmacokinetic analysis assessing the feasibility of efavirenz dose reduction to 400 mg in pregnant women. Clin Pharmacokinet. 57:1421-1433
37. Francis J, Zvada SP, Denti P et al (2018) AADAC gene polymorphism and HIV infection affect the exposure of Rifapentine: a population pharmacokinetics analysis. PAGE 27. Abstr 8695. Available from: www.page-meeting.org/?abstract=8695
38. Bienczak A, Cook A, Wiesner L et al (2016) Effect of diurnal variation, CYP2B6 genotype and age on the pharmacokinetics of nevirapine in African children. J Antimicrob Chemother 72:190-199
39. Polepally AR, Pennell PB, Brundage RC et al (2014) Model-based lamotrigine clearance changes during pregnancy: clinical implication. Ann Clin Transl Neurol 1:99-106
40. Wilkins JJ, Langdon G, McIlleron H, Pillai G, Smith PJ, Simonsson US (2011) Variability in the population pharmacokinetics of isoniazid in South African tuberculosis patients. Br J Clin Pharmacol 72:51-62
41. Lavielle, M. & Ribba, B. Enhanced Method for Diagnosing Pharmacometric Models (2016) Random sampling from conditional distributions. Pharm Res 33:2979.

Chapter 4

Enzyme autoinduction by mitotane supported by population pharmacokinetic modelling in a large cohort of adrenocortical carcinoma patients

Usman Arshad[1], Max Taubert[1], Max Kurlbaum[2], Sebastian Frechen[1], Sabine Herterich[3], Felix Megerle[2], Stephanie Hamacher[4], Martin Fassnacht[2,3,5], Uwe Fuhr[1], Mathias Kroiss[2,3,5].

European Journal of Endocrinology 2018. 179(5):287–297

[1] Department I of Pharmacology, University Hospital Cologne, Germany

[2] Division of Endocrinology and Diabetology, Department of Internal Medicine I, University Hospital, University of Würzburg, Germany

[3] Clinical Chemistry and Laboratory Medicine, University Hospital Würzburg, Germany

[4] Institute of Medical Statistics and Computational Biology, University of Cologne, Germany

[5] Comprehensive Cancer Center Mainfranken, University of Würzburg, Würzburg, Germany

Abstract

Objective: Mitotane is used for the treatment of adrenocortical carcinoma. High oral daily doses of typically 1- 6 g are required to attain therapeutic concentrations. The drug has a narrow therapeutic index and patient management is difficult because of a high volume of distribution, very long elimination half-life, and drug interaction through induction of metabolizing enzymes. The present evaluation aimed at the development of a population pharmacokinetic model of mitotane to facilitate therapeutic drug monitoring.

Methods: Appropriate dosing information, plasma concentrations (1137 data points) and covariates were available from therapeutic drug monitoring (TDM) of 76 adrenocortical carcinoma patients treated with mitotane. Using nonlinear mixed effects modeling, a simple structural model was first developed, with subsequent introduction of metabolic autoinduction. Covariate data were analyzed to improve overall model predictability. Simulations were performed to assess the attainment of therapeutic concentrations with clinical dosing schedules.

Results: A one-compartment pharmacokinetic model with first order absorption was found suitable to describe the data, with an estimated central volume of distribution of 6086 L related to a high interindividual variability of 81.5%. Increase in clearance of mitotane during treatment could be modeled by a linear enzyme autoinduction process. Body mass index was found to have an influence upon disposition kinetics of mitotane. Model simulations favor a high dose regimen to rapidly attain therapeutic concentrations, with the first TDM suggested on day 16 of treatment to avoid systemic toxicity.

Conclusion: The proposed model describes mitotane pharmacokinetics and can be used to facilitate therapy by predicting plasma concentrations.

Introduction

The adrenolytic drug mitotane (1-chloro-2-[2,2-dichloro-1-(4-chlorophenyl) ethyl] benzene) is the only approved treatment of the orphan malignant disease adrenocortical carcinoma (ACC). ACC has a high rate of recurrence after complete tumor resection and a dismal prognosis in advanced stages (1, 2). Mitotane is used both as an adjuvant treatment after complete tumor resection (3, 4) and for palliative treatment of advanced disease (5). Clinically used drug effects of mitotane include reduction of tumor related steroid hormone excess and a direct cytotoxic effect leading to objective treatment response in ~20% of cases (6) which appears to be relatively specific to cells of the adrenal cortex. Several molecular mechanisms for mitotane action appear to contribute to mitotane efficacy (7, 8, 9). We recently found sterol-O-acyl transferase 1 to be inhibited by mitotane which leads to impaired steroidogenesis and lipid induced endoplasmic reticulum stress (10). Published data on the pharmacokinetics of mitotane are scarce and have been conducted in small patient series only. It has been shown that mitotane has a low oral bioavailability (F) of 35-40% (11) and a high volume of distribution which is likely due to its lipophilic nature and extensive accumulation in adipose tissue (12). The majority of mitotane has been found to be bound to lipoprotein particles in circulation with pharmacological activity limited to the unbound fraction (13, 14, 15).

Efficacy of mitotane treatment is associated with plasma concentrations >14 mg/L which could be demonstrated in several retrospective series both in adjuvant and palliative treatment with mitotane monotherapy (6, 16, 17, 18, 19, 20) but also in combination with cytotoxic drugs in advanced disease (21, 22). Adverse effects, including CNS toxicity are associated with plasma concentrations exceeding 20 mg/L (23). However, the time interval to achieve therapeutic plasma concentrations of mitotane limits the clinical utility of the drug regardless of the dosing regimen applied (24, 25, 26). Accordingly, therapeutic drug monitoring (TDM) is needed for continuous treatment evaluation and decision making. There is a poor correlation of mitotane dose with plasma concentrations, which suggests the involvement of other factors influencing the attainment of therapeutic concentrations (27).

Main metabolites of mitotane are o,p′-dichlorodiphenyl-ethene (o,p'-DDE) and –acetate (o,p'-DDA) (28, 29). o,p'-DDA can be detected at ten-fold higher concentration in blood

than mitotane itself whereas o,p'-DDE is barely detectable in most cases (19, 30). Small amounts of these derivatives apparently undergo aromatic hydroxylation and glycine conjugation (28). The compound is a strong inducer of hepatic CYP3A4 *in vitro* and *in vivo*, which causes interactions with co-administered drugs such as sunitinib (31, 32, 33, 34). Orally administered mitotane is excreted in urine and bile and has a long elimination half-life ranging from 18-159 days (35).

In vitro, drug metabolizing enzymes and transporters beyond CYP3A4 were induced by mitotane, probably via the pregnane X receptor (PXR) (32). PXR ligands transcriptionally induce the activity of a broad range of processes in drug metabolism, which in turn often also accelerate the metabolism of PXR ligands, a phenomenon called autoinduction (36, 37). It is therefore conceivable that mitotane metabolism may be affected by autoinduction, and variability in autoinduction may contribute to differences in clinical toxicity and efficacy among patients. Thus, it might be helpful to account for enzyme induction in order to appropriately describe the pharmacokinetics of mitotane during a long-term treatment. A quantitative description of enzyme induction by mitotane in patients may also be useful to predict drug interactions that may limit the exposure to co-administered chemotherapeutic or targeted agents (3). Previous modeling efforts have not considered autoinduction (38).

The objective of the present evaluation is thus to develop a model describing mitotane pharmacokinetics incorporating enzyme autoinduction, which should contribute to optimizing mitotane dosing schedules.

Subjects and methods

Patients characteristics and data preparation

Clinical and demographical data were retrieved from records of patients participating in the German ACC Registry and the European Network for the Study of Adrenal Tumors (ENSAT) at a single reference center. Both registries have been approved by the ethics committee of the University of Würzburg (approval number 86/03 and 88/11) and all patients provided written informed consent to participate in the study. The following parameters were collected: age, sex, weight, height, body mass index, ENSAT tumor stage, treatment intention, concomitant systemic therapy, albumin, triglyceride, high

and low-density lipoprotein, cholesterol, creatinine, and γ-glutamyltransferase (γ-GT) plasma concentrations. Mitotane plasma concentrations were measured within the Lysosafe® TDM provided on behalf of the manufacturer, HRA-Pharma (Paris, France) using LCMS. A total number of 103 patients with adrenocortical carcinoma were treated with oral mitotane doses (0.5-10g per day, with interruptions).

R (version 3.2.3) with 'dyplyr', 'tidyr' 'lubridate' and 'ggplot2' packages was used for data manipulation, cleaning and visualization (39, 40, 41, 42). All patients treated with mitotane over the age of 18 were eligible. Only patients with missing dosing at the initiation of therapy were excluded from analysis. Data from patients with missing dosing information during the treatment course was excluded partly by evaluating only data gathered during the period prior up to the missing information. Exploratory data analysis was performed to judge general trends in the data.

Data analysis and pharmacokinetic model development

Nonlinear mixed effect modeling was performed for data analysis. Estimation of pharmacokinetic parameters was performed by first order conditional estimation with interaction (FOCE-I) using NONMEM 7.4.1 (ICON, Development Solutions, Elliot City, MD, USA) (43). Model development was aided by Pearl-speaks-NONMEM toolkit (Version 4.7.0) (44). Graphical user interface Pirana (Version 2.9.6) was used for model management and execution, output generation and interpretation of results (45). Xpose4 package with R was used for visualizing output data, post processing and analyzing NONMEM output (46).

A compartmental approach was adapted in a stepwise manner to develop a pharmacokinetic model. In the first step, pharmacokinetic parameters representing a typical individual of the population were estimated using the basic structural model, followed by estimation of interindividual variability (IIV). Subsequently, a hypothetical mitotane metabolizing enzyme compartment was introduced.

Change in amount of drug in the central compartment ($A_{D,cent}$) was described by equation 1.

$$dA_{D,cent}/dt = ka \cdot A_{D,gut} - C_p \cdot CL_{baseline} \cdot A_{enz} \qquad (1)$$

Where,

ka is the absorption rate constant,

$A_{D,gut}$ is the amount of drug in gut compartment,

C_p is the mitotane plasma concentration,

$CL_{baseline}$ is the baseline mitotane clearance,

A_{enz} is the relative amount of enzyme in hypothetical enzyme compartment.

Mitotane plasma concentrations influenced enzyme turnover rate and enhanced enzyme synthesis as described in equation 2.

$$\frac{dA_{enz}}{dt} = K_{in} \cdot (1 + Slope \cdot C_p) - K_{out} \cdot A_{enz} \quad (2)$$

The enzyme induction model assumes that the rate of enzyme synthesis (K_{in}) follows zero-order kinetics, while the rate of degradation (K_{out}) follows first-order kinetics dependent upon relative amount of enzyme.

At steady state enzyme concentrations,

$$K_{in} = K_{out} \quad (3)$$

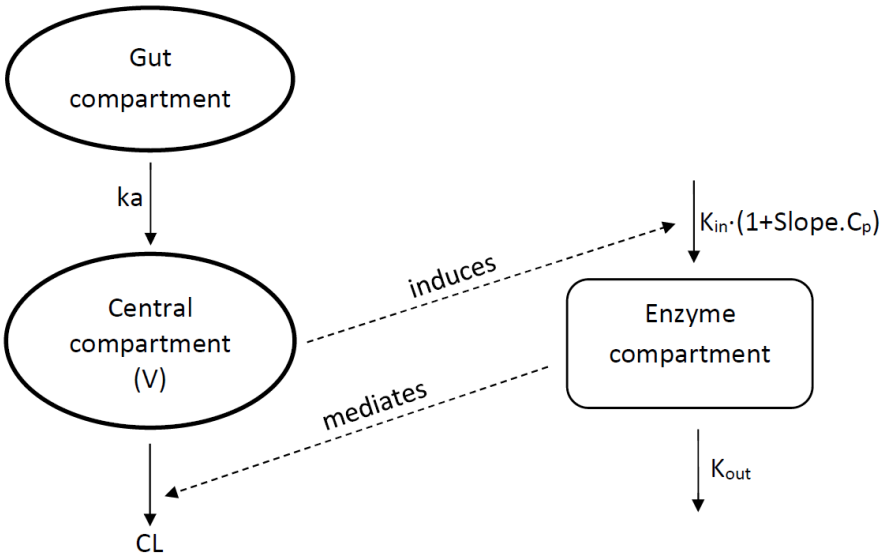

Fig 1. A schematic representation of one compartment pharmacokinetic model linked to the enzyme induction model. Mitotane plasma concentrations increasing the enzyme formation rate and enzyme amount is in turn affecting the mitotane clearance.

Parameters which could not be estimated from the data because of insufficient information were fixed according to published values or to arbitrary and/or physiologically plausible values which were subsequently evaluated by sensitivity analysis.

Other models tested included: (i) a two-compartment model; (ii) models with mitotane being eliminated by two distinct inducible and uninducible pathways; and (iii) models incorporating both gut wall and hepatic enzyme induction. A more complex physiologically based approach was also tested including (iv) a minimal physiologically based pharmacokinetic model (47); and (v) a semiphysiological well stirred liver model to incorporate the first pass effect (48). Both linear and nonlinear relationships (E_{max} and sigmoidal E_{max} models) were tested to describe the effect of mitotane on enzyme formation.

IIV was introduced to volumes of distribution and slope (Equation 4) assuming a normal distribution of η with mean zero and variance ω^2.

$$\phi_{i,j} = \theta_j \cdot exp(\eta_{i,j}) \qquad (4)$$

Where $\phi_{i,j}$ is the jth individual pharmacokinetic parameter of the ith subject, θ_j the population estimate of the respective pharmacokinetic parameter and $\eta_{i,j}$ the deviation of the subject's individual parameter from the population point estimate.

Additive, proportional and combined error models were scrutinized to obtain estimates for residual unexplained variability (RUV). For nested (hierarchical) models, the likelihood ratio test was used which assumes that the difference in objective function values (OFV) (representating an overall prediction error) between two models is chi-squared distributed. Decisions regarding model preference were based on a preselected level of significance (p=0.05), degrees of freedom (difference in total number of parameters), and a critical chi-square value (for the chosen level of significance and degrees of freedom). Nested models with fewer parameters and an OFV lower by an amount larger than the critical chi-square value was finally given a preference. For non-nested (non-hierarchical) models, the Akaike Information Criterion (AIC: OFV plus two times the number of parameters) was used and the model with a lower AIC value was preferred. Goodness of fit (GOF) plots were evaluated to assess the discrepancy between

the observed and predicted data and included individual/population predicted concentrations (IPRED/PRED) vs. the observed concentrations and conditional weighted residuals (CWRES) vs. observed concentrations and vs. time range. Physiological plausibility and precision of parameter estimates assessed via bootstrap statistics with 1,000 samples were further criteria of model selection.

Covariate analysis

After successful development of a basic structural model, covariates were analyzed to provide an explanation for IIV and to improve overall model performance. Covariate pre-selection was based primarily on physiological plausibility. Graphical screening for potential covariates was performed including CWRES and individual pharmacokinetic parameters estimates versus covariates. Correlated covariates were avoided to be tested together and preference among those was given to the covariate with greater scientific plausibility if they provided a similar improvement of the model. Mitotane is reported to alter γ-GT (49) and triglyceride levels in patients and it is suggested to closely monitor the lipid profile during mitotane treatment (50). As the drug is known to be accumulated in the adipose tissue, greater body fat proportion in women might have an impact influence upon its volume of distribution (51). Considering these facts, parameter covariate relationships were tested on volume of distribution (BMI and sex) and Slope (CL_{CR}, plasma γ-GT and triglyceride levels).

Categorical covariate relationship (sex) was tested as a fractional change (θ_{COV}) from the typical value of a parameter estimate (θ_1)

$$TVP\ (typical\ value\ of\ parameter) = \theta_1 \cdot [1 + \theta_{COV} \cdot (COV)] \qquad (5)$$

Whereas, continuous covariates (BMI, CL_{CR}, plasma γ-GT and triglyceride levels) were analyzed as linear relationships,

$$TVP = \theta_1 \cdot [1 + \theta_{COV} \cdot (COV - COV_{median})] \qquad (6)$$

Final covariate inclusion in the model was mainly based upon the decrease in OFV and IIV.

Simulation study

Relative change in clearance over time was evaluated graphically by designing stochastic simulations with model estimates. Both high dose (day1: 1.5 g, day2: 3g, day3: 4.5g, day4-onwards: 6g daily) and low dose (day1-2: 1g, day3-5: 1.5g, day6-8: 2g, day 9-11: 2.5g, day12-onwards: 3g daily) regimens used in clinical practice (24, 25) were tested in simulated population over a period of 3 months. Statistical and graphical evaluation was performed with the aim to attain therapeutic mitotane concentrations (14-20mg/L), avoiding toxic concentrations and to define appropriate timing of first TDM.

Results

Data regarding 76 patients out of 103, 45 females and 31 males, could finally be included in the model development process. These patients were aged between 17 and 75 years, the body weight was between 44 and 129 kg. 1137 observations of concentration data were part of the analysis. Descriptive statistics of patient, disease and treatment characteristics are presented in Table 1.

Absorption from gut compartment was modeled as a first order process. A one-compartment model was given preference over a two-compartment model, apparently because there was not sufficient information available in the data to precisely estimate peripheral volume of distribution and intercompartmental clearance. Although an empirical two-compartment model provided a lower OFV, this was at the expense of highly imprecise parameter estimates for volume of distribution and intercompartmental clearance. Attempt to fix these parameters according to published fat to plasma concentration ratios (12) resulted in even a higher IIV with regard to central volume of distribution and therefore conflicted with the model selection criteria. Fig. 1 provides a schematic representation of the model.

The parameter value for F was fixed to 0.35 (11) and value for ka (49.9 day^{-1}) was also taken from the literature because of insufficient information available during the absorption phase of mitotane in the present data (52). Model simulations demonstrated that parameter estimate for K_{out} did not have any substantial impact upon concentration time profile. Therefore, the parameter value for K_{out} was fixed to 0.23 day^{-1} according to literature (33). $CL_{baseline}$ was a priori assumed to be not estimable and sensitivity

analysis using different $CL_{baseline}$ values of up to 60 L/day did not exhibit any changes in OFV, hence a value of 1 was used to describe the relative change over time. The drug was

Table 1. Patient, disease and treatment characteristics

Patient characteristic	**total (n = 76)**
Age, years [mean ± sd]	48.6 ± 11.8
Sex, female [n (%)]	45 (59.2%)
Body height, m [mean ± sd]	1.71 ± 0.92
Body weight, kg [mean ± sd]	75.4 ± 14.5
BMI, kg/m² [mean ± sd]	25.6 ± 4.2
Plasma cholesterol, mg/dL [mean ± sd]	267.6 ± 83
Plasma creatinine, mg/dL [mean ± sd]	0.82 ± 0.26
Plasma γ-glutamyltransferase, U/L [mean ± sd]	187.3 ± 158.8
Disease characteristics	**patient n (%)**
Stage at treatment initiation	
ENSAT I	1 (1)
ENSAT II	23 (30)
ENSAT III	11 (14)
ENSAT IV	37 (49)
local recurrence	3 (4)
unknown	1 (1)
Treatment characteristics	**patient n (%) / Median (range)**
treatment intention at start of mitotane	
adjuvant	12 (16)
adjuvant and palliative*	21 (28)
palliative	37 (49)
unknown	1 (1)
Concomitant systemic therapy any time during observation period	44 (58)
yes	2 (3)
unknown	
Chemotherapy regimens	
Number of regimens	5 (1-5)
EDP	34 (45)
Streptozotocin	29 (38)
Gemcitabine/Capecitabine	13 (17)
other	16 (21)
unknown	2 (3)

*Treatment initiation in adjuvant intention, later continued as palliative treatment
BMI: Body Mass Index, ENSAT: European Network for the Study of Adrenal Tumors, EDP: Etoposide, Doxorubicin, Cisplatin regimen.

estimated to have a high central volume of distribution of 6086 L (4743-7676L; bootstrap 95% CI). Clearance of the drug was found to increase over time due to the enzyme induction process. A relative linear increase of 3.97 L/day ("Slope", 3.22-4.80; bootstrap 95% CI) per day per mg/L mitotane plasma concentration was observed. A

simple linear model was preferred over E_{max} and sigmoidal E_{max} models because of implausible estimates for EC_{50} and E_{max}.

High IIV was associated with the volume of distribution (81.5%; point estimate). Extent of induction (Slope) was also found to be highly variable among the population (78.8%; point estimate). Estimates for RUV were adequately obtained with a combined error model. BMI was found to be a significant covariate for the volume of distribution, with an objective function value (OFV) decrease by 11 points. IIV was marginally reduced by 4.1% upon volume of distribution and 3.5% upon Slope. The comparison of the basic model and the covariate model in terms of decrease in IIV and OFV is represented in table 2. Table 3 presents bootstrap parameter estimates.

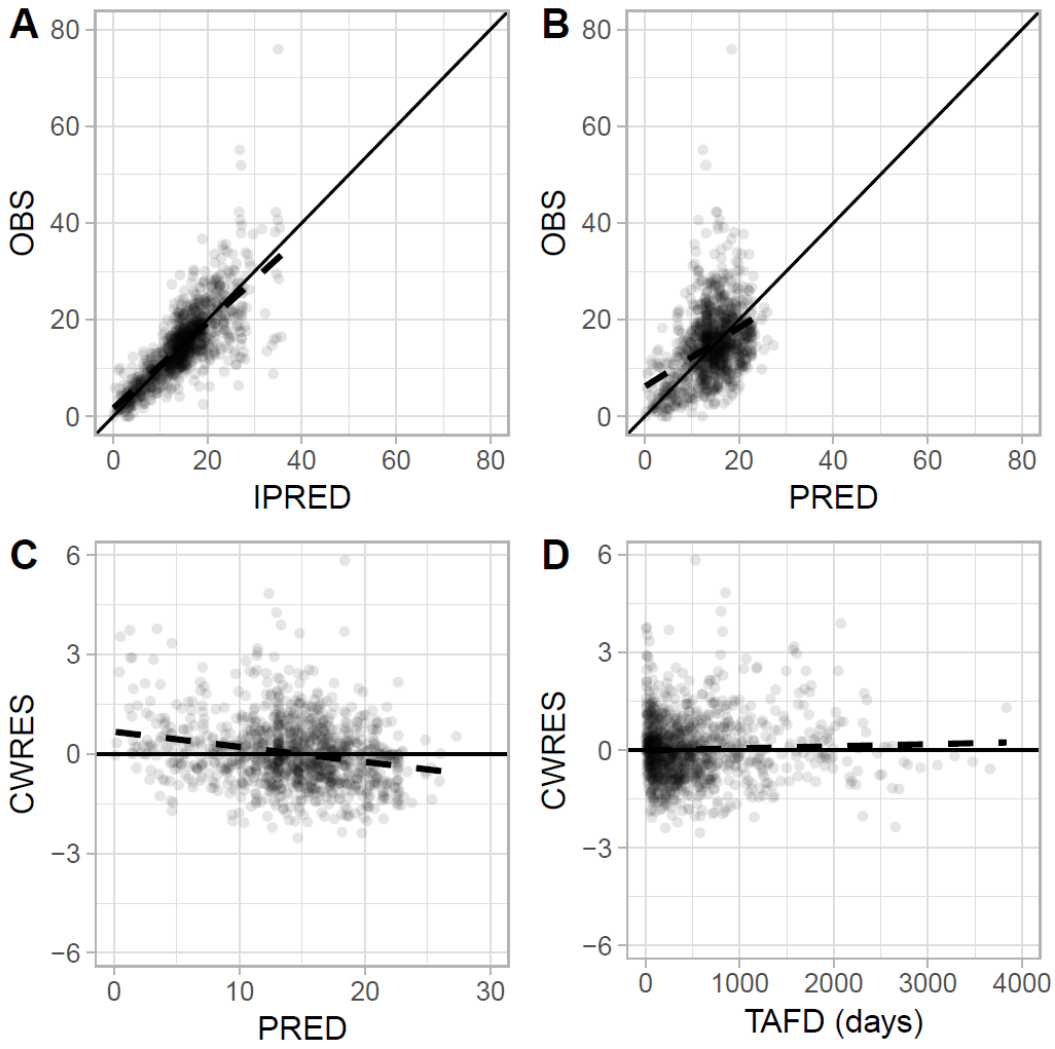

Fig 2. Goodness fo fit plots; observed vs individual predicted concentration (A) observed vs population predicted concentrations (B) conditional weighted residuals vs population predicted concentrations (C) conditional weighted residuals (CWRES) vs time after first dose (D).

Fig. 2 displays the basic goodness-of-fit (GOF) plots for the developed model. The IPRED were symmetrically distributed along the line of unity without any major outlier trends and PRED were adequate. CWRES were evenly distributed around zero depicting an adequate model performance over the concentration and time range. Individual plots (Fig. 3) exhibit the concentration time profiles for the observed and model predicted concentrations for four individuals exposed to mitotane treatment over different time periods ranging from 150 to 600 days. These plots illustrate that the model appropriately describes the diverse pharmacokinetic profiles across the studied population.

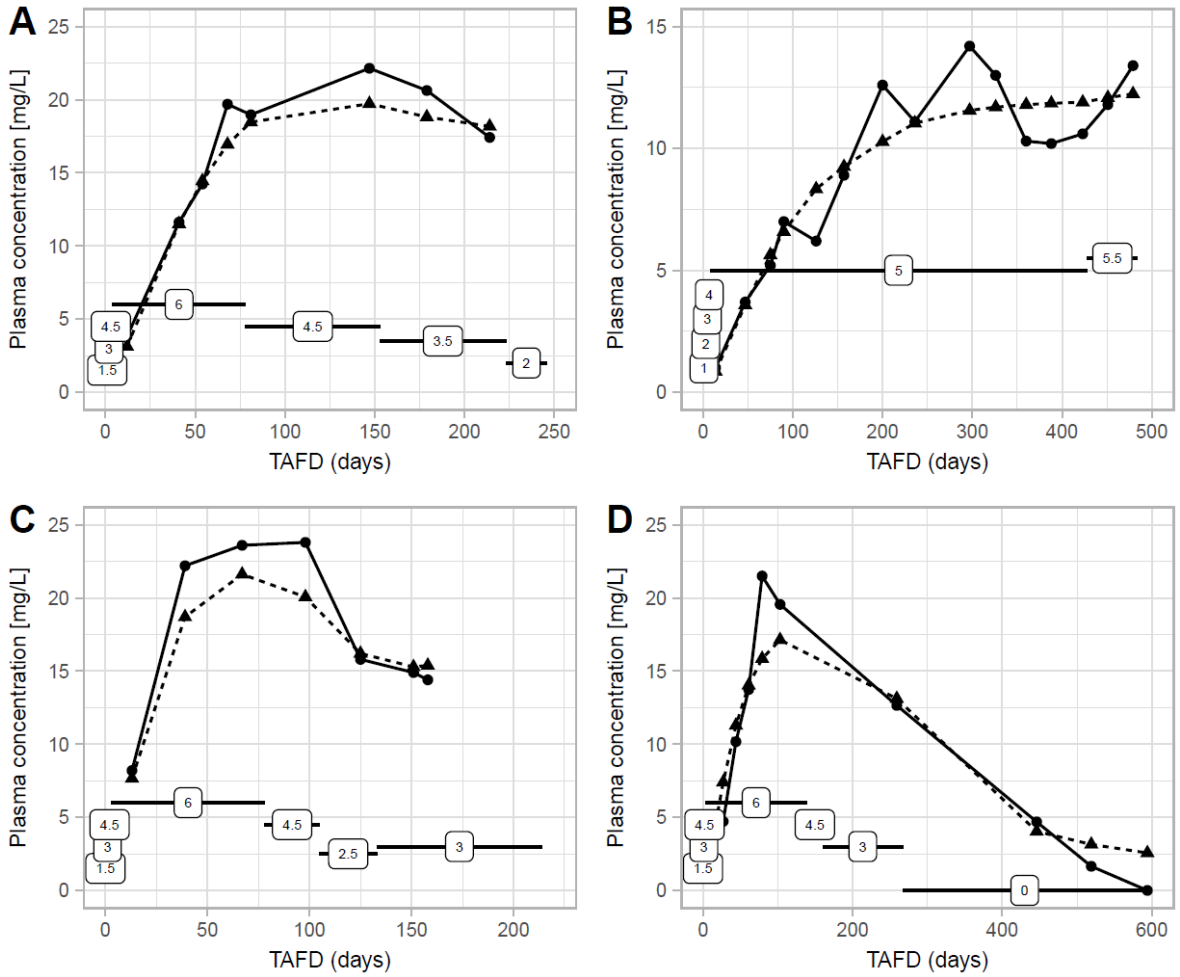

Fig 3. Individual plots of 4 patients treated with mean mitotane doses of 4.12g (A), 4.57g (B), 3.91g (C) and 4.77g over different periods of time (TAFD, time after first dose; -●-observed concentrations; -▲-predicted concentrations). Doses (rectangular boxes with associated lines) represent actual daily doses.

Monte-Carlo simulations

Temporal changes in clearance over time in a simulated population are depicted in Fig. 4. Median simulated plasma mitotane concentrations and respective percentiles (5th and 99th) with the high and the low dose regimen, respectively, are shown in Fig. 5. Persistent increase in plasma concentrations was observed. The 99th percentile reached the upper range of the therapeutic window at around day 16 for the high dose regimen and on day 55 for the low dose regimen.

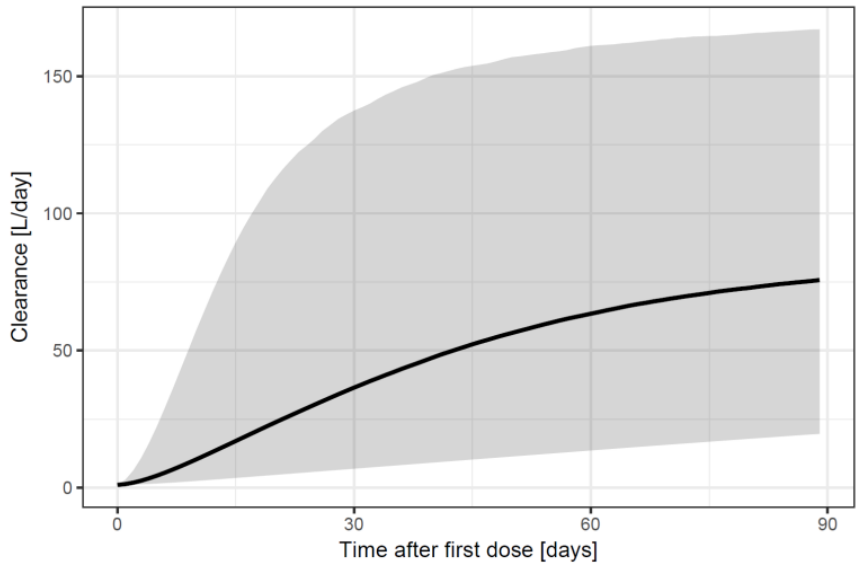

Fig 4. Change in clearance over time in a simulated population of 500 virtual subjects (median with 5th and 95th percentiles).

Table 2. Comparison of base and covariate model

Model	Objective function value	Interindividual variability (%CV)
Base model	4764.4	81.5 (V), 78.8 (Slope)
Covariate model	4753.3	77.3 (V), 75.2 (Slope)

CV: coefficient of variation, V: volume of distribution

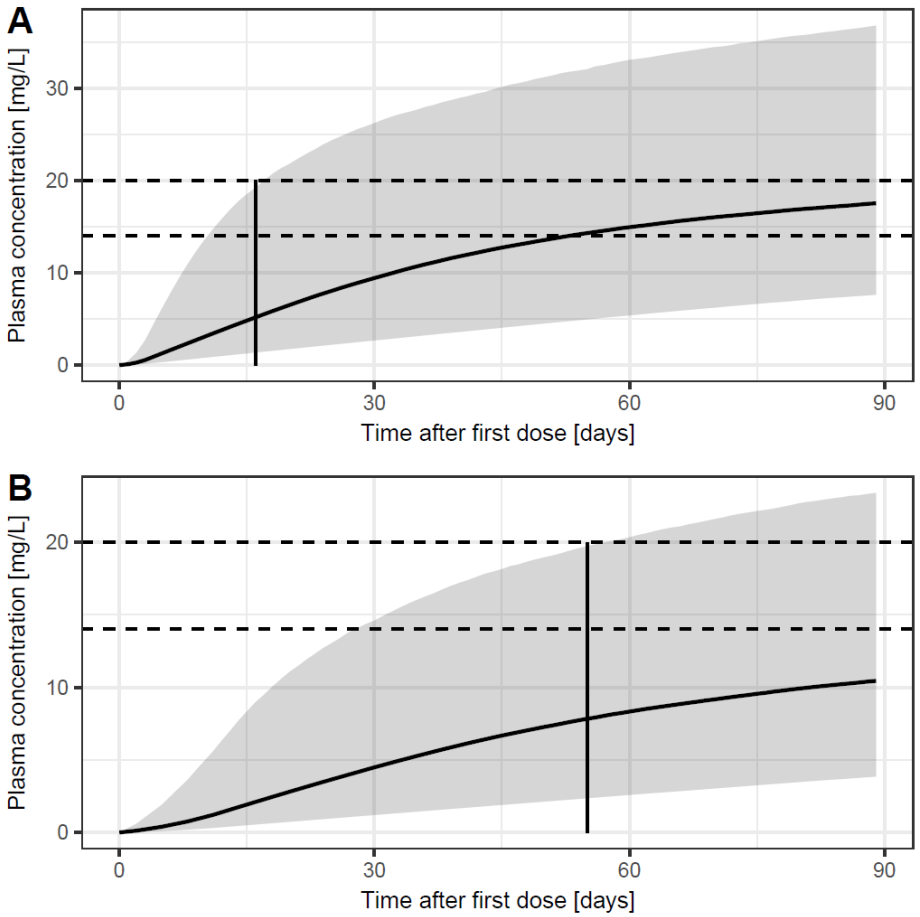

Fig 5. Concentration vs time plot for a simulated population of 500 virtual subjects administered with the clinically used highy dose (A) and low dose (B) mitotane regimens (median, 5th and 99th percentiles). The region between the dashed lines represents the therapeutic window. The vertical lines identify the time points proposed for the first TDM sampling for the two dosing regimens.

Discussion

In this by far largest and well characterized series of ACC patients on mitotane treatment, we investigate the pharmacokinetics of mitotane by implementing a nonlinear mixed effect modeling approach. The approach not only considers the fixed effects (descriptors of a process e.g., pharmacokinetic parameters and respective covariates) but also estimates the random variability (reflected by IIV and RUV) across the population by making use of nonlinear regression techniques. Mitotane showed a large and highly variable volume of distribution, partly explained by interindividual differences in BMI. Pronounced variability was also found for concentration dependent mitotane clearance attributable to autoinduction of mitotane metabolism.

Table 3: Model parameter estimates

Pharmacokinetic parameters		
Parameter	**median estimate**	**95% CI**
ka (day^{-1})	49.9	Fixed
F (%)	35	Fixed
V/F (L)	6086	4743-7673
K_{in} (day^{-1})	0.23	Fixed
K_{out} (day^{-1})	0.23	Fixed
slope (L day^{-1} day^{-1})	3.97	3.22-4.80
BMI covariate effect upon V (fractional change from typical value of V per unit of BMI)	0.055	0.01-0.11
Interindividual variability		
Parameter	**median estimate**	**95% CI**
η_i^v (ω^2)	0.54	0.28-0.87
η_i^{slope} (ω^2)	0.56	0.35-0.84
Residual variability (combined error model)		
Type	**median estimate**	**95% CI**
Additive (σ^2)	0.24	0.18-0.29
Proportional (σ^2)	2.28	1.50-3.13

ka: absorption rate constant, F: bioavailability, V: volume of distribution, K_{in}: rate of enzyme synthesis, K_{out}: rate of enzyme degradation, η_i^v: interindividual variability in V, η_i^{slope}: interindividual variability in slope, ω^2 and σ^2: variance, BMI: body mass index as kg m^{-2}, CI: confidence interval.

Sparsity of data points as well as the complex pharmacokinetics were well handled by the population pharmacokinetic model as indicated by the GOF plots. A high volume of distribution is compatible with the extensive distribution of mitotane drug to adipose tissue (53). Moreover, high IIV associated with volume of distribution suggests a significant influence of individual patient characteristics. Individual patient demographics and lipid profiles were analyzed as possible sources of variability. While BMI was found to be a significant covariate for the volume of distribution, the reduction in IIV was marginal and individualization of therapy based on BMI seems not useful.

Our study has the particular strength of a uniform mode of measurement in regular time intervals and a large individual number of data points and corresponding clinical and laboratory data available. In comparison with a previous modeling effort (38) we come to a similar conclusion regarding high volume of distribution. Nevertheless, the published study has some important limitations although the data were informative

enough to develop a three-compartmental model. Thus, the estimate for absorption rate constant (0.005 hr^{-1}) corresponds to a physiologically implausible absorption half-life of 138 hours in that study. Importantly, this model does not take enzyme autoinduction into account. Empirical modeling approaches of metabolic autoinduction are frequently based on either of the two following approaches. The drug may be assumed to increase the rate of enzyme synthesis as demonstrated in case of rifampin, or it may decrease the rate of enzyme degradation as modeled in the case of ifosfamide (55, 56). Studies elucidating the mechanism of enzyme induction responsible for drug interactions concluded that mitotane increases gene expression of a number of transporters and enzymes, including CYP3A4 (57). Therefore, we assumed an increase in enzyme synthesis as an approach for modeling enzyme induction. An attempt was made to estimate a baseline value for mitotane clearance prior to any enzyme induction process but limited information in the initial phase of dosing precluded a reliable estimate. The sparsity of initial TDM data reflects the current practice of monitoring mitotane 3-4 weeks after the first dose. Therefore, the enzyme compartment which represented a time changing clearance of the drug was initialized to a baseline value of 1 (100%). With regard to the magnitude of mitotane induction of drug metabolizing enzymes, a limited parallel group comparison study revealed 18.3 fold and 5.0 fold decrease in midazolam (a CYP3A probe drug) and sunitinib AUCs (both administered orally) by mitotane, respectively (31). As a comparison, the very potent known CYP3A inducer rifampin caused a 4-fold reduction in oral sunitinib plasma exposure (58), while it decreased AUC of orally and intravenously administered CYP3A probe substrates by 10-20 fold and 1.9-3.5 fold respectively (33). The effect on intravenously administered CYP3A probe substrates reflects hepatic CYP3A induction. A reasonable estimate for maximal induction of hepatic CYP3A activity by mitotane may therefore be about 5-fold. The larger changes in mitotane clearance according to our empirical model (Fig. 4) suggest an additional induction of gut wall enzymes.

In order to quickly establish antitumor efficacy, it is imperative to attain target concentrations as early as possible. Previously, efforts have been made to develop an appropriate dosing regimen with mitotane considering ≥14 mg/L as the target concentration. Appropriate plasma levels can be ultimately achieved with a chronic dose from the beginning of treatment but at the expense of a lag time to achieve therapeutic concentrations (24). This period may be shortened with high loading dose regimens but

at the cost of a higher risk to attain potentially toxic concentrations (25). Studies indicating high variation in plasma concentration buildup suggest the involvement of factors other than the dosage regimen such as enzyme induction and differences in intestinal absorption due to dietary variation (26). Our model was not able to identify major sources of interindividual variability; therefore, an exact prediction of the individual required dose is not possible. Hence TDM remains essential for mitotane treatment. Simulations based on our model however were supportive of using the high dose regimen for the rapid attainment of therapeutic concentrations (Fig 5).

The current model is expected to be helpful for decision making in clinical management of ACC with mitotane. It can be used for *a posteriori* dose adjustments in patients using Maximum *a posteriori* (MAP) Bayesian methods (59) based on limited TDM measurements (two or three) to estimate individual pharmacokinetic parameters. MAP Bayesian approaches have proven their benefit in TDM of a number of anticancer drugs including methotrexate and carboplatin (60, 61). Another important aspect regarding decision making is the addition of cytotoxic chemotherapy in patients who are not predicted to attain therapeutic concentrations within a clinically useful time frame (e.g. 90 days) when using their individual maximum tolerated dose. Also, in a palliative setting where response to mitotane monotherapy is limited (6), optimal dosing may be supported when drug exposure related parameters are taken into account in addition to tissue based markers of response (10). From a research perspective, the model may be used to link mitotane pharmacokinetics to pharmacodynamic endpoints such as tumor growth inhibition.

The limitations of the evaluation related to retrospective nature of the present study suggest to design a prospective study for a more physiological and a more detailed description of mitotane pharmacokinetics. It would be desirable to (i) take more samples (e.g., 1 per day) during the initial build-up of plasma concentration; (ii) occasionally apply a dense sampling scheme including several samples within the first hour after dose during one dosing interval to describe mitotane absorption kinetics; (iii) evaluate the effect of additional covariates such as food intake, disease state and co-medications on mitotane pharmacokinetics, and (iv) to quantify enzyme induction during therapy by separate CYP3A probe drugs such as midazolam.

Conclusion

The proposed model appropriately describes plasma concentrations during chronic treatment with mitotane. It includes concentration dependent induction of metabolizing enzymes that considerably accelerates mitotane elimination. If tolerated, using the high dose regimen with a first TDM on day 16 of treatment might be a good treatment strategy. The model is a next important step to use pharmacokinetic modeling to improve personalized dose selection as well as establishing the timing of TDM, while more data are urgently needed.

Declaration of interest

We declare that there is no conflict of interest that could be perceived as prejudicing the impartiality of the research reported.

Funding

The study was supported by a scholarship grant from Higher Education Commission, Pakistan in collaboration with German Academic Exchange Program (DAAD), Germany (to U.A.), a fellowship by the Comprehensive Cancer Center Mainfranken (to M.K.) and an individual research grant by the German Research Council (FA 466/4-1, FA 466/4-2, KR 4371/1-1, KR 4371/1-2) to M.K. and M.F. and within the CRC/Transregio 205/1 “The Adrenal: Central Relay in Health and Disease“ to MK and MF.

Acknowledgments

We thank all patients and their families for contributing their data, Michaela Haaf and Henriette Herbst for data curation as part of the ENSAT registry.

References

1. Fassnacht M, Libé R, Kroiss M & Allolio B. Adrenocortical carcinoma: a clinician's update. *Nature Reviews Endocrinology* 2011 **7** 323–335.

2. Else T, Kim AC, Sabolch A, Raymond VM, Kandathil A, Caoili EM, Jolly S, Miller BS, Giordano TJ & Hammer GD. Adrenocortical carcinoma. *Endocrine Reviews* 2014 **35** 282–326.

3. Terzolo M, Angeli A, Fassnacht M, Daffara F, Tauchmanova L, Conton PA, Rossetto R, Buci L, Sperone P, Grossrubatscher E *et al*. Adjuvant mitotane treatment for adrenocortical carcinoma. *New England Journal of Medicine* 2007 **356** 2372–2380.

4. Berruti A, Grisanti S, Pulzer A, Claps M, Daffara F, Loli P, Mannelli M, Boscaro M, Arvat E, Tiberio G *et al*. Long-term outcomes of adjuvant mitotane therapy in patients with radically resected adrenocortical carcinoma. *The Journal of Clinical Endocrinology & Metabolism* 2017 **102** 1358–1365.

5. Temple TE, Jones DJ, Liddle GW & Dexter RN. Treatment of Cushing's disease. *New England Journal of Medicine* 1969 **281** 801–805.

6. Megerle F, Herrmann W, Schloetelburg W, Ronchi CL, Pulzer A, Quinkler M, Beuschlein F, Hahner S, Kroiss M & Fassnacht M. Mitotane monotherapy in patients with advanced adrenocortical carcinoma. *The Journal of Clinical Endocrinology & Metabolism* 2018 **103** 1686–1695.

7. Hescot S, Slama A, Lombes A, Paci A, Remy H, Leboulleux S, Chadarevian R, Trabado S, Amazit L, Young J *et al*. Mitotane alters mitochondrial respiratory chain activity by inducing cytochrome c oxidase defect in human adrenocortical cells. *Endocrine Related Cancer* 2013 **20** 371–381.

8. Cai W, Counsell RE, Djanegara T, Schteingart DE, Sinsheimer JE & Wotring LL. Metabolic activation and binding of mitotane in adrenal cortex homogenates. *Journal of Pharmaceutical Sciences* 1995 **84** 134–138.

9. Scheidt HA, Haralampiev I, Theisgen S, Schirbel A, Sbiera S, Huster D, Kroiss M & Müller P. The adrenal specific toxicant mitotane directly interacts with lipid membranes and alters membrane properties depending on lipid composition. *Molecular and Cellular Endocrinology* 2016 **428** 68–81.

10. Sbiera S, Leich E, Liebisch G, Sbiera I, Schirbel A, Wiemer L, Matysik S, Eckhardt C,

Gardill F, Gehl A *et al*. Mitotane inhibits sterol-O-acyl transferase 1 triggering lipid-mediated endoplasmic reticulum stress and apoptosis in adrenocortical carcinoma cells. *Endocrinology* 2015 **156** 3895–3908.

11. MOY RH. Studies of the pharmacology of o,p'DDD in man. *The Journal of laboratory and clinical medicine* 1961 **58** 296–304.

12. van Slooten H, van Seters AP, Smeenk D & Moolenaar AJ. O,p′-DDD (Mitotane) levels in plasma and tissues during chemotherapy and at autopsy. *Cancer Chemotherapy and Pharmacology* 1982 **9** 85–88.

13. Gebhardt DOE, Moolenaar AJ, van Seters AP, van der Velde EA & Gevers Leuven JA. The distribution ofo,p′-DDD (Mitotane) among serum lipoproteins in normo- and hypertriglyceridemia. *Cancer Chemotherapy and Pharmacology* 1992 **29** 331–334.

14. Hescot S, Seck A, Guerin M, Cockenpot F, Huby T, Broutin S, Young J, Paci A, Baudin E & Lombès M. Lipoprotein-free mitotane exerts high cytotoxic activity in adrenocortical carcinoma. *The Journal of Clinical Endocrinology & Metabolism* 2015 **100** 2890–2898.

15. Kroiss M, Plonné D, Kendl S, Schirmer D, Ronchi CL, Schirbel A, Zink M, Lapa C, Klinker H, Fassnacht M *et al*. Association of mitotane with chylomicrons and serum lipoproteins: practical implications for treatment of adrenocortical carcinoma. *European Journal of Endocrinology* 2016 **174** 343–353.

16. van Slooten H, Moolenaar AJ, van Seters AP & Smeenk D. The treatment of adrenocortical carcinoma with o,p'-DDD: prognostic implications of serum level monitoring. *European journal of cancer & clinical oncology* 1984 **20** 47–53.

17. Haak H, Hermans J, Velde C van de, Lentjes E, Goslings B, Fleuren GJ & Krans H. Optimal treatment of adrenocortical carcinoma with mitotane: results in a consecutive series of 96 patients. *British Journal of Cancer* 1994 **69** 947–951.

18. Baudin E, Pellegriti G, Bonnay M, Penfornis A, Laplanche A, Vassal G & Schlumberger M. Impact of monitoring plasma 1,1-dichlorodiphenildichloroethane (o,p?DDD) levels on the treatment of patients with adrenocortical carcinoma. *Cancer* 2001 **92** 1385–1392.

19. Hermsen IG, Fassnacht M, Terzolo M, Houterman S, Hartigh J den, Leboulleux S, Daffara F, Berruti A, Chadarevian R, Schlumberger M *et al*. Plasma Concentrations

of o,p′DDD, o,p′DDA, and o,p′DDE as Predictors of Tumor Response to Mitotane in Adrenocortical Carcinoma: Results of a Retrospective ENS@T Multicenter Study. *The Journal of Clinical Endocrinology & Metabolism* 2011 **96** 1844–1851.

20. Terzolo M, Baudin AE, Ardito A, Kroiss M, Leboulleux S, Daffara F, Perotti P, Feelders RA, DeVries JH, Zaggia B *et al*. Mitotane levels predict the outcome of patients with adrenocortical carcinoma treated adjuvantly following radical resection. *European Journal of Endocrinology* 2013 **169** 263–270.

21. Fassnacht M, Terzolo M, Allolio B, Baudin E, Haak H, Berruti A, Welin S, Schade-Brittinger C, Lacroix A, Jarzab B *et al*. Combination chemotherapy in advanced adrenocortical carcinoma. *New England Journal of Medicine* 2012 **366** 2189–2197.

22. Henning JEK, Deutschbein T, Altieri B, Steinhauer S, Kircher S, Sbiera S, Wild V, Schlötelburg W, Kroiss M, Perotti P *et al*. Gemcitabine-based chemotherapy in adrenocortical carcinoma: A Multicenter Study of Efficacy and Predictive Factors. *The Journal of Clinical Endocrinology & Metabolism* 2017 **102** 4323–4332.

23. Mauclère-Denost S, Leboulleux S, Borget I, Paci A, Young J, Al Ghuzlan A, Deandreis D, Drouard L, Tabarin A, Chanson P *et al*. High-dose mitotane strategy in adrenocortical carcinoma: Prospective analysis of plasma mitotane measurement during the first 3 months of follow-up. *European Journal of Endocrinology* 2012 **166** 261–268.

24. Terzolo M, Pia A, Berruti A, Osella G, Alì A, Carbone V, Testa E, Dogliotti L & Angeli A. Low-dose monitored mitotane treatment achieves the therapeutic range with manageable side effects in patients with adrenocortical cancer 1. *The Journal of Clinical Endocrinology & Metabolism* 2000 **85** 2234–2238.

25. Faggiano A, Leboulleux S, Young J, Schlumberger M & Baudin E. Rapidly progressing high o,p'DDD doses shorten the time required to reach the therapeutic threshold with an acceptable tolerance: preliminary results. *Clinical Endocrinology* 2006 **64** 110–113.

26. Kerkhofs TM, Baudin E, Terzolo M, Allolio B, Chadarevian R, Mueller HH, Skogseid B, Leboulleux S, Mantero F, Haak HR *et al*. Comparison of two mitotane starting dose regimens in patients with advanced adrenocortical carcinoma. *The Journal of Clinical Endocrinology & Metabolism* 2013 **98** 4759–4767.

27. Daffara F, De Francia S, Reimondo G, Zaggia B, Aroasio E, Porpiglia F, Volante M,

Termine A, Di Carlo F, Dogliotti L *et al*. Prospective evaluation of mitotane toxicity in adrenocortical cancer patients treated adjuvantly. *Endocrine Related Cancer* 2008 **15** 1043–1053.

28. Reif VD, Sinsheimer JE, Ward JC & Schteingart DE. Aromatic hydroxylation and alkyl oxidation in metabolism of mitotane (o,p'-DDD) in humans. *Journal of pharmaceutical sciences* 1974 **63** 1730–1736.

29. Sinsheimer JE, Guilford J, Bobrin LJ & Schteingart DE. Identification of o,p'-dichlorodiphenyl acetic acid as a urinary metabolite of 1-(o-chlorophenyl)-1-(p-chlorophenyl)-2,2-dichloroethane. *Journal of Pharmaceutical Sciences* 1972 **61** 314–316.

30. Mornar A, Sertić M, Turk N, Nigović B & Koršić M. Simultaneous analysis of mitotane and its main metabolites in human blood and urine samples by SPE-HPLC technique. *Biomedical Chromatography* 2012 **26** 1308–1314.

31. van Erp NP, Guchelaar HJ, Ploeger BA, Romijn JA, Hartigh JD & Gelderblom H. Mitotane has a strong and a durable inducing effect on CYP3A4 activity. *European Journal of Endocrinology* 2011 **164** 621–626.

32. Theile D, Haefeli WE & Weiss J. Effects of adrenolytic mitotane on drug elimination pathways assessed in vitro. *Endocrine* 2015 **49** 842–853.

33. Baneyx G, Parrott N, Meille C, Iliadis A & Lavé T. Physiologically based pharmacokinetic modeling of CYP3A4 induction by rifampicin in human: Influence of time between substrate and inducer administration. *European Journal of Pharmaceutical Sciences* 2014 **56** 1–15.

34. Chortis V, Taylor AE, Schneider P, Tomlinson JW, Hughes BA, O'Neil DM, Libé R, Allolio B, Bertagna X, Bertherat J *et al*. Mitotane therapy in adrenocortical cancer induces CYP3A4 and inhibits 5α-reductase, explaining the need for personalized glucocorticoid and androgen replacement. *The Journal of Clinical Endocrinology & Metabolism* 2013 **98** 161–171.

35. Moolenaar AJ, van Slooten H, van Seters AP & Smeenk D. Blood levels of o,p'-DDD following administration in various vehicles after a single dose and during long-term treatment. *Cancer chemotherapy and pharmacology* 1981 **7** 51–54.

36. Ihunnah CA, Jiang M & Xie W. Nuclear receptor PXR, transcriptional circuits and

metabolic relevance. *Biochimica et Biophysica Acta (BBA) - Molecular Basis of Disease* 2011 **1812** 956–963.

37. Sinz MW. Evaluation of pregnane X receptor (PXR)-mediated CYP3A4 drug-drug interactions in drug development. *Drug Metabolism Reviews* 2013 **45** 3–14.

38. Kerkhofs TMA, Derijks LJJ, Ettaieb H, den Hartigh J, Neef K, Gelderblom H, Guchelaar HJ & Haak HR. Development of a Pharmacokinetic model of mitotane. *Therapeutic Drug Monitoring* 2015 **37** 58–65.

39. Wickham H, Francois R, Henry L & Müller K. dplyr: A Grammar of Data Manipulati on 2017. [R package version 0.7.4]. Available from: https://CRAN.R-project.org/p ackage=dplyr

40. Wikham H. Easily Tidy Data with 'spread()' and 'gather()' Functions 2017. [R pack age tidyr version 0.8.0]. Available from: https://CRAN.R-project.org/package=tidy r

41. Grolemund G & Wickham H. Dates and Times Made Easy with lubridate. *Journal of Statistical Software* 2011 **40** 1–25.

42. Wickham H. ggplot2: Elegant Graphics for Data Analysis. Springer International Publishing 2016.

43. Zhang L, Beal SL & Sheiner LB. Simultaneous vs. sequential analysis for population PK/PD data I: best-case performance. *Journal of pharmacokinetics and pharmacodynamics* 2003 **30** 387–404.

44. Lindbom L, Ribbing J & Jonsson EN. Perl-speaks-NONMEM (PsN)—a Perl module for NONMEM related programming. *Computer Methods and Programs in Biomedicine* 2004 **75** 85–94.

45. Keizer RJ, van Benten M, Beijnen JH, Schellens JHM & Huitema ADR. Piraña and PCluster: A modeling environment and cluster infrastructure for NONMEM. *Computer Methods and Programs in Biomedicine* 2011 **101** 72–79.

46. Jonsson EN & Karlsson MO. Xpose--an S-PLUS based population pharmacokinetic/pharmacodynamic model building aid for NONMEM. *Computer methods and programs in biomedicine* 1999 **58** 51–64.

47. Cao Y & Jusko WJ. Applications of minimal physiologically-based pharmacokinetic

models. *J Pharmacokinet Pharmacodyn* 2012 **39** 711–723.

48. Brill MJE, Valitalo PAJ, Darwich AS, van Ramshorst B, van Dongen HP, Rostami-Hodjegan A, Danhof M & Knibbe CAJ. Semiphysiologically based pharmacokinetic model for midazolam and CYP3A mediated metabolite 1-OH-midazolam in morbidly obese and weight loss surgery patients. *CPT: Pharmacometrics and Systems Pharmacology* 2016 **5** 20–30.

49. Fassnacht M, Kroiss M & Allolio B. Update in adrenocortical carcinoma. *The Journal of Clinical Endocrinology & Metabolism* 2013 **98** 4551–4564.

50. Larumbe T, Soto C, Goyogana A, De Linares UL, Sesmero A, Vina V, Olmedo C, Garcia M, Roussel O & Munoz A. Severe hypertriglyceridemia in relation to toxic levels of mitotane in a patient with stage IV adrenocortical carcinoma (ACC). *Endocrine Abstracts* 2017 .

51. Schwartz JB. The Influence of sex on pharmacokinetics. *Clinical Pharmacokinetics* 2003 **42** 107–121.

52. Watson AD, Rijnberk A & Moolenaar AJ. Systemic availability of o,p'-DDD in normal dogs, fasted and fed, and in dogs with hyperadrenocorticism. *Research in veterinary science* 1987 **43** 160–165.

53. Paci A, Hescot S, Seck A, Jublanc C, Mercier L, Vezzosi D, Drui D, Quinkler M, Fassnacht M, Bruckert E *et al*. Dyslipidemia causes overestimation of plasma mitotane measurements. *Endocrinology, Diabetes & Metabolism Case Reports* 2016 .

55. Smythe W, Khandelwal A, Merle C, Rustomjee R, Gninafon M, Bocar Lo M, Sow OB, Olliaro PL, Lienhardt C, Horton J *et al*. A semimechanistic pharmacokinetic-enzyme turnover model for rifampin autoinduction in adult tuberculosis patients. *Antimicrobial agents and chemotherapy* 2012 **56** 2091–2098.

56. Kerbusch T, Huitema AD, Ouwerkerk J, Keizer HJ, Mathôt RA, Schellens JH & Beijnen JH. Evaluation of the autoinduction of ifosfamide metabolism by a population pharmacokinetic approach using NONMEM. *British journal of clinical pharmacology* 2000 **49** 555–561.

57. Takeshita A, Igarashi-Migitaka J, Koibuchi N & Takeuchi Y. Mitotane induces CYP3A4 expression via activation of the steroid and xenobiotic receptor. *Journal of*

Endocrinology 2013 **216** 297–305.

58. Bello C, Houk B, Sherman L, Misbah S, Sarapa N, Smeraglia J & Haung X. Effect of rifampin on the pharmacokinetics of SU11248 in healthy volunteers. *Journal of Clinical Oncology* 2005 **23** 3078–3078.

59. Rousseau A & Marquet P. Application of pharmacokinetic modelling to the routine therapeutic drug monitoring of anticancer drugs. *Fundamental & Clinical Pharmacology* 2002 **16** 253–262.

60. Pignon T, Lacarelle B, Duffaud F, Guillet P, Catalin J, Durand A & Favre R. Dosage adjustment of high dose methotrexate using Bayesian estimation: a comparative study of two different concentrations at the end of 8-h infusions. *Therapeutic Drug Monitoring* 1995 **17** 164–169.

61. Guillet P, Monjanel S, Nicoara A, Duffaud F, Lacarelle B, Baqarry-Liegey D, Durand A, Catalin J & Favre R. A Bayesian dosing method for carboplatin given by continuous infusion for 120h. *Cancer Chemotherapy and Pharmacology* 1997 **40** 143–149.

Chapter 5

Prediction of exposure driven myelotoxicity of continuous infusion 5-fluorouracil by a semi-physiological pharmacokinetic-pharmacodynamic model in gastrointestinal cancer patients

Usman Arshad[1], Su-arpa Ploylearmsaeng[1], Mats O. Karlsson[2], Oxana Doroshyenko[1], Dorothee Frank[1], Edgar Schömig[1], Sabine Kunze[3], Semih A. Güner[3], Roman Skripnichenko[3], Sami Ullah[1], Ulrich Jaehde[4], Alexander Jetter[5], Uwe Fuhr[1], Max Taubert[1].

Cancer Chemotherapy and Pharmacology 2020 [In press]

[1] University of Cologne, Faculty of Medicine and University Hospital Cologne, Center for Pharmacology, Department I of Pharmacology, Cologne, Germany

[2] Department of Pharmaceutical Biosciences, Uppsala University, Uppsala, Sweden

[3] University of Cologne, Faculty of Medicine and University Hospital Cologne, Department of Radiotherapy, Cologne, Germany

[4] Institute of Pharmacy, Clinical Pharmacy, University of Bonn, An der Immenburg 4, 53121, Bonn, Germany

[5] Department of Clinical Pharmacology and Toxicology, University Hospital Zurich, University of Zurich, Zürich, Switzerland

Abstract

Purpose: To describe 5-fluorouracil (5FU) pharmacokinetics, myelotoxicity and respective covariates using a simultaneous nonlinear mixed effect modelling approach.

Methods: Thirty patients with gastrointestinal cancer received 5FU 650 or 1000 mg/m^2/day as 5-days continuous venous infusion (14 of whom also received cisplatin 20 mg/m^2/day). 5FU and 5-fluoro-5,6-dihydrouracil (5FUH2) plasma concentrations were described by a pharmacokinetic model using NONMEM. Absolute leukocyte counts were described by a semi-mechanistic myelosuppression model. Covariate relationships were evaluated to explain the possible sources of variability in 5FU pharmacokinetics and pharmacodynamics.

Results: Total clearance of 5FU correlated with body surface area (BSA). Population estimate for total clearance was 249 L/h. Clearances of 5FU and 5FUH2 fractionally changed by 77% per m^2 difference from the median BSA. 5FU central and peripheral volumes of distribution were 5.56 L and 28.5 L, respectively. Estimated 5FUH2 clearance and volume of distribution were 121 L/h and 96.7 L, respectively. Baseline leukocyte count of 6.86×10^9/L, as well as mean leukocyte transit time of 281 h accounting for time delay between proliferating and circulating cells were estimated. The relationship between 5FU plasma concentrations and absolute leukocyte count was found to be linear. A higher degree of myelosuppression was attributed to combination therapy (slope=2.82 L/mg) with cisplatin as compared to 5FU monotherapy (slope=1.17 L/mg).

Conclusions: BSA should be taken into account for predicting 5FU exposure. Myelosuppression was influenced by 5FU exposure and concomitant administration of cisplatin.

Key words: *5-fluorouracil, pharmacokinetics, pharmacodynamics, pharmacogenetics, myelosuppression.*

Introduction

The pyrimidine antimetabolite 5-fluorouracil (5FU) is being used since decades for the treatment of gastrointestinal solid malignancies [1]. Dose, but also route and schedule of administration have been identified to influence 5FU pharmacokinetics (PK) and effects [2, 3]. Considerable variations in PK and toxicity are associated with a given 5FU dosing regimen [4]. Investigations have been carried out evaluating patient's factors to predict 5FU exposure, where a relationship between body surface area (BSA) and 5FU clearance (CL_{5FU}) was reported [3, 5]. CL_{5FU} was found to be lower in females [6] and at older age [5, 7]. Due to saturable hepatic degradation, 5FU PK is considered to be non-linear in nature [8]. Additionally, elimination of the drug was reported to be influenced by hepatic metastases [3] and by glomerular filtration rate as measured by creatinine clearance [6].

Being a prodrug, 5FU requires enzymatic activation. A small fraction of an administered dose is metabolised into cytotoxic nucleotides, while most of the drug is degraded to 5-fluoro-5,6-dihydrouracil (5FUH2) mainly by hepatic dihydropyrimidine dehydrogenase (DPD) [9]. Some rare variants of the highly polymorphic DPD gene (*DPYD)* are responsible for complete or partial loss of DPD activity, which is related to increased 5FU toxicity [10]. Belonging to the class of antimetabolites, 5FU inhibits thymidylate synthase (TS), ultimately leading to the impairment of DNA synthesis [11]. Polymorphisms in the gene encoding TS influence toxicity and response of 5FU based therapeutic regimens [12]. Methylenetetrahydrofolate reductase (MTHFR) is involved in formation of the reduced folate cofactor, which is required for the inhibition of TS. Genetic polymorphisms in the gene encoding MTHFR are associated with altered enzymatic activity, thereby influencing sensitivity towards 5FU [13].

5FU is commonly used in combination with other antineoplastic drugs and with radiotherapy. A therapeutic regimen known as FOLFIRINOX including 5FU, folinic acid, oxaliplatin and irinotecan is frequently employed for the treatment of colorectal and pancreatic cancer [14]. Another regimen, called de Gramont, includes a combination of 5FU and leucovorin (folinic acid) and has been reported to possess low toxicity profile, increased response rate and progression-free survival [15]. For oesophageal cancer, combination with cisplatin is one of the recommend drug treatments [16].

Approximately 10%–30% of 5FU treated patients experience severe treatment-related toxicity [17], where myelosuppression and mucositis have been reported as main dose limiting side effects in 5FU treatment [18]. Continuous infusions exhibit lower myelosuppression with greater efficacy and are considered superior over the bolus administrations [19]. Furthermore, 5FU has a narrow therapeutic index with severe toxicities tending to occur with AUC values >25 mg h/L during continuous venous infusion [20]. Therefore, therapeutic drug monitoring is considered valuable to achieve optimal 5FU exposure with minimal serious toxicity [21].

Semiphysiological myelosuppression models were developed in both animals and human beings to understand time course and extent of leukopenia following administration of cytotoxic antineoplastic drugs, thus facilitating the drug development and therapy [22]. Models incorporating white blood cell (WBC) count over time are helpful to predict the time (T_{nadir}) and depth (WBC_{nadir}) of lowest total WBC count and the duration of the recovery period in order to administer the next cycle of a regimen [23]. Efforts have been made to predict the time course of myelosuppression by 5FU in rats [24]. Population analysis was carried out for the hematological toxicity in breast cancer patients treated with combined 5FU, epirubicin and cyclophosphamide regimen [25] but such a study with 5FU monotherapy is lacking.

The objective of the present study was to describe the PK and associated variability of 5FU and its metabolite by developing an empirical model. Subsequently, it was aimed to establish the relationship between 5FU exposure and myelotoxicity through a semi-mechanistic PKPD model. The study was further focused towards the identification and quantitative description of covariates on 5FU PK and myelotoxicity, especially patient demographics and genotypes (*DPYD*, *MTHFR*, *TS*).

Methods

Patients and treatment plan

The study was approved by the Ethics Committee of the Medical Faculty of the University of Cologne, Germany (application number 02-171) and was conducted according to the Declaration of Helsinki and national and international legal stipulations and guidelines in 2002 to 2005 [26, 27]. Sample size was estimated using WinBiAS

(version 7.01, epsilon Verlag, Darmstadt, Germany) considering interindividual variability (IIV) in 5FU pharmacokinetics to be at least 30%. To assess the effect of a covariate on 5FU pharmacokinetics, assuming a linear coefficient of correlation ρ = 0.5477 (explaining a fraction of ρ^2 = 0.3 of variability) with a power of 90% and α = 0.05, n = 30 patients were required. To account for possible dropouts, thirty-three patients with colorectal or oesophageal cancer were planned to be enrolled in the study after the provision of written informed consent. Eligibility criteria included age ≥ 18 years; Karnofsky performance status ≥ 70%; life expectancy ≥ 3 months; adequate haematopoietic, hepatic, and renal function. Exclusion criteria were prior chemotherapy or radiotherapy, and concomitant drugs (not included in the chemotherapeutic regimen) known to interfere with 5FU PK and/or pharmacodynamics. The patients with colorectal cancer received 5FU 650 or 1000 mg/m^2/day as 24-hours continuous venous infusion for 5 days, and radiotherapy. The patients with oesophageal cancer additionally obtained cisplatin 20 mg/m^2/day for 5 days before, or together with 5FU administration. Any decision on treatment was made according to the clinical situation and was not influenced by the study. WBC count was evaluated once prior to and 1-3 times per week after 5FU administration, but prior to the second cycle starting on day 28, as the assessment of myelosuppression was aimed to be investigated under the influence of single cycle of treatment. Only the first cycle was monitored in each participant. Covariate data regarding patient demographics and essential laboratory values were collected prior to the treatment.

Genotyping

DNA was extracted from peripheral blood using the QIAamp DNA Blood Mini Kit (Qiagen, Hilden, Germany). For *DPYD* genotyping [28], PCR amplification of all 23 coding exons and exon-intron boundaries of the *DPYD* gene was carried out. PCR products were separated on 1.6% agarose gels, visualized with ethidium bromide and purified using a QIA quick Gel Extraction Kit (Qiagen, Hilden, Germany). Samples were sequenced on an ABI 3100 automated DNA sequencer (Applied Biosystems, Foster City, CA, USA). TS genotyping was carried by PCR amplification [29] of the *TS* promoter enhancer region containing the double and triple tandem repeats using the following primers: forward 5´AAAAGGCGCGCGGAAGGGGTCCT3´; reverse 5´TCCGAGCCGGCCACAGGCAT3´. A total of 32 cycles (94°C for 40 sec, 62°C for 40 sec and 72°C for 1 min) and extension at 72°C for

5 min were carried out following hot start at 94°C for 4 min. The PCR product was analyzed in a 3% agarose gel. The triple repeat (3R/3R) had a 144 bp PCR product, the double repeat (2R/2R) a 116 bp product. For *MTHFR* genotyping [30], the PCR reaction used forward primer 5´TGAAGGAGAAGGTGTCTGCGGGA3´ and reverse primer 5´AGGACGGTGCGCTGAGAGTG3´. Restriction fragment analysis was carried out using *Hinf* I (Fermentas, St. Leon-Rot, Germany). The C→T substitution at nucleotide 667 creates a *Hinf* I digestion site resulting in two fragments (175 bp and 23 bp) of the PCR product.

Table 1: Patient characteristics (n = 30)

Characteristics	**Value**
Sex (n male/ n female)	25/5
Median age, years (range)	59.5 (37-73)
Median Karnofsky performance status (range)	100% (100-100)
Tumour primary site (n)	
Oesophagus	14
Rectal	2
Colorectal	13
Anus	1
Median body height, m (range)	1.75 (1.61-1.86)
Median body weight, kg (range)	76 (46-111)
Median BMI, kg/m^2 (range)	24.2 (16.9-33.2)
Median BSA, m^2 (range)	1.95 (1.48-2.33)
Median baseline laboratory values (range)	
Haemoglobin (g/dL)	13.7 (10.1-16.6)
Platelet count (x10^3/uL)	277 (48-426)
Erythrocyte count (x10^6/uL)	4.6 (3.8-5.5)
Leukocyte count (x10^9/L)	6.90 (4.68-11.28)
Plasma albumin (g/dL)	42 (35-47)
Plasma ASAT (U/L)	18 (9-50)
Plasma ALAT (U/L)	15 (8-90)
Plasma γ-GT (U/L)	24 (13-81)
Plasma total bilirubin (mg/dL)	0.45 (0.4-0.5)
Plasma creatinine (mg/dL)	0.85 (0.44-1.06)
Comedication with cisplatin (n)	14

BSA = body surface area, BMI = body mass index, ASAT = aspartate aminotransferase, ALAT = alanine aminotransferase, γ-GT = gamma-glutamyl transferase

Analysis of 5FU and 5FUH2 plasma concentrations

Analytical grade reagents were purchased from Merck (Darmstadt, Germany). 5FU (Sigma, St. Louis, MO, USA) was purchased as crystalline form, pure > 95%, 5FUH2

(26.5% pure) was supplied by Syncom (Groningen, The Netherlands), and 5-chlorouracil (5-CU), the internal standard, was obtained from Arcos Organics (Geel, Belgium).

Blood samples (4.5 mL each) were withdrawn during the first cycle using Li^+-heparinized tubes pre-dose, 36, 48, and 108 hours after the start of 5FU infusion, at the end of infusion, and 5, 30, 60 and 90 min thereafter. The samples were immediately placed in an ice water bath and centrifugated at +4°C. Plasma was stored at -80°C until analysis. 5FU and 5FUH2 in plasma were quantified by reverse-phase HPLC method with UV detection. Briefly, 0.7 mL of plasma was mixed with 20 µL of 100 µg/mL 5-CU (internal standard) and extracted with 7 mL of isopropranol/ethyl acetate (5:95, v/v). Samples were mixed and centrifuged (3500 rpm, 10 min) to separate the organic phase, which was evaporated to dryness. The samples were reconstituted with 100 µL of 50 mM K_2HPO_4 (pH 4.0), and 40 µL were injected into the HPLC system. 5FU and 5FUH2 were separated on an Ultrasphere ODS C_{18} column (5 µm, 250x4.6 mm, Beckman Coulter, Brea, CA, USA). Elution was performed under gradient condition as follows: 50 mM K_2HPO_4 (A) for 17 min, acetonitrile (B) 0-50% over 1 min and maintained at 50% for 5 min; initial conditions were restored by decreasing B to 0% over 1 min, and the column was equilibrated with 100% A for 5 min. The chromatographic instrument was a Waters 2690 Separations Module (Waters, Milford, MA, USA) with a Waters 996 photodiode array detector. Detection of 5FU, 5FUH2 and 5-CU were carried out at 265, 220 and 270 nm, respectively. Data analysis was performed by the Millennium 2.1 software (Waters, Milford, MA, USA). The LLOQs were 0.005 and 0.01 µg/mL for 5FU and 5FUH2, respectively. The 5FU and 5FUH2 intra-assay coefficients of variation ranged from 0.34 to 7.15% and from 0.53 to 2.76%, respectively, while the inter-assay coefficients of variation for a 5-day validation were 0.1–3.4% and 2.3–9.0%, respectively.

Data analysis

Model development and selection criteria

R (version 3.2.3) was used for data manipulation and exploratory evaluation [31]. Population parameter estimates were obtained using first order conditional estimation with interaction (FOCE-I) algorithm in NONMEM 7.4.2 (ICON, Development Solutions, Elliot City, MD, USA) [32]. Model development process was aided by Perl-speaks-

NONMEM (PsN) toolkit (Version 4.7.0) [33]. IIV in model parameters was estimated assuming a log-normal distribution. Additive, proportional and combined error models were implemented to estimate residual unexplained variabilities (RUV) for 5FU and 5FUH2. Model selection/rejection was guided by decrease in objective function value (OFV) which was assumed to be chi-squared distributed ($p<0.05$, corresponding to a $\Delta OFV \geq 3.84$ given a change by one degree of freedom), diagnostic plots, scientific plausibility and precision of parameter estimates. Precision of population parameter estimates was assessed with the help of a bootstrap procedure using 1000 sample replicates.

Table 2: Allele frequencies of polymorphisms in the *DPYD* gene found in patients

Polymorphisms in the *DPYD* gene		**Effect (nucleotide change)**	**Wild-type (*n*)**	**Heterozygous mutant (*n*)**	**Homozygous mutant (*n*)**	**Allelic frequency (%)**
DPYD* nomenclature	**Exon**					
*DPYD*9A*	2	Cys29Arg (85T>C)	20	8	2	12/60 (20%)
-	6	Met166Val (496A>G)	22	8	0	8/60 (13.33%)
-	11	Glu412Glu (1236G>A)	29	1	0	1/60 (1.67%)
*DPYD*4*	13	Ser534Asn (1601G>A)	29	1	0	1/60 (1.67%)
*DPYD*5*	13	Ile543Val (1627A>G)	19	9	2	13/60 (21.67%)
*DPYD*6*	18	Val732Ile (2194G>A)	28	2	0	2/60 (3.33%)

DPYD = dihydropyrimidine dehydrogenase gene
*Source of nomenclature: Mcleod *et al.,* 1998 [45]

Pharmacokinetic analysis

An empirical compartmental model for 5FU was first developed and then expanded to a combined model incorporating 5FUH2 data. The drug was presumed to be eliminated from the central compartment where elimination was tested to follow either a linear behaviour or nonlinear Michaelis-Menten kinetics. The fraction of 5FU converted to 5FUH2 was fixed *a priori* to 0.85, according to the literature [6, 34]. PK parameters were estimated based on the absolute dose administered.

Pharmacodynamic analysis

The PD model was developed according to Friberg *et al* [24, 34] using simultaneous approach. The model was driven by 5FU plasma concentrations from the PK model and comprised a compartment of proliferating leukocytes (rate constant describing the proliferation of cells: k_{prol}), transit compartments representing leukocytes undergoing maturation (rate constant describing the transfer between transit compartments: k_{tr}) and a compartment of circulating leukocytes (rate constant describing the rate of exit from the circulating compartment: k_{circ}). Parameters were the baseline circulating leukocyte count ($Circ_0$) representing the number of cells prior to 5FU administration, mean transit time (MTT = [n +1] / $k_{tr,}$ where n denotes the number of transit compartments) and a parameter γ describing a negative feedback of circulating cells on the rate of self-renewal of the proliferative cells (feedback = $[Circ_0 / Circ]^{\gamma}$). The number of parameters to be estimated were minimized by assuming $k_{prol} = k_{tr} = k_{circ}$. 5FU plasma concentrations were assumed to inhibit the proliferation of leukocytes.

The drug effect (E_{drug}) on proliferating cells was assumed to be driven by individual predicted 5FU plasma concentrations (C_p) and was incorporated in to the model as $k_{prol} \times (1 - E_{drug})$. E_{drug} was either formulated as a linear model ($E_{drug} = slope \times C_p$) or a nonlinear model ($E_{drug} = E_{max} \times C_p / (EC_{50} + C_p)$).

Covariate analysis

Covariates tested in the PK analysis included demographics (age, weight, height, sex, body mass index, lean body weight, BSA); predose plasma concentrations of alanine

aminotransferase (ALT), aspartate aminotransferase (AST) γ-glutamyltransferase (γ-GT), and albumin; and *DPYD, TS*, and *MTHFR* genotypes. The effect of co-medication with cisplatin was tested on the slope of the linear effect model. Scientific plausibility was the primary basis for covariate pre-selection, while graphical evaluation (residuals and individual PK estimates versus covariates) was performed to assist the inclusion decision. A comparative analysis was carried out to assess any possible superiority of other indices representing body mass over the BSA such as BMI, LBW and allometric scaling with body weight.

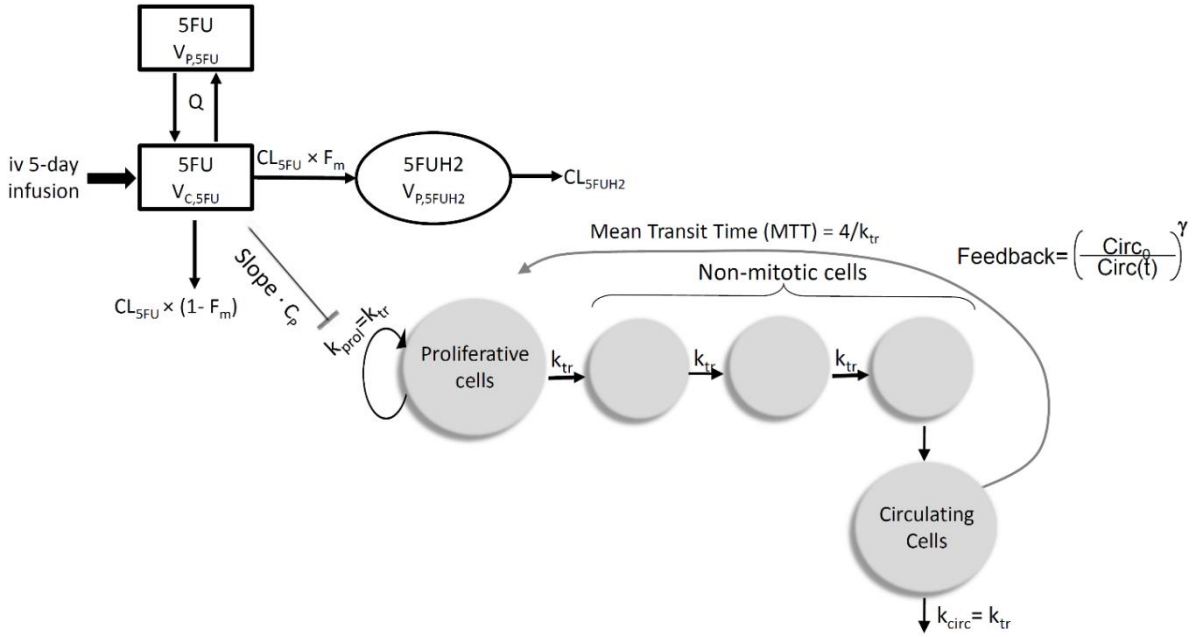

Fig. 1: Schematic representation of PKPD model. Compartments with white background reflect the PK model describing 5FU and 5FUH2 plasma concentrations, while those with grey background reflect the PD model describing total WBC count over time. k_{prol}: 1st order rate constant of proliferation, k_{tr}: 1st order rate constant of transit, k_{circ}: 1st order rate constant of elimination of circulating cells, $Circ_0$: baseline leucocyte count, γ: feedback parameter, C_p: 5FU plasma concentration, $V_{C,5FU}$: 5FU central volume of distribution, $V_{P,5FU}$: 5FU peripheral volume of distribution, CL_{5FU}: 5FU total clearance, Q: intercompartmental clearance, F_m: fraction of 5FU converted to 5FUH2, $V_{C,5FUH2}$: 5FUH2 central volume of distribution, CL_{5FUH2}: 5FUH2 clearance, drug effect: E_{drug}=slope · C_p.

Simulation design

The effect of concomitant cisplatin administration on leukocyte suppression was evaluated. WBC counts over time were simulated for virtual subjects receiving a 5 day

continuous infusion with and without cisplatin co-medication. WBC_{nadir} and T_{nadir} for the respective regimens were determined to assess the degree of myelosuppression.

Another simulation scenario aimed towards the comparative assessment of the time course of myelosuppression theoretically produced by the 5FU component contained in a single cycle of the two standard dosage regimens used in current clinical practice; to this end, the effects of the other components of the regimens were ignored. The standard FOLFIRINOX regimen combines oxaliplatin (85 mg/m^2 over 2 hours) with folinic acid (200 mg/m^2) followed by irinotecan (180 mg/m^2 over 90 min) and 5FU (400 mg/m^2 bolus) followed by 2400 mg/m^2 5FU over 46 h, all on day 1 and repeated every 2 weeks [14]. The de Gramont regimen is described as follows: high-dose folinic acid (200 mg/m^2) followed by 5FU i.v. bolus (300 mg/m^2) and continuous infusion (300 mg/m^2) on days 1, 2, 14 and 15, repeated every 4 weeks. In the absence of toxicity, 5-FU is increased to 400 mg/m^2 i.v. bolus and continuous infusion at course 2 and to 500 mg/m^2 at course 3 and from course 4 maintained at 500 mg/m^2 [15]. Simulated WBC_{nadir} and T_{nadir} were observed for treatment with FOLFIRINOX (400 mg/m^2 bolus 5FU followed by 2400 mg/m^2 5FU over 46 h) and de Gramont (5FU 300 mg/m^2 i.v. bolus followed by 300 mg/m^2 continuous infusion over 24 hrs) regimens.

Results

Patient characteristics

Thirty-three patients were included in the study; of these, 3 patients dropped out prior to the first administration of 5-FU. The remaining 30 patients who all completed the study comprised 5 women and 25 men with an age ranging between 37 and 73 years. 16 patients with colorectal cancer were administered 5FU only, while 14 with oesophageal cancer were treated with the combination of 5FU with cisplatin. Patient demographics, primary tumor location, pre-treatment values of haematology and clinical chemistry parameters are summarized in table 1.

Genotypes

Analysis of the *DPYD* gene revealed the presence of 6 polymorphisms in 22 of 30 patients. Eight patients had multiple mutations in the coding region of the *DPYD* gene

(table 2). None of the known rare (<2%) mutations causing extremely reduced or absent DPD activity, such as exon 14 (*DPYD*2A*) G>A skipping mutation [36] were found in the study population. The six *DPYD* polymorphisms detected in our study were considered to result in either normal (i.e. 1236G>A [37]) or partially reduced enzyme activity [38].

With regard to the *TS* genotype, 5 (16.7%) patients were homozygous for the triple repeat (3R/3R), 19 (63.3%) were heterozygous (2R/3R), and 6 (20%) were homozygous (2R/2R) for the double repeat variant within the *TS* promoter region. As for C677T *MTHFR* genotype, 13 of 30 patients (43.3%) were CC (wild-type), 12 (40%) - CT (heterozygous mutant), and 5 (16.7%) - TT (homozygous mutant).

Pharmacokinetic model

199 and 251 quantifiable plasma concentrations of 5FU and 5FUH2, respectively, were part of the pharmacokinetic model development. Fig. 1 provides a schematic representation of the PKPD model. A two-compartment model with linear elimination (ΔOFV of 210 compared to one-compartment model) best described the 5FU concentration-time data, and a one-compartment model was appropriate for the 5FUH2 data. IIV in the combined model was included for CL_{5FU}, CL_{5FUH2}, $V_{C,5FU}$ and $V_{C,5FUH2}$. IIV on $V_{P,5FU}$ was removed because of a high shrinkage value, while IIV on intercompartmental clearance (Q) was negligible and hence removed from the final model. A proportional error model was appropriate to model RUV for both 5FU and 5FUH2. Visual predictive checks (VPCs) indicated an adequate prediction of the 5FU and 5FUH2 concentrations by the model (fig. 2). Population pharmacokinetic parameter estimates are presented in table 3.

Pharmacodynamic model

In total, 135 observations for total WBC count were available for 29 patients. None of the patients received a WBC count-modifying drug (e.g. filgrastim). The semi-mechanistic model with three transit compartments adequately described the time course of myelosuppression (fig. 2). A linear model was preferred over an E_{max} model, as the E_{max} model did not provide any additional goodness-of-fit to describe the PK / PD relationship. The estimated parameter γ for the feedback mechanism was inconsistent across different runs and was therefore fixed to a value of 0.17 according to available

literature [22]. Fixing the parameter estimate for γ did not have a significant impact on the model fit (ΔOFV=3.68). IIV on MTT and slope were not kept in the final model as they displayed high shrinkage and provided no further improvement with ΔOFV values of 1.32 and 0.09, respectively. A proportional error model was found adequate to model RUV. Pharmacodynamic parameter estimates are presented in table 3.

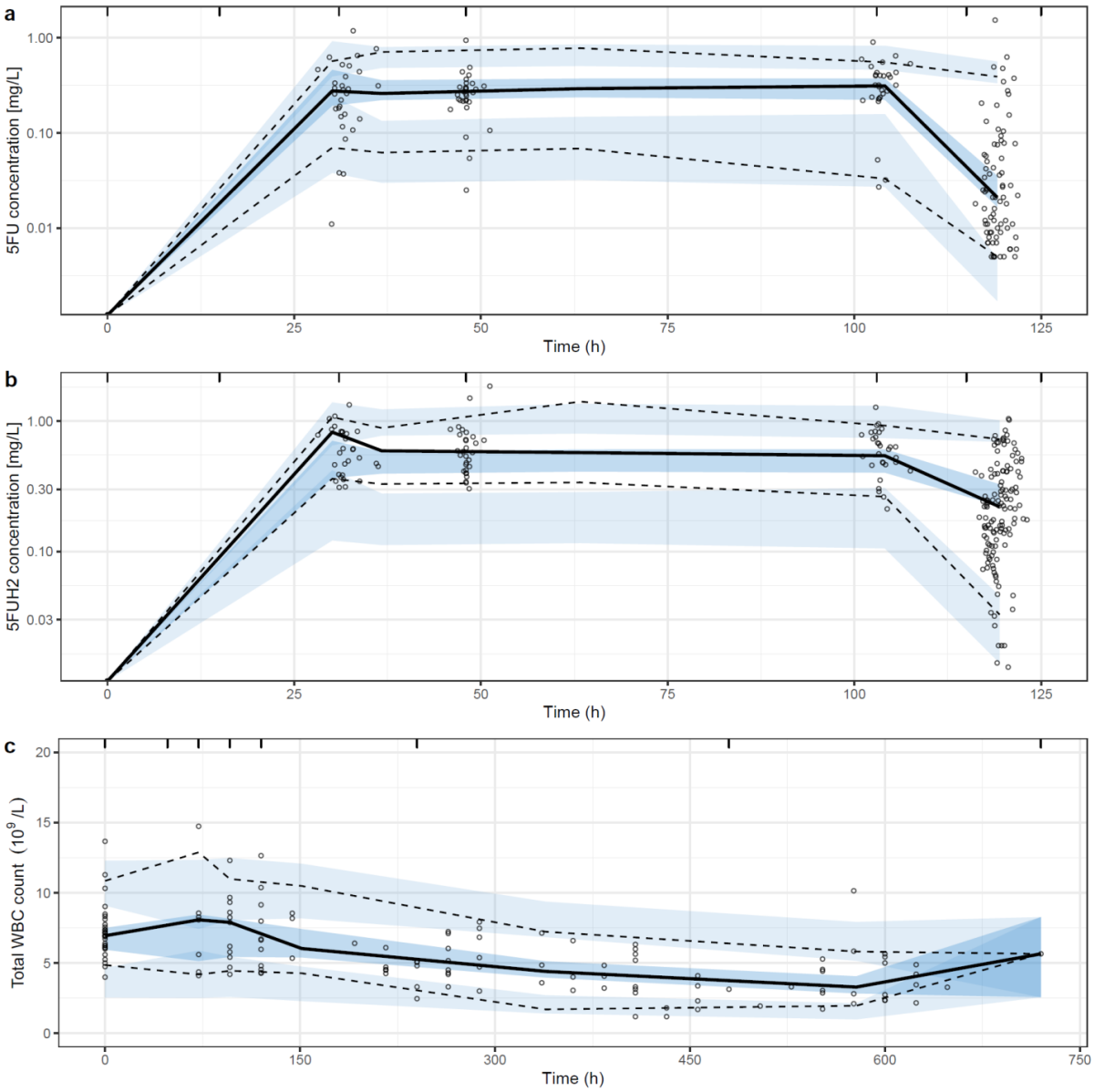

Fig. 2: Visual predictive checks for 5FU (a) and 5FUH2 (b) plasma concentration data and total WBC count (c) over time. Continuous and dashed lines represent median, 2.5th and 97.5th percentiles of the observed data. Shaded areas are the 95% confidence interval for median, 2.5th and 97.5th percentiles of the simulated data. 5FU and 5FUH2 plasma concentrations are presented on a log scale.

Covariate relationships

Estimated IIV in CL_{5FU} in the covariate-free model was 32.8% (CV), whereas a 9% reduction in IIV resulted from the inclusion of BSA as covariate. Scaling with BSA (ΔOFV=10.1) was found superior to that with LBW (ΔOFV=6.4), BMI (ΔOFV=4.3) and body weight (ΔOFV=5.0). CL_{5FU} point estimates were 263 L/h [231-295] and 175 L/h [87-263] in patients with wild-type *DPYD* genotype and homozygous mutations, respectively. Precision of these estimates was poor, and the effect of *DPYD* was not statistically significant, probably due to small number of mutations in the *DPYD* gene found in the studied population. IIV of CL_{5FU} was correlated to *MTHFR* genotype with a ΔOFV of 8.98, but the covariate effect was not included in the model because of limitations with regard to mechanistic plausibility. Scaling CL_{5FUH2} with individual BSA reduced OFV by 6.76 points with a marginal reduction in IIV (~2.1%). The estimate for BSA effect on CL_{5FUH2} (0.73 m^{-2}) was close to that on CL_{5FU} (0.79 m^{-2}), therefore the BSA effect was included as a single parameter in the final model assuming a similarity in disposition kinetics between 5FU and 5FUH2. Using single parameter instead of two separate parameters provided no significant change in model fit (ΔOFV = 0.35). Inclusion of cisplatin co-medication as a covariate upon slope parameter provided an improvement in model fit by reduction of 18.6 OFV points. Thus, the covariate relationships part of the PKPD model included effects of BSA on CL_{5FU} and CL_{5FUH2}, and of cisplatin comedication on slope.

Bootstrap analysis using the final PKPD model including the covariate relationships resulted in 681 runs with successful minimization, 318 runs with rounding errors, whereas only a single run failed during the execution. Parameter estimates obtained from bootstrapping were very close to NONMEM estimates (Table 3).

Simulated total WBC count over time

Differences in simulated WBC count over time for 5FU monotherapy ($5FU_{mono}$) and combination therapy ($5FU_{comb}$) are presented in fig. 3 (left panel). A higher degree of myelosuppression was observed for the typical individual receiving $5FU_{comb}$ in comparison to the individual receiving $5FU_{mono}$. Simulated temporal changes in total WBC count (fig. 3, right panel) showed a higher degree of myelosuppression for virtual

subjects administered with the higher 5FU exposure in FOLFIRINOX regimen in comparison to de Gramont regimen.

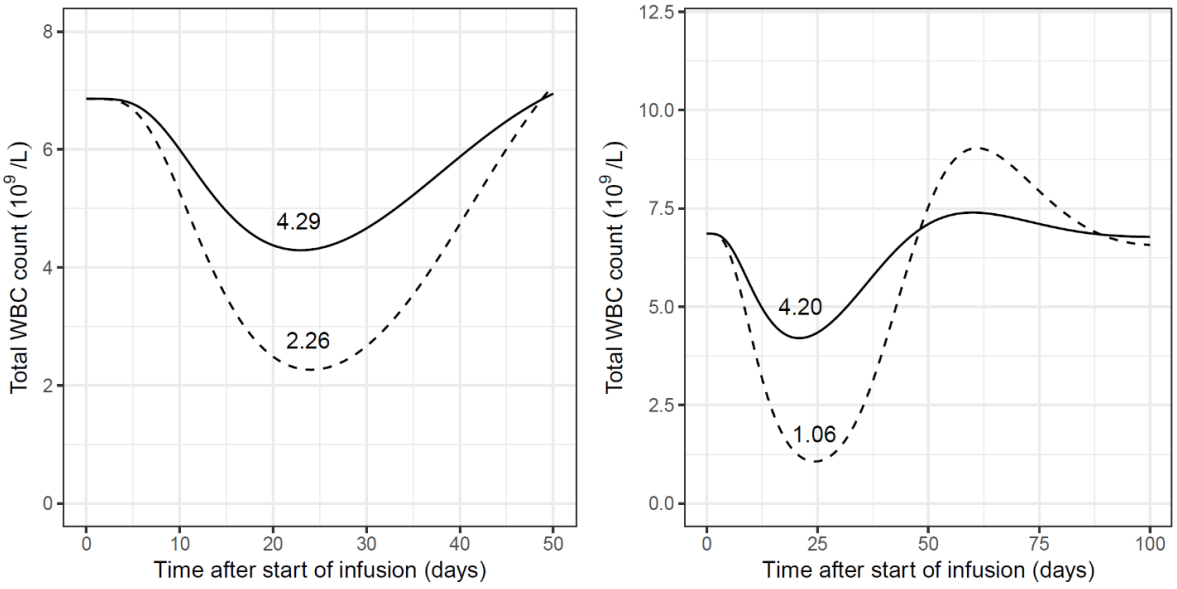

Fig. 3: Left panel; Simulated total WBC count over time. Continuous line represents individuals receiving5FU monotherapy. Dashed line represents individuals receiving combination therapy with 5FU and cisplatin. Numbers represent corresponding WBC_{nadir} values. **Right panel**: Simulated total WBC over time for effects attributable to a 5FU dose as used in the FOLFIRINOX (400 mg/m² bolus 5FU followed by 2400 mg/m² over 46 h) versus the de Gramont regimens (300 mg/m² i.v. bolus followed by 300 mg/m² continuous infusion over 24 hrs): Continuous lines represent an individual receiving 5FU according to de Gramont regimen, while dashed lines represent an individual receiving the dose according to FOLFIRINOX regimen. Effects apply for a single treatment course, and those of the other components of the respective regimens are ignored in this figure. Numbers represent corresponding WBC_{nadir} values.

Discussion

A semi-physiological PK/PD model of 5FU during continuous venous infusion was developed. Covariate effects including genetic variants of the main enzymes involved in 5FU PK and myelosuppression were tested. BSA was identified as a factor significantly influencing 5FU pharmacokinetics. Cisplatin co-administration was found to aggravate myelotoxicity. The current investigations are of particular value because they establish a link between 5FU PK and myelosuppression in the same patients, where we were also able to characterize the PD interaction between 5FU and cisplatin.

Approaches adapted to describe pharmacokinetics of 5FU have been nicely summarized by Deyme *et al* [14]. In most of the cases, a two-compartment model was found adequate to describe 5FU PK [3, 38, 39, 40], while some studies presented a one-compartment model [6, 41]. Most of these studies demonstrated a linear elimination [6, 38, 41], whereas a nonlinear elimination was also observed occasionally [3, 40]. Both linear and nonlinear elimination kinetics were reported in one case [40]. In the current evaluation, a two-compartment model with linear elimination was the best to describe 5-FU PK. CL_{5FU} of 249 L/h was comparable to the estimates obtained in similarly designed studies. Non-compartmental analysis with a 5-day continuous infusion estimated the CL_{5FU} to be 257 L/h [43], while an estimate of 270 L/h was reported for a 3-day continuous infusion [44]. Population pharmacokinetic analysis performed by Etienne *et al*. presented an estimate of 235 L/h, where the data was described by a one-compartment model with first order elimination [7].

BSA and C677T *MTHFR* genotype were significant covariates in our model. Despite the long-term use of BSA for 5FU dose individualization in clinical practice, existing studies provided conflicting results regarding suitability of BSA for prediction of 5FU exposure. Some studies did not report any significant relationship between BSA and 5FU exposure [7, 38, 44], while others considered BSA as the best predictor of CL_{5FU} [5]. In a PKPD study, principally aiming to describe hematological toxicity under a combination regimen with 5FU, neither BSA nor body weight were found to influence the variability in 5FU PK [46]. Significant, but moderate, effects of either BSA [3] or body weight [45] on 5FU PK were confirmed in most population pharmacokinetic studies using nonlinear mixed-effect modelling. In the comparative covariate analysis, none of the indices representing body mass provided superiority over BSA regarding the improvement of model fit principally guided by reduction in OFV and % IIV. Patient's gender was not found to influence CL_{5FU} in the present study, which is consistent with a previous population pharmacokinetic analysis [7]. Gender effect on CL_{5FU} observed in some studies [5, 41] might possibly be accounted for by differences in individual BSA. A considerably higher IIV of 145% was associated with $V_{c,5FU}$ in comparison to previously reported values ranging from 19% to 114% [6, 38, 39, 41]. The CL_{5FUH2} (126 L/h) and $V_{C,5FUH2}$ (91.9 L) estimates in our study were comparable to those reported by Mueller *et al*. [6]. An 18% higher CL_{5FUH2} in men was reported, but the gender influence is not supported by the present evaluation, probably because of the lower proportion of

female patients in the studied population. It is worth mentioning that exploratory covariate analyses in small to medium sized studies are expected to result in different sets of covariates, especially in case the covariates demonstrate moderate to high correlation such as body size, age, sex, creatinine clearance etc.

Table 3: Population pharmacokinetic and pharmacodynamic parameter estimates

Parameter	NONMEM Estimates	NONMEM RSE (%)	Bootstrap Estimates	Bootstrap RSE (%)	95% CI
5FU					
CL_{5FU} (L/h)	256	5.47	249	6.36	224-276
$V_{C,\,5FU}$ (L)	5.85	39.3	5.56	42.0	2.41-9.87
$V_{P,\,5FU}$ (L)	24.0	22.9	28.5	81.5	13.3-59.3
Q (L/h)	17.3	30.7	14.8	29.8	9.66-23.4
BSA effect (m^{-2})[a]	0.71	23.5	0.77	28.0	0.44-1.14
$AUC_{24,5FU}$ (mg h/L)[b]	6.72	-	6.72	-	4.76-8.74
5FUH2					
F_m (%)	85	-	85	-	Fixed
CL_{5FUH2} (L/h)	124	6.61	121	7.11	108-136
$V_{C,\,5FUH2}$ (L)	100	13.0	96.7	14.37	74.8-119
$AUC_{24,5FUH2}$ (mg h/L)[b]	12.2	-	12.2	-	7.12 - 19.2
Total WBC count					
$CIRC_0$ ($\times 10^9$/L)	7.16	5.23	6.86	4.50	6.38-7.37
MTT (h)	261	6.70	281	13.1	224-344
$Slope_{comb}$ (L/mg)	2.10	18.9	2.82	27.2	1.53-3.77
$Slope_{mono}$ (L/mg)	1.31	44.2	1.17	25.0	0.78-1.72
γ	0.17	-	0.17	-	Fixed
IIV (%CV)					
CL_{5FU}	24.9	17.2	23.0	43.1	12.3-30.1
$V_{C,\,5FU}$	130	45.4	145	57.0	75.3-204
CL_{5FUH2}	30.5	27.1	28.9	28.0	21.8-35.1
$V_{C,\,5FUH2}$	58.9	62.7	59.6	76.8	30.7-96.3
$CIRC_0$	16.8	69.6	16.4	52.0	8.29-22.8
RUV (σ2)					
Proportional error 5FU	0.36	10.2	0.32	9.37	0.23-0.44
Proportional error 5FUH2	0.14	8.06	0.14	9.61	0.10-0.18
Proportional error Total WBC count	0.08	8.70	0.08	8.97	0.06-0.11

RSE = relative standard error, CI = confidence interval, CL_{5FU} = total clearance of 5FU, $V_{C,\,5FU}$ = 5FU central volume of distribution, $V_{P,\,5FU}$ = 5FU peripheral volume of distribution, Q = intercompartmental clearance, BSA = body surface area, F_m = fraction of 5FU converted to 5FUH2, CL_{5FUH2} = clearance of 5FUH2, $CIRC_0$ = baseline leukocyte count, MTT = mean transit time, $Slope_{comb}$ = slope parameter for combination therapy with cisplatin, $Slope_{mono}$ = slope parameter for 5FU monotherapy, The "Slope" parameter represents the relationship between efffect and drug concentration into bone marrow (E_{drug}=slope×Cp), Cp = plasma concentration, IIV = interindividual variability, RUV = residual unexplained variability, CV = coefficient of variation.

[a] fractional change in CL per m^2 difference from median BSA value, [b] calculated by obtaining time integral of drug concentrations using an additional compartment in NONMEM.

The effect of the *MTHFR* C677T mutation on CL_{5FU} was found to be statistically significant. Population estimates for total clearance were 278 L/h (*MTHFR* 677CT or 677CC genotype) and 150 L/h (*MTHFR* 677TT genotype), but the genotype effect was not made part of the model due to lack of mechanistic plausibility as a predictor of 5FU PK. Published studies analysed this mutation primarily in relationship to 5FU efficacy and showed its favourable role in treatment response [47] and survival [48], considering the *MTHFR* genotype as an important predictor for the therapeutic effect of 5FU [49]. The common C677T polymorphism in the *MTHFR* gene results in a considerably lower enzyme activity [48] that probably increases intracellular folate concentrations, making tumors exhibiting mutated *MTHFR* genotypes more sensitive to cytotoxicity than wild-type *MTHFR* tumors [50], if there are no differences in *MTHFR* genotype between tumor and somatic cells of the patient. It is difficult to deduce plausible mechanisms describing the influence of *MTHFR* on CL_{5FU} based on the current knowledge on the metabolic pathways which provides a motivation to investigate this effect in further studies.

The Friberg model [24] is the standard approach to study the myelotoxicity under antineoplastic treatment. The model was originally developed using total WBCs count data from rats treated with 5FU. A subsequent study comprised of a number of myelosuppression models demonstrated parameter consistency across different drugs [35]. The developed models performed adequately to predict the time course of myelosuppression using both neutrophil and total leukocyte counts data separately. The semi-mechanistic myelosuppression model appropriately described the total WBC count over time after 5FU administration. Transit compartments accounted for a delay between drug administration and the observed effect. Self-renewal/mitosis in the proliferating cells compartment was dependent on the number of cells, a rate constant for cell division (k_{prol}), and a feedback mechanism from the circulating cells $(Circ_0/Circ)^{\gamma}$ which describes the rebound of cells as the proliferation rate is regulated by endogenous growth factors and cytokines [51]. An estimate of 6.86×10^9/L for baseline leukocyte count ($Circ_0$) was in the expected range [22]. The Parameter estimates for γ (indicative of hematopoietic viability) were highly inconsistent across model runs; therefore, the value representative of a typical population was fixed according to the available literature [22] in order to avoid an overshoot compared to $Circ_0$. Myelosuppression was found to be significantly higher in patients receiving additional cisplatin (slope=2.82

L/mg) as compared to the patients undergoing monotherapy (slope=1.17 L/mg). In an attempt using a semi-physiological model to describe the relationship between the PK and the myelotoxicity contributed by respective components of the combination regimen comprised of 5FU, epirubicin and cyclophosphamide, the authors assumed negligible contribution by 5FU as it was not possible to estimate the effect contributed by 5FU and cyclophosphamide simultaneously [25]. The hypotheses underlying this strong assumption was a lower hematological toxicity observed with continuous infusions as compared to 5FU bolus administration [52], and a relatively stronger myelosuppression previously reported with epirubicin and cyclophosphamide in comparison to 5FU in rats [53]. When 5FU is investigated alone, the present results demonstrate a significant amount of myelosuppression related to 5FU continuous infusion with WBC_{nadir} values of 2.26 ($\times 10^9$) and 4.29 ($\times 10^9$) in patients receiving $5FU_{comb}$ and $5FU_{mono}$ regimens, respectively. T_{nadir} is typically expected between day 9 and day 14 with 5FU, however the simulated T_{nadir} in the present study was observed between day 22 to day 25 after start (=17 to 20 days after end) of infusion, which may possibly be attributed to the continuous nature of the infusion.

A comparative evaluation of the theoretical contribution of a 5FU dose to myelosuppression expectedly predicted a more pronounced effect for the higher dose administered in the FOLFIRINOX regimen in comparison to de Gramont regimen. Although, hematological toxicities in case of combination based regimens are often additive in nature [53, 54, 55], a true prediction of the time course of myelosuppression under these therapeutic regimens may demands the incorporation of the effect of the other components, especially leucovorin, as one may expect differences in WBC_{nadir} and T_{nadir}. Nevertheless, the simulations nicely show that just the FU component of even a single treatment course would put a considerable fraction of patients at risk for infections, as these doses are repeated every other week. Model based prediction of WBC_{nadir} and T_{nadir} along with monitoring during the course of treatment can be imperative for suitable sampling schedules, assessment of the patient's immune competence, and the expected consequence of additional treatment cycles [23]. Thus, it would be interesting to develop myelotoxicity models for 5-FU incorporating the effect of leucovorin in present regimens. Predictions may further be useful to identify patients or patient subgroups at a higher risk of toxicity.

Conclusions

A semi-physiological PKPD model of 5FU is presented. IIV in the CL_{5FU} was partially explained by individual BSA. Frequent leukocyte count monitoring and model based predictions may be used to take the contribution of 5-FU to myelosuppression into account, especially in case of polychemotherapy regimens.

Acknowledgements

The authors are thankful to all the patients and their families for their contribution. The study was supported by a PhD scholarship (to UA) from the Higher Education Commission, Pakistan, in collaboration with the German Academic Exchange Service, Germany.

Conflict of interest

The authors declare that there is no conflict of interest.

References

1. Capitain O, Boisdron-Celle M, Poirier A-L, et al (2008) The influence of fluorouracil outcome parameters on tolerance and efficacy in patients with advanced colorectal cancer. Pharmacogenomics J 8:256–267. https://doi.org/10.1038/sj.tpj.6500476

2. Kosmas C, Kallistratos MS, Kopterides P, et al (2007) Cardiotoxicity of fluoropyrimidines in different schedules of administration: a prospective study. J Cancer Res Clin Oncol 134:75–82. https://doi.org/10.1007/s00432-007-0250-9

3. Terret C, Erdociain E, Guimbaud R, et al (2000) Dose and time dependencies of 5-fluorouracil pharmacokinetics. Clin Pharmacol Ther 68:270–279. https://doi.org/10.1067/mcp.2000.109352

4. Lee JJ, Beumer JH, Chu E (2016) Therapeutic drug monitoring of 5-fluorouracil. Cancer Chemother Pharmacol 78:447–464. https://doi.org/10.1007/s00280-016-3054-2

5. Port RE, Daniel B, Ding RW, Herrmann R (1991) Relative importance of dose, body surface area, sex, and age for 5-fluorouracil clearance. Oncology 48:277–81. https://doi.org/10.1159/000226942

6. Mueller F, Büchel B, Köberle D, et al (2013) Gender-specific elimination of continuous-infusional 5-fluorouracil in patients with gastrointestinal malignancies: results from a prospective population pharmacokinetic study. Cancer Chemother Pharmacol 71:361–370. https://doi.org/10.1007/s00280-012-2018-4

7. Etienne M-C, Chatelut E, Pivot X, et al (1998) Co-variables influencing 5-fluorouracil clearance during continuous venous infusion. A NONMEM analysis. Eur J Cancer 34:92–97. https://doi.org/10.1016/S0959-8049(97)00345-6

8. Bouché O, Laurent-Puig P, Boisdron-Celle M, et al (2013) 5-fluorouracile : MSI, pharmacocinétique, DPD, TYMS et MTHFR. Médecine Personnal en cancérologie Dig 75–92. https://doi.org/10.1007/978-2-8178-0527-6_6

9. Diasio RB, Harris BE (1989) Clinical Pharmacology of 5-Fluorouracil. Clin Pharmacokinet 16:215–237. https://doi.org/10.2165/00003088-198916040-00002

10. van Kuilenburg AB. (2004) Dihydropyrimidine dehydrogenase and the efficacy and toxicity of 5-fluorouracil. Eur J Cancer 40:939–950. https://doi.org/10.1016/J.EJCA.2003.12.004

11. Köhne CH, Peters GJ (2000) UFT: Mechanism of drug action. Oncology 14:13–18. https://doi.org/10.1201/9781315383293-2

12. Pullarkat ST, Lenz HJ (2001) Thymidylate synthase gene polymorphism determines response and toxicity of 5-FU chemotherapy. Pharmacogenomics J 1:65–70. https://doi.org/10.1038/sj.tpj.6500012

13. Etienne-Grimaldi M-C, Francoual M, Formento J-L, Milano G (2007) Methylenetetrahydrofolate reductase *(MTHFR)* variants and fluorouracil-based treatments in colorectal cancer. Pharmacogenomics 8:1561–1566. https://doi.org/10.2217/14622416.8.11.1561

14. Deyme L, Barbolosi D, Gattacceca F (2018) Population pharmacokinetics of FOLFIRINOX: a review of studies and parameters. Cancer Chemother Pharmacol 83:27–42. https://doi.org/10.1007/s00280-018-3722-5

15. Hanna CL, McKinna FE, Williams LB, et al (1995) High-dose folinic acid and 5-fluorouracil bolus and continuous infusion in advanced colorectal cancer: Poor response rate in unselected patients. Br J Cancer 72:774–776. https://doi.org/10.1038/bjc.1995.409

16. Tepper J, Krasna MJ, Niedzwiecki D, et al (2008) Phase III Trial of Trimodality Therapy With Cisplatin, Fluorouracil, Radiotherapy, and Surgery Compared With Surgery Alone for Esophageal Cancer: CALGB 9781. J Clin Oncol 26:1086–1092. https://doi.org/10.1200/JCO.2007.12.9593

17. Meulendijks D, Henricks LM, Jacobs BAW, et al (2017) Pretreatment serum uracil concentration as a predictor of severe and fatal fluoropyrimidine-associated

toxicity. Br J Cancer 116:1415–1424. https://doi.org/10.1038/bjc.2017.94

18. Garg MB, Lincz LF, Adler K, et al (2012) Predicting 5-fluorouracil toxicity in colorectal cancer patients from peripheral blood cell telomere length: a multivariate analysis. Br J Cancer 107:1525–33. https://doi.org/10.1038/bjc.2012.421

19. Macdonald JS (1999) Toxicity of 5-fluorouracil. Oncology (Williston Park) 13:33–34

20. Alnaim L (2010) Individualization of 5-Fluorouracil in the Treatment of Colorectal Cancer. SRX Pharmacol 2010:1–12. https://doi.org/10.3814/2010/352491

21. Wilhelm M, Mueller L, Miller MC, et al (2016) Prospective, Multicenter Study of 5-Fluorouracil Therapeutic Drug Monitoring in Metastatic Colorectal Cancer Treated in Routine Clinical Practice. Clin Colorectal Cancer 15:381–388. https://doi.org/10.1016/j.clcc.2016.04.001

22. Soto E, Keizer RJ, Trocóniz IF, et al (2011) Predictive ability of a semi-mechanistic model for neutropenia in the development of novel anti-cancer agents: two case studies. Invest New Drugs 29:984–995. https://doi.org/10.1007/s10637-010-9437-z

23. Netterberg I, Nielsen EI, Friberg LE, Karlsson MO (2017) Model-based prediction of myelosuppression and recovery based on frequent neutrophil monitoring. Cancer Chemother Pharmacol 80:343–353. https://doi.org/10.1007/s00280-017-3366-x

24. Friberg LE, Freijs A, Sandstrom M, Karlsson MO (2000) Semiphysiological model for the time course of leukocytes after varying schedules of 5-fluorouracil in rats. J Pharmacol Exp Ther 295:734–740

25. Sandström M, Lindman H, Nygren P, et al (2006) Population analysis of the pharmacokinetics and the haematological toxicity of the fluorouracil-epirubicin-cyclophosphamide regimen in breast cancer patients. Cancer Chemother Pharmacol 58:143–156. https://doi.org/10.1007/s00280-005-0140-2

26. The Declaration of Helsinki, as established by the 18th WMA General Assembly, Helsinki, Finland, June 1964 and amended by the 52nd WMA General Assembly, Edinburgh, Scotland, October 2000. Fortaleza (Brazil)

27. German Drug Act (Arzneimittelgesetz). Available at https://www.gesetze-im-internet.de/amg_1976/. Applicable version: Elftes Gesetz zur Änderung des Arzneimittelgesetzes vom 21. August 2002/BGBl. I, S. 3348.

28. Lazar A, Mau-Holzmann UA, Kolb H, et al (2004) Multiple Organ Failure due to 5-Fluorouracil Chemotherapy in a Patient with a Rare Dihydropyrimidine Dehydrogenase Gene Variant. Oncol Res Treat 27:559–562. https://doi.org/10.1159/000081338

29. Iacopetta B, Grieu F, Joseph D, Elsaleh H (2001) A polymorphism in the enhancer region of the thymidylate synthase promoter influences the survival of colorectal cancer patients treated with 5-fluorouracil. Br J Cancer 85:827–830. https://doi.org/10.1054/bjoc.2001.2007

30. Shrubsole MJ, Gao Y-T, Cai Q, et al (2004) MTHFR polymorphisms, dietary folate intake, and breast cancer risk: results from the Shanghai Breast Cancer Study. Cancer Epidemiol Biomarkers Prev 13:190–196. https://doi.org/10.1158/1055-9965.epi-03-0273

31. R Core Team (2018) R: a language and environment for statistical computing. In: R Found. Stat. Comput. Vienna, Austria.

32. Zhang L, Beal SL, Sheiner LB (2003) Simultaneous vs. Sequential Analysis for Population PK/PD Data I: Best-Case Performance. J Pharmacokinet Pharmacodyn 30:387–404. https://doi.org/10.1023/B:JOPA.0000012998.04442.1f

33. Lindbom L, Ribbing J, Jonsson EN (2004) Perl-speaks-NONMEM (PsN)—a Perl module for NONMEM related programming. Comput Methods Programs Biomed 75:85–94. https://doi.org/10.1016/j.cmpb.2003.11.003

34. Ezzeldin H, Diasio R (2004) Dihydropyrimidine dehydrogenase deficiency, a pharmacogenetic syndrome associated with potentially life-threatening toxicity

following 5-fluorouracil administration. Clin Colorectal Cancer 4:181–189. https://doi.org/10.3816/ccc.2004.n.018

35. Friberg LE, Henningsson A, Maas H, et al (2002) Model of chemotherapy-induced myelosuppression with parameter consistency across drugs. J Clin Oncol 20:4713–4721. https://doi.org/10.1200/JCO.2002.02.140

36. Van Kuilenburg ABP, Muller EW, Haasjes J, et al (2001) Lethal outcome of a patient with a complete dihydropyrimidine dehydrogenase (DPD) deficiency after administration of 5-fluorouracil: Frequency of the common IVS14+1G>A mutation causing DPD deficiency. Clin Cancer Res 7:1149–1153

37. Seck K, Riemer S, Kates R, et al (2005) Analysis of the DPYD gene implicated in 5-fluorouracil catabolism in a cohort of Caucasian individuals. Clin Cancer Res 11:5886–5892. https://doi.org/10.1158/1078-0432.CCR-04-1784

38. Ploylearmsaeng S, Fuhr U, Jetter A (2006) How may Anticancer Chemotherapy with Fluorouracil be Individualised? Clin Pharmacokinet 45:567–592. https://doi.org/10.2165/00003088-200645060-00002

39. Porta-Oltra B, Pérez-Ruixo J, Climente-Martí M, et al (2004) Population pharmacokinetics of 5-fluorouracil in colorectal cancer patients. J Oncol Pharm Pract 10:155–167. https://doi.org/10.1191/1078155204jp129oa

40. Woloch C, Di Paolo A, Marouani H, et al (2012) Population Pharmacokinetic Analysis of 5-FU and 5-FDHU in Colorectal Cancer Patients: Search for Biomarkers Associated with Gastro-Intestinal Toxicity. Curr Top Med Chem 12:1713–1719. https://doi.org/10.2174/156802612803531414

41. van Kuilenburg ABP, Häusler P, Schalhorn A, et al (2012) Evaluation of 5-Fluorouracil Pharmacokinetics in Cancer Patients with a C.1905+1G>A Mutation in DPYD by Means of a Bayesian Limited Sampling Strategy. Clin Pharmacokinet 51:163–174. https://doi.org/10.1007/BF03257473

42. Bressolle F, Joulia JM, Pinguet F, et al (1999) Circadian rhythm of 5-fluorouracil population pharmacokinetics in patients with metastatic colorectal cancer. Cancer

Chemother Pharmacol 44:295–302. https://doi.org/10.1007/s002800050980

43. Fleming RA, Milano GA, Etienne MC, et al (1992) No effect of dose, hepatic function, or nutritional status on 5-fu clearance following continuous (5-day), 5-fu infusion. Br J Cancer 66:668–672. https://doi.org/10.1038/bjc.1992.335

44. Grem JL, McAtee N, Balis F, et al (1993) A phase II study of continuous infusion 5-fluorouracil and leucovorin with weekly cisplatin in metastatic colorectal carcinoma. Cancer 72:663–668. https://doi.org/10.1002/1097-0142(19930801)72:3<663::AID-CNCR2820720307>3.0.CO;2-V

45. Climente-Martí M, Merino-Sanjuán M, Almenar-Cubells D, Jiménez-Torres NV (2003) A Bayesian Method for Predicting 5-Fluorouracil Pharmacokinetic Parameters Following Short-Term Infusion in Patients With Colorectal Cancer. J Pharm Sci 92:1155–1165. https://doi.org/10.1002/JPS.10374

46. Sandström M, Lindman H, Nygren P, et al (2006) Population analysis of the pharmacokinetics and the haematological toxicity of the fluorouracil-epirubicin-cyclophosphamide regimen in breast cancer patients. Cancer Chemother Pharmacol 58:143–156. https://doi.org/10.1007/s00280-005-0140-2

47. Etienne-Grimaldi M-C, Milano G, Maindrault-Goebel F, et al (2010) Methylenetetrahydrofolate reductase (MTHFR) gene polymorphisms and FOLFOX response in colorectal cancer patients. Br J Clin Pharmacol 69:58–66. https://doi.org/10.1111/j.1365-2125.2009.03556.x

48. Etienne MC, Formento JL, Chazal M, et al (2004) Methylenetetrahydrofolate reductase gene polymorphisms and response to fluorouracil-based treatment in advanced colorectal cancer patients. Pharmacogenetics 14:785–792. https://doi.org/10.1097/00008571-200412000-00001

49. Schwab M, Zanger UM, Marx C, et al (2008) Role of genetic and nongenetic factors for fluorouracil treatment-related severe toxicity: a prospective clinical trial by the German 5-FU Toxicity Study Group. J Clin Oncol 26:2131–2138. https://doi.org/10.1200/JCO.2006.10.4182

50. Gusella M, Ferrazzi E, Ferrari M, Padrini R (2002) New limited sampling strategy for determining 5-fluorouracil area under the concentration-time curve after rapid intravenous bolus. Ther Drug Monit 24:425–431. https://doi.org/10.1097/00007691-200206000-00016

51. Takatani H, Soda H, Fukuda M, et al (1996) Levels of recombinant human granulocyte colony-stimulating factor in serum are inversely correlated with circulating neutrophil counts. Antimicrob Agents Chemother 40:988–991. https://doi.org/10.1128/aac.40.4.988

52. Hansen RM, Ryan L, Anderson T, et al (1996) Phase III Study of Bolus Versus Infusion Fluorouracil With or Without Cisplatin in Advanced Colorectal Cancer. J Natl Cancer Inst 88:668–674. https://doi.org/10.1093/jnci/88.10.668

53. De Brulin EA, Driessen OMJ, Hermans J (1991) The CMF-regimen. Toxicity patterns following stepwise combinations of cyclophosphamide, methotrexate and fluorouracil. Int J Cancer 48:67–72. https://doi.org/10.1002/ijc.2910480113

54. Sandström M, Lindman H, Nygren P, et al (2005) Model Describing the Relationship Between Pharmacokinetics and Hematologic Toxicity of the Epirubicin-Docetaxel Regimen in Breast Cancer Patients. J Clin Oncol 23:413–421. https://doi.org/10.1200/JCO.2005.09.161

55. Zandvliet AS, Schellens JHM, Dittrich C, et al (2008) Population pharmacokinetic and pharmacodynamic analysis to support treatment optimization of combination chemotherapy with indisulam and carboplatin. Br J Clin Pharmacol 66:485–97. https://doi.org/10.1111/j.1365-2125.2008.03230.x

56. Zandvliet AS, Siegel-Lakhai WS, Beijnen JH, et al (2008) PK/PD model of indisulam and capecitabine: interaction causes excessive myelosuppression. Clin Pharmacol Ther 83:829–39. https://doi.org/10.1038/sj.clpt.6100344

Supplementary material

Supplementary Fig. 1: Goodness of fit plots for 5FU; observed vs individual predicted (IPRED) concentration (mg/L) (A); observed vs population predicted (PRED) concentrations (B); conditional weighted residuals (CWRES) vs population predicted concentrations (C); conditional weighted residuals vs time after first dose (D). Continuous line represents the line of unity (A & B) and zero line (C & D), while dashed lines are the lines of smooth.

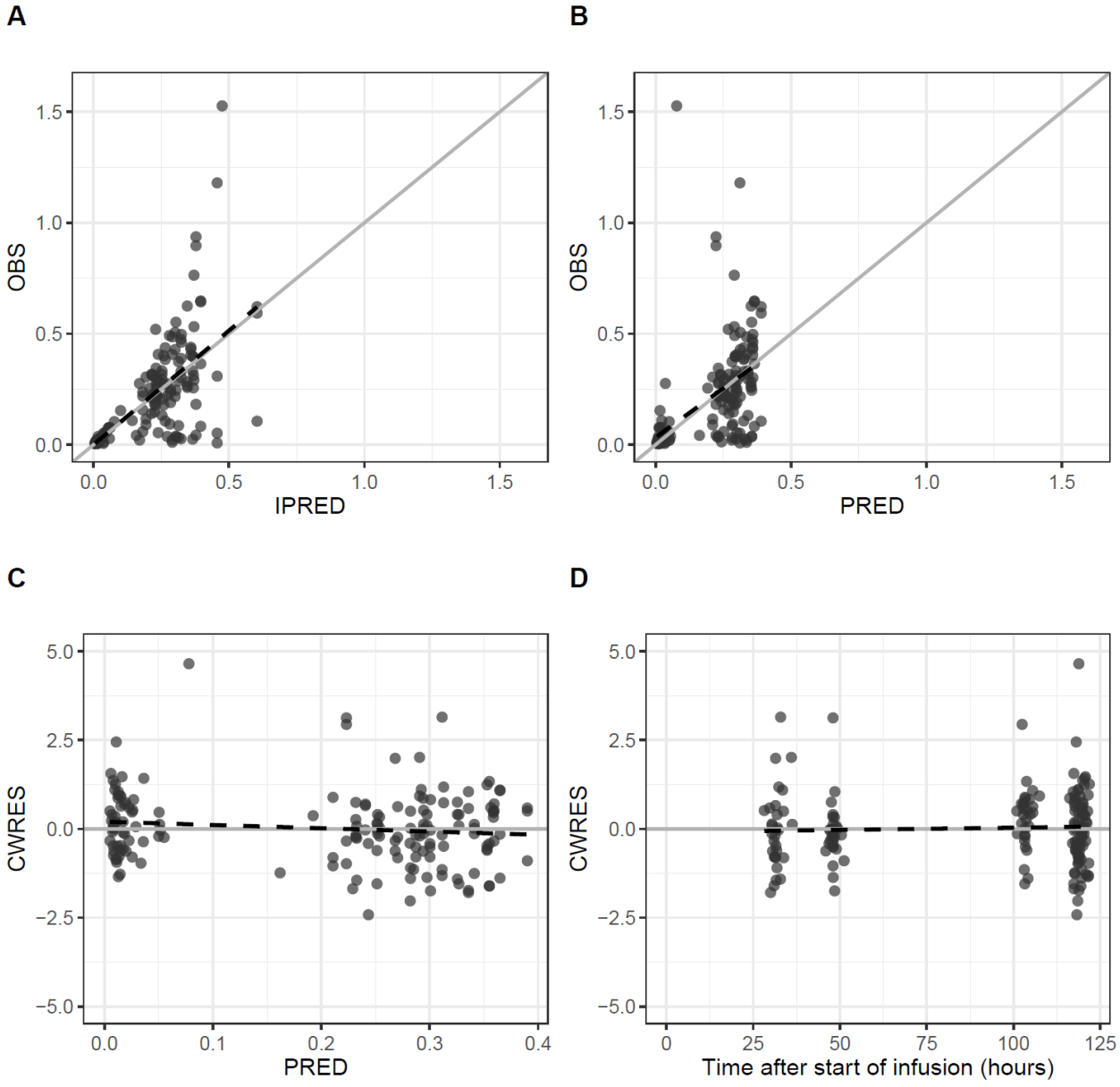

Supplementary Fig. 2: Goodness of fit plots for 5FUH2; observed vs individual predicted (IPRED) concentration (mg/L) (A); observed vs population predicted (PRED) concentrations (B); conditional weighted residuals (CWRES) vs population predicted concentrations (C); conditional weighted residuals vs time after first dose (D). Continuous line represents the line of unity (A & B) and zero line (C & D), while dashed lines are the lines of smooth.

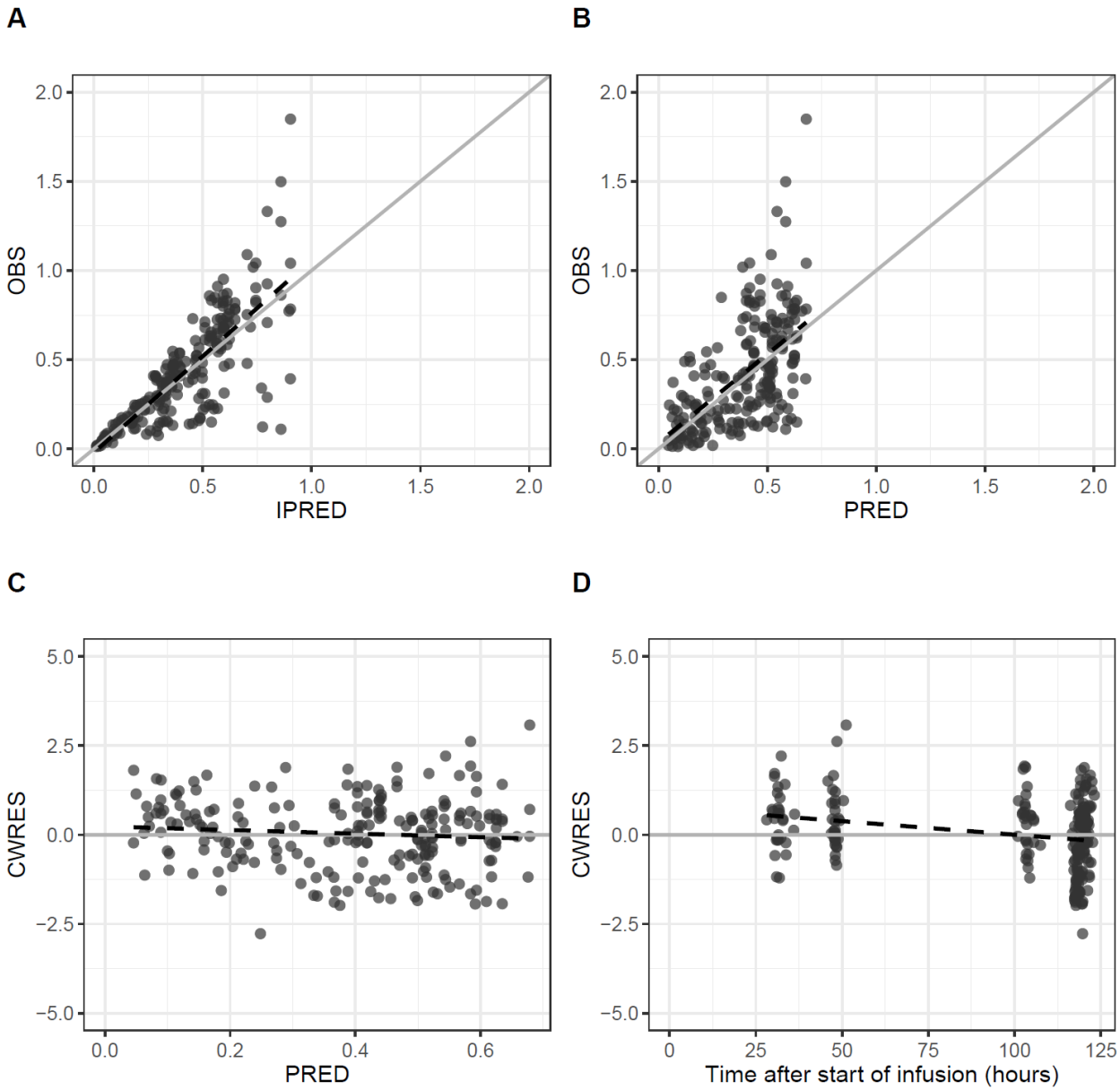

Supplementary Fig. 3: Goodness of fit plots for total WBC count data; observed (OBS)vs individual predicted (IPRED) WBC count (10^9/L) (A); observed vs population predicted (PRED) WBC count (B); conditional weighted residuals (CWRES) vs population predicted WBC count (C); conditional weighted residuals vs time after first dose (D). Continuous line represents the line of unity (A & B) and zero line (C & D), while dashed lines are the lines of smooth.

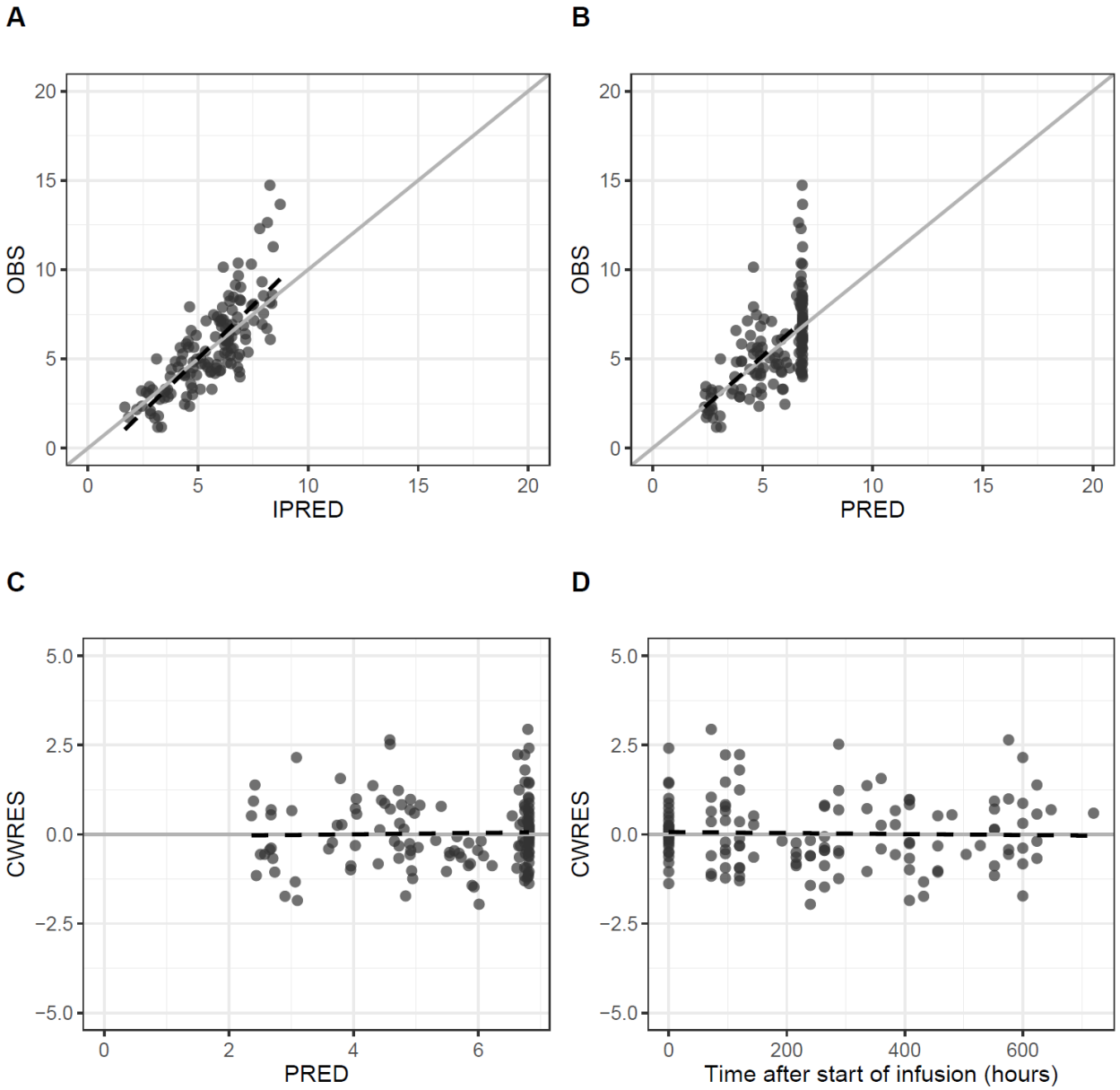

Supplementary Fig. 4: Individual plots for 5FU; points connected with dashed lines represent observed concentrations whereas continuous lines are the individual predicted concentrations.

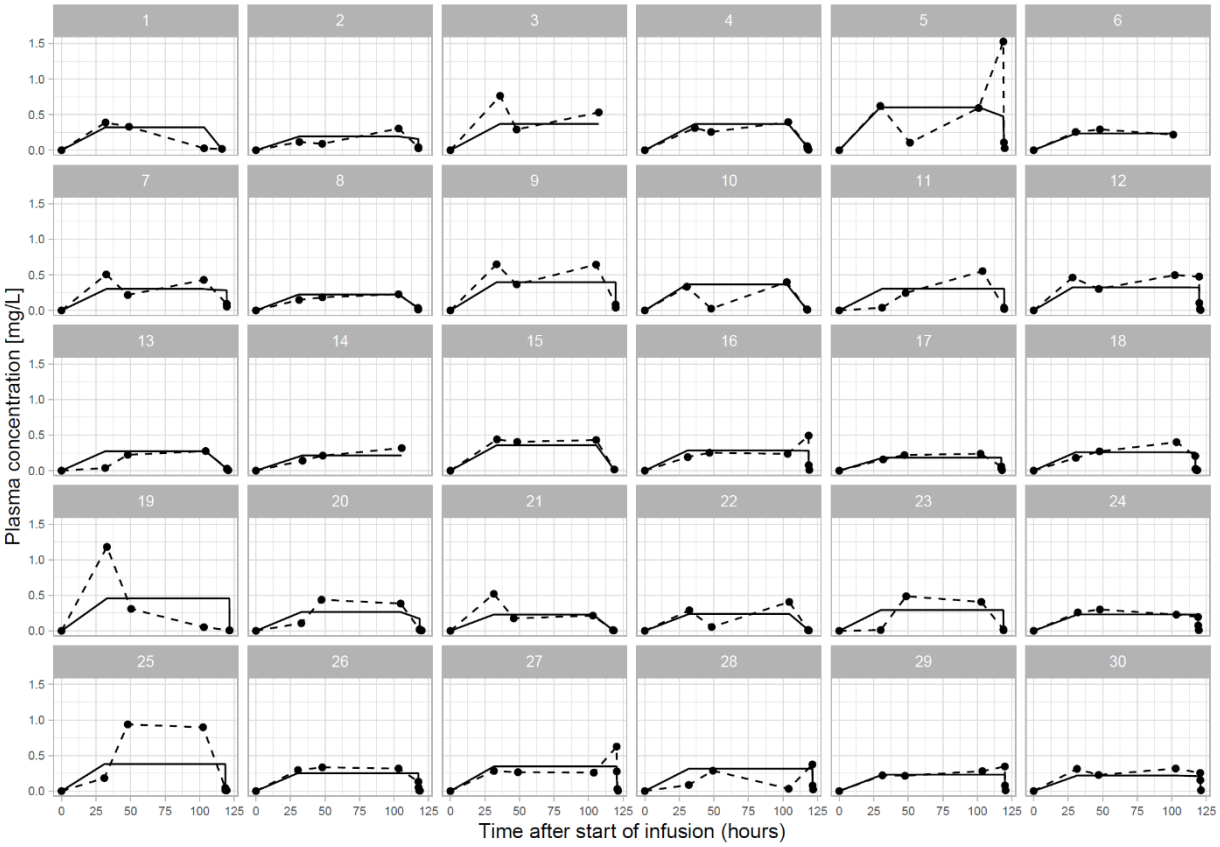

Supplementary Fig. 5: Individual plots for 5FUH2; points connected with dashed lines represent observed concentrations whereas continuous lines are the individual predicted concentrations.

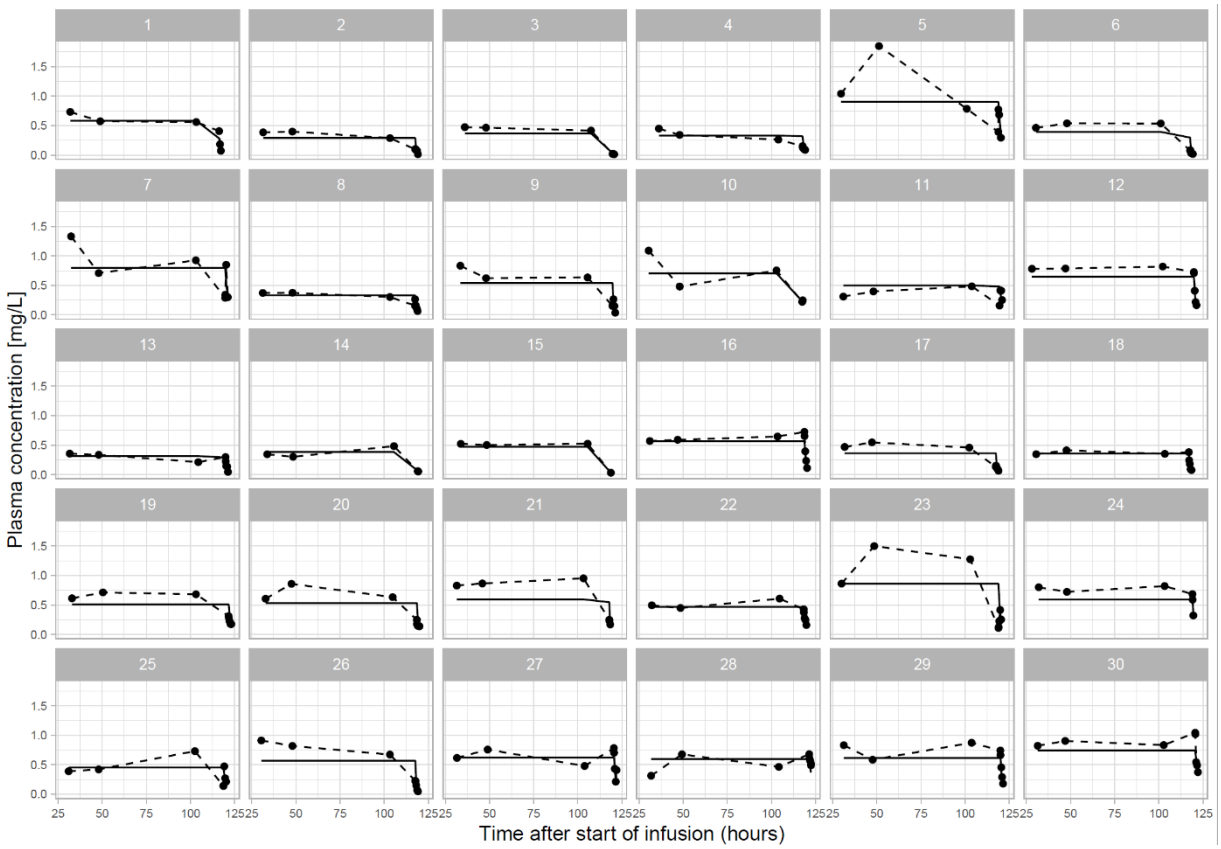

Supplementary Fig. 6: Individual plots for total WBC count data. points connected with dashed lines represent observed WBC count whereas continuous lines are the individual predicted WBC count.

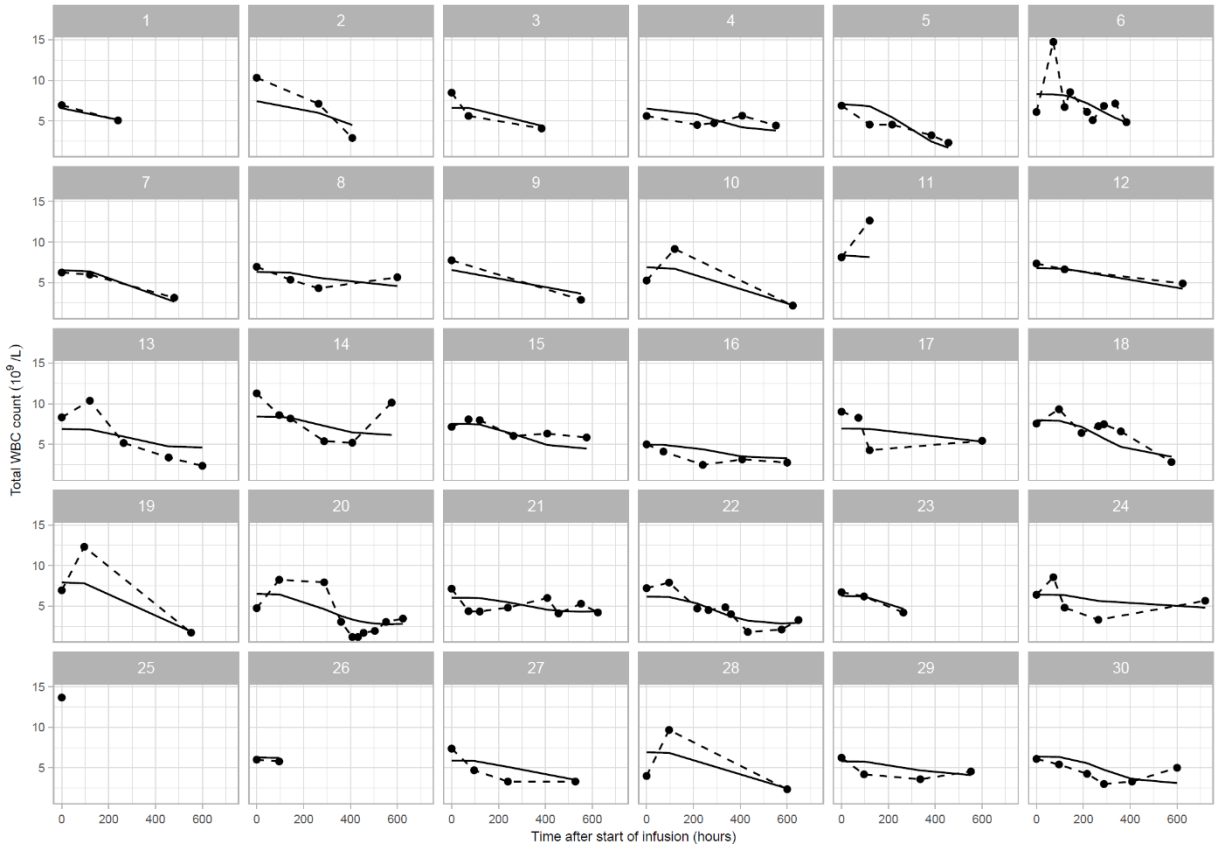

Chapter 6

BSA adjusted dosing of methotrexate continuous infusion is not supported by population pharmacokinetics in a large cohort of cancer patients.

Usman Arshad[1,3], Max Taubert[1], Tamina Seeger-Nukpezah[2], Sami Ullah[1,3], Ulrich Jaehde[3], Uwe Fuhr[1], Jörg Janne Vehreschild[2], Carolin Jakob[2].

[Manuscript under revision by co-authors]

[1] University of Cologne, Faculty of Medicine and University Hospital Cologne, Center for Pharmacology, Department I of Pharmacology, Cologne, Germany

[2] University of Cologne, Faculty of Medicine and University Hospital Cologne, Department I of Internal Medicine, Cologne, Germany

[3] Institute of Pharmacy, Clinical Pharmacy, University of Bonn, Bonn, Germany

Abstract

Objective: The aim of this study was to identify sources of variability including gender in pharmacokinetic exposure for methotrexate continuous infusion by a population pharmacokinetic approach applied in a large cohort of patients with hematological and solid malignancies.

Methods: Plasma concentration data (2182 measurements) from therapeutic drug monitoring was available for 229 subjects receiving methotrexate through 4 or 24 hours continuous intravenous infusion. Nonlinear mixed effects modeling was performed using NONMEM 7.4.3. Covariate data on patient demographics and clinical chemistry parameters was incorporated to assess and to quantify relationships with pharmacokinetic parameters. Simulations were developed to compare pharmacokinetic exposure under BSA adjusted and flat dosing regimens.

Results: Pharmacokinetics of methotrexate were best described by a three-compartment model. Values for clearance (CL) of 4.52 [2.98-6.36] L h^{-1} and central volume of distribution of 4.44 [2.09-8.21] L were estimated. An inter-occasion variability of 23.1% (coefficient of variation) and an inter-individual variability of 29.7% were associated to methotrexate CL, which was 16% lower in female patients. Serum creatinine, patient age, and BSA were also significantly related to methotrexate CL. The simulations suggested only marginal differences in drug exposure between flat dosing and adjusted dosing regimens.

Conclusion: Superiority of BSA guided dosing over flat dosing regimens is not supported by the present analysis. Influence of patient gender on methotrexate CL is present but small and needs to be further investigated.

Key words: methotrexate, pharmacokinetics, covariates, dosing.

1. Introduction

Methotrexate is considered an efficacious, cost-effective and acceptably safe drug for the treatment of many malignancies and autoimmune diseases.[1] The folate analogue methotrexate acts as an antineoplastic agent via competitive inhibition of dihydrofolate dehydrogenase, resulting in depletion of purines and thymidylate leading to impairment of DNA synthesis.[2 3] The drug can be administered via multiple routes of administrations and has a wide variation in dosing regimens including low (<50 mg/m^2), intermediate (50-500 mg/m^2) and high (>500 mg/m^2) dose regimens.[1 4] The pronounced inter-individual variability (IIV) of methotrexate pharmacokinetics and toxicity[8 9 10] renders individualization of dosing regimens difficult.

Hepatic metabolism accounts for a considerably lower fraction of its clearance compared to renal elimination, as the main fraction (80-90%) of the drug is primarily eliminated via glomerular filtration and active tubular secretion.[12 13] Nephrotoxicity associated with methotrexate impairs its clearance (CL), leading to further aggravation of toxicity such as myelosuppression and mucositis. In subjects with extracellular fluid accumulations, methotrexate has been shown to undergo delayed elimination.[11] To handle the various sources of variability, monitoring of methotrexate plasma concentrations (therapeutic drug monitoring, TDM) and serum creatinine (SCr) is recommended to safeguard a relatively constant circulating drug concentration with an acceptable risk/benefit ratio particularly in patients with impaired renal function.[14]

Modeling of pharmacokinetic data has the potential to optimize TDM, where tailored dose adjustments can be made according to the model predicted concentrations.[16] Bayesian population pharmacokinetic analysis has been used to assist TDM guided dose adjustments for methotrexate.[16] In addition, population pharmacokinetic analysis provides the possibility to identify and quantify covariate effects on drug exposure.[17 18] This may provide a better understanding of drug's pharmacology and assist adjustments in dosage regimen according to patient's individual characteristics e.g., renal/hepatic function, genotype of drug metabolizing enzymes or transporters, and/or anthropometric characteristics. Models capturing covariate relationships have been found useful in oncology for individualized dose adaptations such as in case of busulfan, topotecan and docetaxel.[17]

The current study was primarily aimed to identify the covariates influencing methotrexate pharmacokinetics, particularly patient gender, by developing a population pharmacokinetic model using the TDM data collected from patients with hematological and solid malignancies. The model was further aimed to be used for the evaluation of ongoing clinical practice of administering methotrexate based on individual BSA.

2. Materials and methods

2.1 Patients, treatment and sampling procedures

Plasma concentration over time data was obtained for patients with hematological malignancies or solid tumors treated with methotrexate during the period of 2005 to 2018 from the CoCoNut database maintained at Department I of Internal Medicine, University Hospital Cologne, Germany. Methotrexate was administered via 4 or 24 hour continuous intravenous infusions. TDM was routinely performed in patients 42h and 48h after infusion for 24 hour MTX and 24h, 42h, and 48h after infusion for 4 hour MTX. When target plasma concentration was not reached TDM was performed every 6h. Methotrexate plasma concentrations were measured. Demographic covariates included patient's age, gender, weight and height. Covariate data from clinical chemistry analysis included SCr, plasma total bilirubin ($Bili_{tot}$), γ-glutamyltransferase (γ-GT), uric acid concentrations, absolute leukocyte counts (ALC), and BSA.

2.2 Dataset preparation

Dosing, concentration and covariate data was subjected to screening prior to pharmacokinetic analysis. R (version 3.5.1) with the 'tidyverse' packages[19] was used to prepare the dataset. Dataset preparation was assisted by visual inspection of individual concentration time profiles. Patients with missing dosing information at treatment initiation were identified for exclusion from subsequent analysis. Subjects with missing dosing information during the treatment were flagged and partially excluded (data points after missing dose information only). Missing covariates within an individual were handled using last observation carried forward approach in case the covariate values were available at start or during the treatment, while next observation was carried backward where the covariate information was present during or at the end of therapy but missing at prior time points. At the very time point of sampling, actual

covariate information was not available in 91.9 %, 82.2 %, 78.2 %, and 40.0 % of the data for γ-GT, weight, $Bili_{tot}$ and SCr respectively.

2.3 Model development, selection and evaluation criteria

Data was analyzed by the nonlinear mixed effect modeling approach using NONMEM 7.4.3 (ICON, Development Solutions, Elliot City, MD, USA). Perl speaks NONMEM (PsN), Pirana and Xpose4 were used to assist model development, evaluation and post processing of output data.[20] [21] [22] A combination of iterative two-stage (ITS) and first order conditional estimation with interaction (FOCE-I) methods was applied for parameter estimation. Likelihood ratio test (LRT) or Akaike information criterion (AIC) were used for evaluation of nested and non-nested models, respectively. A nested model with fewer parameters or decrease in OFV by 3.84 (i.e., $p<0.05$) was given preference. The model with a lower AIC value in case of non-nested models was preferred.

Model evaluation criteria comprised of plausibility of parameter estimates, reduction in unexplained and residual variability, shrinkage and precision in parameter estimates. Visual inspection through goodness of fit (GOF) plots included observed versus individual/population predicted concentrations (IPRED/PRED) over time. Residual error model was evaluated with the help of CWRES versus observed concentrations and versus time after first dose (TAFD). Numerical predictive checks (NPCs) were used for further assessment by comparing the empirical cumulative distribution function of the observed methotrexate concentrations with the theoretical cumulative distribution, computed from simulated data.

2.4 Structural model development

Compartmental analysis was performed in a step-wise manner. Both linear and nonlinear (Michaelis-Menten) elimination models were evaluated. IIV was incorporated using exponential terms η_{iiv}.[18] Interoccasion variability (IOV) defined as variability between individual cycles of methotrexate therapy was incorporated in the model as random effects (η_{iov}).[23] Population parameters (P) were therefore estimated as,

$$P = \theta \times e^{\eta_{iiv} + \eta_{iov}}$$

Where, θ represent the population estimate of the pharmacokinetic parameter. η_{iiv} describes the deviation of pharmacokinetic parameter values of an individual from the population estimate. η_{iov} account for the variability on part of subsequent cycles of methotrexate infusions. Additive, proportional and combined error models were tested to estimate the residual unexplained variability (RUV).

2.5 Covariate model development

Covariate data was analyzed to identify covariate-parameter relationships.

Continuous covariates were included as linear relationships or power relationships centered around their median values as follows,

$$\text{Covariate}_{\text{effect}} = 1 + (\text{Covariate}_{\text{i}} - \text{Covariate}_{\text{median}}) \times \theta_{\text{Covariate}}$$

$$\text{Covariate}_{\text{effect}} = \left(\text{Covariate}_{\text{i}} / \text{Covariate}_{\text{median}}\right)^{\theta_{\text{Covariate}}}$$

Categorical relationships were given the following functional form,

$$\text{Covariate}_{\text{effect}} = 1 + \text{Covariate}_{\text{i}} \times \theta_{\text{Covariate}}$$

Where, $\text{Covariate}_{\text{i}}$ is the individual covariate value and $\theta_{\text{Covariate}}$ represents the effect size of covariate relationship to a pharmacokinetic parameter. Covariate preselection was performed considering scientific plausibility as an essential criterion. Graphical evaluation of covariates was performed including conditional weighted residuals (CWRES) vs covariate, empirical bayes estimates (EBEs) versus covariate, and covariate versus covariate plots. Inclusion of highly correlated covariates was abstained by assigning superiority on basis of physiological plausibility. Significance of covariate relationship was principally guided by decrement in OFV and/or unexplained variability. A univariate analysis was performed as a first step followed by inclusion/elimination of further covariate data in a stepwise manner. During forward inclusion, the covariate providing maximum reduction in OFV was selected at each step, while covariate relationships demonstrating no significant impact on OFV during the backward elimination process were disregarded. Selection criteria during forward

inclusion was a ΔOFV of 3.84 ($p<0.05$), whereas a ΔOFV of 6.63 ($p<0.01$) was considered during the backward elimination procedure.

Population parameter estimates with respective confidence intervals (CI) and relative standard errors (RSE) were obtained by performing a bootstrap analysis using 1000 sample replicates.

2.6 Evaluation of BSA versus flat dosing regimens

Simulations were designed using the final model for comparative evaluation of drug exposure under BSA based and flat dosing 24 hours infusion regimens. A typical high dose regimen of 3000 mg/day, was given either as a flat (scaled with the median BSA of 1.96 for all patients) or a BSA based dose (linear scaling with individual BSA), where each subject was simulated 100 times (22900 subjects in total). Considering the current TDM protocol at University Hospital of Cologne, plasma concentrations were supposed not to exceed 1.0 and 0.3 mg/L at 42 and 48 hours after the start of infusion, respectively. Subjects exceeding the target concentrations at respective time points were flagged and the dose reduction needed to provide a plasma concentration below the thresholds was identified for these subjects. The fraction of subjects requiring a dose reduction stratified by BSA percentiles (<10%, 10–90%, and >90%) was calculated and compared for both regimens.

Another simulation was designed to visualize the exposure achieved with BSA based dosing and flat dosing regimens, where the probability of attaining concentrations higher than the above mentioned thresholds at respective time points was calculated and visualized.

3. Results

3.1. Patient and treatment characteristics

The majority of the patients received 4 or 24 hours infusions with median methotrexate doses of 5.60 and 2.61 g/m^2 respectively, while some received 12 or 48 hours infusions with median doses of 4.54 and 5.39 g/m^2 respectively. Only a single patient received a 72 hours infusion with a dose of 8.09 g/m^2. A median of 3 dosing cycles (range, 1 – 9) per patient were part of the available data. In total, 229 cancer patients (83 females)

with 2182 plasma concentration measurements were included in the pharmacokinetic analysis. The number of plasma concentration measurements per patient ranged from 1 to 65 with a median of 7 measurements. Patients were 19 to 82 years old and had a median BSA of 2.06 m^2 (range: 1.56 - 3.42). The underlying disease characteristics of the study population are provided in Table 1. Further information on patient demographics and clinical laboratory parameters is summarized in table 2.

Table 1: Population characteristics

Characteristics (n=229, females=83)	**Median [Min, Max]**
Age (years)	58.0 [19.0, 82.0]
Weight (kg)	78.4 [41.5, 227]
Height (cm)	176 [154, 203]
Body surface area (m^2)	1.96 [1.34, 3.42]
Body mass index (kg/m^2)	25.4 [15.7, 66.3]
Serum creatinine (mg/dL)	0.76 [0.30, 7.31]
Total plasma bilirubin (mg/dL)	0.48 [0.09, 2.90]
Plasma γ-glutamyltransferase (mg/dL)	69.8 [14.0, 442]
Plasma urea (mg/dL)	32.0 [2.90, 949]
Absolute leucocyte count ($\times 10^9/L$)	6.28 [0.05, 61.1]

Table 2: Population disease characteristics

Tumor type	**n**
Solid tumors	
Sarcoma	4
Carcinoma	2
Hodgkin lymphoma	5
Non-Hodgkin lymphoma	9
Leukemia / very aggressive Non-Hodgkin lymphoma	
Acute lymphoblastic leukemia	64
Acute Myeloid leukemia	1
Others	48
Low aggressive Non-Hodgkin lymphoma	101

3.2. Pharmacokinetic model

A three-compartment model with linear elimination adequately described methotrexate plasma concentrations well as shown by a ΔOFV of 389 compared to two-compartment model (fig. 1, fig. 2). Population estimates for V_1 and plasma CL of methotrexate were 4.44 L and 4.52 L/h, respectively. A linear CL model was preferred over a model with an additive nonlinear CL component (combined model), although the latter provided a better fit with a ΔOFV of 70 points. The fraction of CL contributed by the linear component in the combined model was 4.77 L/h, whereas nonlinear CL contributed 0.42 L/h at median methotrexate concentrations (2.20 mg/L). It was not feasible to proceed further with the combined model because of the much longer run times of ~60 hours compared to ~1 hour for linear model, preventing proper covariate analysis. Moreover, a decreased stability with frequent rounding errors was observed with the combined model. Therefore, the linear model was used for subsequent analysis.

An IIV of 34.1%, and an IOV of 27.9% was associated with methotrexate CL. Covariance between IIV parameters on CL and V_1 was estimated to be 49.4%. RUV was appropriately described by a combined (additive and exponential) error model. Mean pharmacokinetic parameters with 95% CI and RSE obtained from the bootstrap analysis are presented in Table 3. Supplementary table presents parameter estimates for the combined model with linear and nonlinear CL components.

3.3. Covariate analysis

SCr was found to be a significant covariate on CL with an OFV reduction by 215. Inclusion of patient's gender and age on CL was further observed to improve the model fit with ΔOFVs of 32.0 and 13.0 respectively. BSA effect on CL and V was devoid of statistical significance during univariate analysis. However, considering the pharmacological relevance due to the fact that individual doses were calculated according to patient's BSA, it was tested as a covariate on CL and V in the final model, demonstrating a further reduction in OFV by 4.4 on CL, but no significant impact on V was observed. A ~16% lower CL was estimated in females. Reduction in IIV of individual parameters was not so eminent as a decrease in 2.40, 0.56 and 1.44 (%) was observed after the inclusion of SCr, age and gender respectively. IIV and IOV on methotrexate CL in the covariate model was estimated to be 29.7% and 23.1% respectively. Individual CL

(CL_i) given the model point estimates, individual Scr, age, BSA and gender can be computed as follows,

$$CL_i = 4.52\left({SCr_i}/{0.77}\right)^{-0.77}\left({Age_i}/{58}\right)^{-0.17}\left({BSA_i}/{1.73}\right)^{-0.41}(1 + Gender_i \times -0.16)$$

Where, gender was coded as 0 for males and 1 for females. Estimates for covariate relationships are summarized in table 3.

Table 3: Population pharmacokinetic parameter estimates from bootstrap analysis

	Mean	**% RSE**	**95% CI**
Pharmacokinetic parameters			
CL (L h^{-1})	4.52	23.6	2.58 - 7.38
V_1 (L)	4.44	46.9	1.65 - 9.52
V_2 (L)	2.73	48.0	0.87 - 6.25
V_3 (L)	2.94	59.0	0.65 - 7.25
Q_1 (L h^{-1})	0.43	52.9	0.13 - 1.04
Q_2 (L/h)	0.03	55.0	0.01 - 0.06
Covariate effects on CL			
SCr (mg^{-1} dL)	-0.77	-14.2	-0.97 - -0.57
Age ($year^{-1}$)	-0.17	-37.1	-0.30 - 0.05
Gender (fractional decrease in females)	-0.16	-29.2	-0.25 - -0.07
BSA (m^{-2})	0.41	68.2	-0.13 - 0.96
IIV (ω^2)			
CL	0.11	15.1	0.08 - 0.14
V_1	1.58	29.7	0.84 - 2.72
COV(CL, V_1)	0.32	21.3	0.19 - 0.44
IOV (ω^2)			
CL	0.08	18.9	0.05 - 0.11
V_1	-	-	-
RUV (σ^2)			
Additive error	0.02	18.6	0.02 - 0.03
Exponential error	0.26	6.89	0.22 - 0.30

RSE = relative standard error, CI = confidence interval, RSE = relative standard error, CL = clearance, V_1 = central volume of distribution, V_2 & V_3 = peripheral volumes of distribution, Q_1 and Q_2 = inter-compartmental clearances, AUC = Area under the curve, SCr = Serum Creatinine, IIV = inter-individual variability, IOV = inter-occasion variability, RUV = residual unexplained variability.

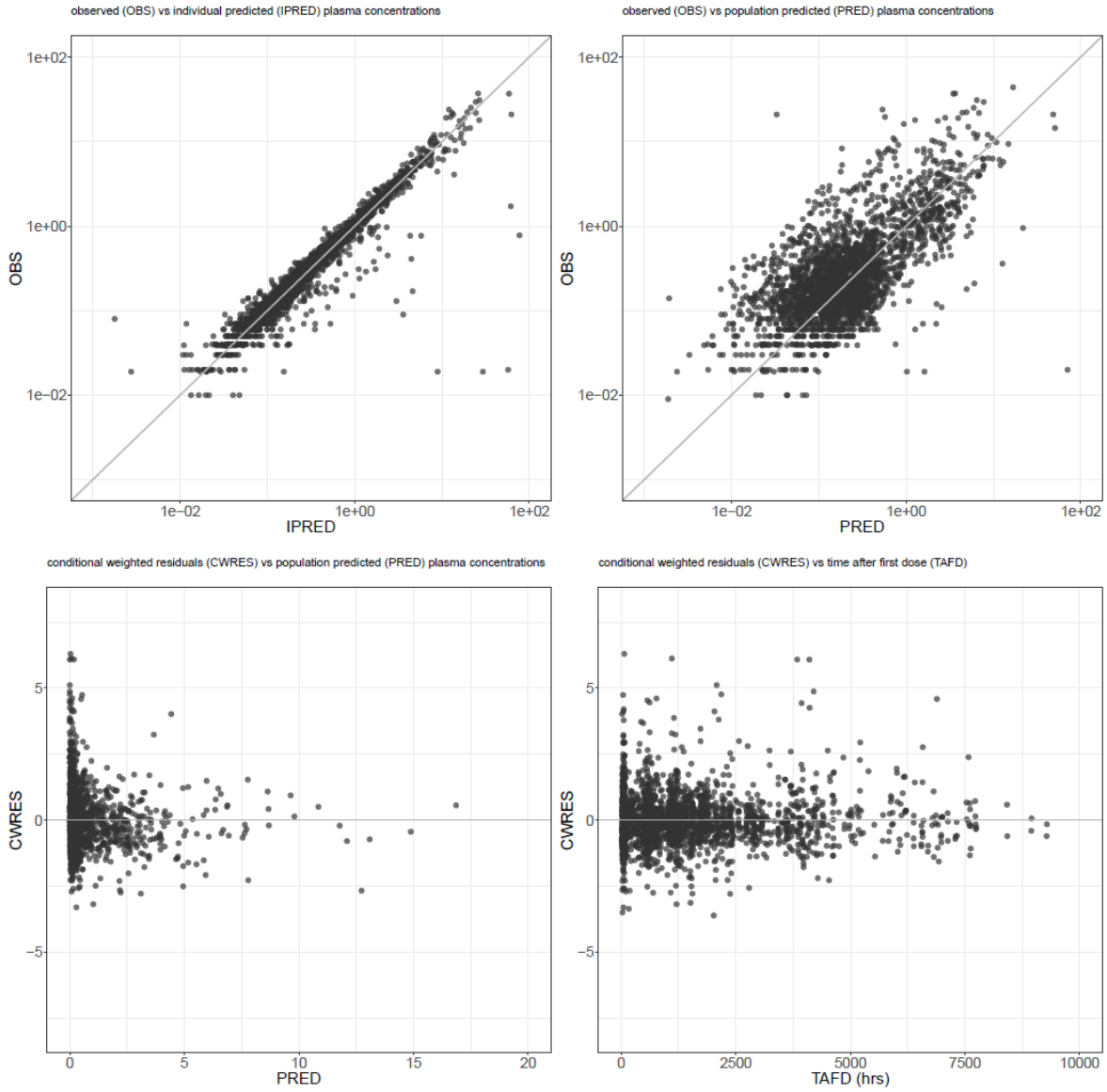

Figure 1: Goodness of fit plots; observed vs individual predicted (IPRED) concentration (mg/L) (top left); observed vs population predicted (PRED) concentrations (top right); conditional weighted residuals (CWRES) vs population predicted concentrations (bottom left); conditional weighted residuals vs time after first dose (bottom right). Concentrations are presented on log scale in the upper panel.

3.4. BSA versus flat dosing regimens

Table 4 presents the fraction of subjects requiring dose reduction for respective BSA percentiles in a simulated population administered with methotrexate flat dosing or scaled on the basis of individual BSA. Overall, marginal differences between the regimens were observed. For the upper BSA percentile (>90%), a higher proportion of

subjects (45.6%) receiving BSA based regimens required dose reduction as compared to the flat dosing (38.5%). The contrary was observed for the lower BSA subgroup (<10%) where 30.5% compared to 37.2% subjects needed dose reduction for BSA based and flat dosing regimens, respectively. A negligible difference (37.3% for flat versus 36.7% for BSA based dosing) was observed for the major proportion (10-90%) of subjects in the simulated population.

Figure 3 displays the probability of attaining plasma concentrations higher than the given threshold across the BSA quartiles for flat and BSA based regimens. Marginal differences between the two regimens across the BSA range were observed.

Table 4: Fraction of subjects requiring dose reduction for BSA based and fixed dosing regimens across the observed BSA percentiles.

BSA percentile	Dosing	Subjects requiring dose reduction (%)
< 10%	BSA based	30.5
	Fixed	37.2
10-90%	BSA based	36.7
	Fixed	37.3
> 90%	BSA based	45.6
	Fixed	38.5

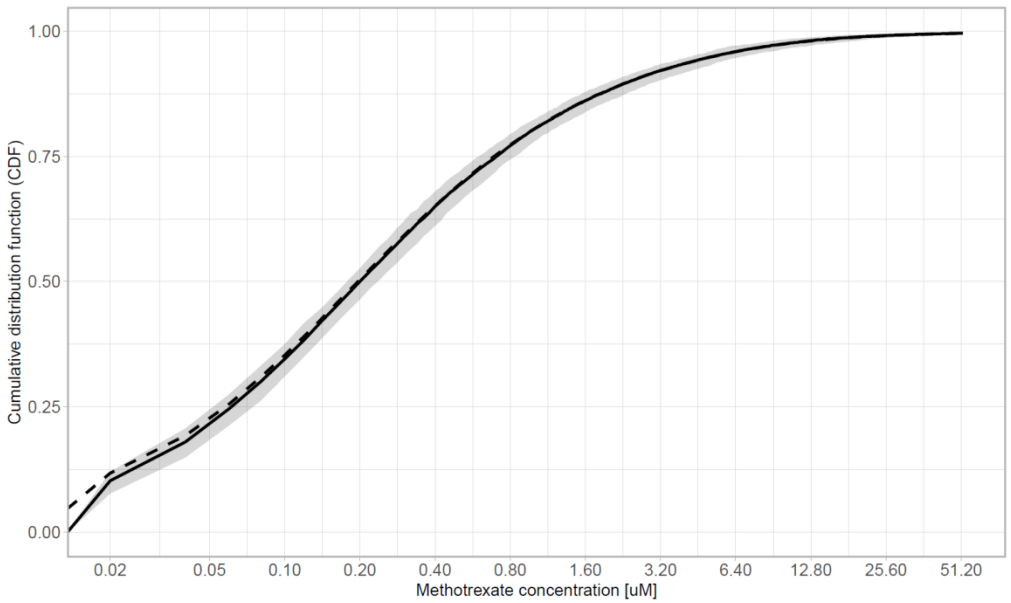

Figure 2: Numerical predictive check: Continuous and dashed lines are the empirical and predicted distributions, respectively. Shaded area represents the 95% prediction interval.

3. Discussion

A three-compartment pharmacokinetic model of methotrexate continuous infusion is presented. Patient gender, age, BSA and Scr were related to methotrexate CL. A 16% lower CL was estimated for females compared to males. Simulations using the final covariate model did not support superiority of BSA based dose adjustments over flat dosing.

Identification of clinically relevant covariates has been main objective of population pharmacokinetic modeling of methotrexate, as numerous studies with inconsistent covariate effects have been presented[24 25 26 27 28 29 30 31 32 33 34] . Gender influence on methotrexate CL was previously presented in a study on patients with acute lymphocytic leukemia[29], but gender effect was not supported by several other population pharmacokinetic studies.[24 30 31 32 33 34] For univariate analysis, a reduction in OFV by 4.4 points was observed with the inclusion of patient gender. The inclusion of gender in the model containing a SCr effect demonstrated an improvement of model fit by ΔOFV of 32.0, where CL was shown to be about 16 % lower in females, independent of the differences in anthropometric characteristics between men and women. Besides statistical significance, a ~30% reduction in IIV with the covariate inclusion is considered to be clinically relevant. [17] Despite of the 16% difference in CL between the two genders, considerable unexplained variability is yet associated with methotrexate CL, thus the effect size is not of considerable importance from a clinical perspective.

Age was related to methotrexate CL in a few studies[30 32], while inconsistencies exist in the majority of studies.[25 34 35 36 37 38] Some studies presented the influence of body weight and patient's age on both the CL and V of methotrexate.[31 33] Mei *et al.,* showed that V of methotrexate increases with increase in age and supported the preference of age over body weight as a covariate influencing V. A relationship between weight and V was reported by some other studies as well.[30 34 31 39 40] Age was found to be significant on methotrexate CL in our study with a ΔOFV of 13.0, however body weight was not concluded to be significant on methotrexate CL and V in the present analysis.

SCr was found to be the most significant covariate with a ΔOFV of 215, where the studied population demonstrated a wide variation in SCr concentration (0.30-7.31 mg/dL). These results are in line with other studies where methotrexate elimination

was found to be correlated with SCr. [34] [41] [42] The observed effect is physiologically plausible as methotrexate is primarily eliminated by the kidneys.[24] Nevertheless, the covariate relationship between SCr concentrations and methotrexate CL faces disagreements in some studies.[31] [30] [33] [37] Creatinine CL (CrCL, estimated from individual Scr) was included as a covariate on methotrexate CL in some studies [29] [26] [43] but CrCL was not found significant during the present analysis.

Identification of true parameter covariate relationship is of considerable importance as it may enhance the model's predictive performance which is primarily the ability of the model to (1) predict the variable of interest, and (2) better estimate individual parameter(s). Lack of predictive performance however does not necessarily mean that the co-variate-parameter relation does not exist. Important aspects influencing covariate selection power and bias are briefly discussed by Ribbing *et al*.[44] The authors concluded that false covariate selection is more probable in case of highly correlated covariates. Under circumstances where a potential covariate contains information from another set of covariates, high correlations may exist. A selection bias may be observed where a true covariate has a weak or insignificant effect which may occur in small sample size, i.e. in the case of lack of power, which may not be a major limitation in the present analysis as a sample size of 229 patients was large enough containing complete covariate information on BSA, age and gender, while SCr values were available for most of the time points (~60%). Covariates with lesser information included γ-GT, $Bili_{tot}$ and uric acid but none of these were previously reported to influence methotrexate pharmacokinetics.

The present analysis led towards the motivation to evaluate BSA guided dosing strategy being employed in current clinical practice in contrast to flat dosing. Preference of BSA based dosing over flat dosing or based on other measures such as patient genotype / phenotype is an ongoing debate. Therapeutic effects with an acceptable tolerability are generally assumed by a linear scaling of the dose according to individual BSA. Flat dosing is proposed for a number of anticancer drugs where BSA was not found to reduce IIV. [45] [46] [47] Prediction of exposure becomes more relevant for anticancer drugs with narrow therapeutic index. Fig 3 displays marginal differences in plasma drug exposure between the two dosing strategies. It can be observed that BSA guided dosing performs slightly better in comparison to flat dosing for subjects having BSA at the lower extreme.

For these subjects, a comparatively lower proportion required dose reduction in case of BSA guided dosing as presented in Table 4. The contrary was observed for subjects with BSA at the upper extreme, while the major proportion of simulated population (between 10th and 90th percentile) had negligible differences.

Estimation of IOV separates the individual differences in pharmacokinetic parameters from residual error, thereby avoiding the overestimation of IIV and RUV.[23] Model-based approaches to assist TDM are challenged under circumstances where IOV is observed to be higher than IIV because IOV lacks the predictive ability.[23 48] A decreased precision in target attainment was reported with increasing magnitudes of IOV. [48] Abrantes *et al*., in a recent study suggested the inclusion of IOV to generate individual pharmacokinetic estimates but dose individualization including IOV should be avoided during model-based TDM.[49]

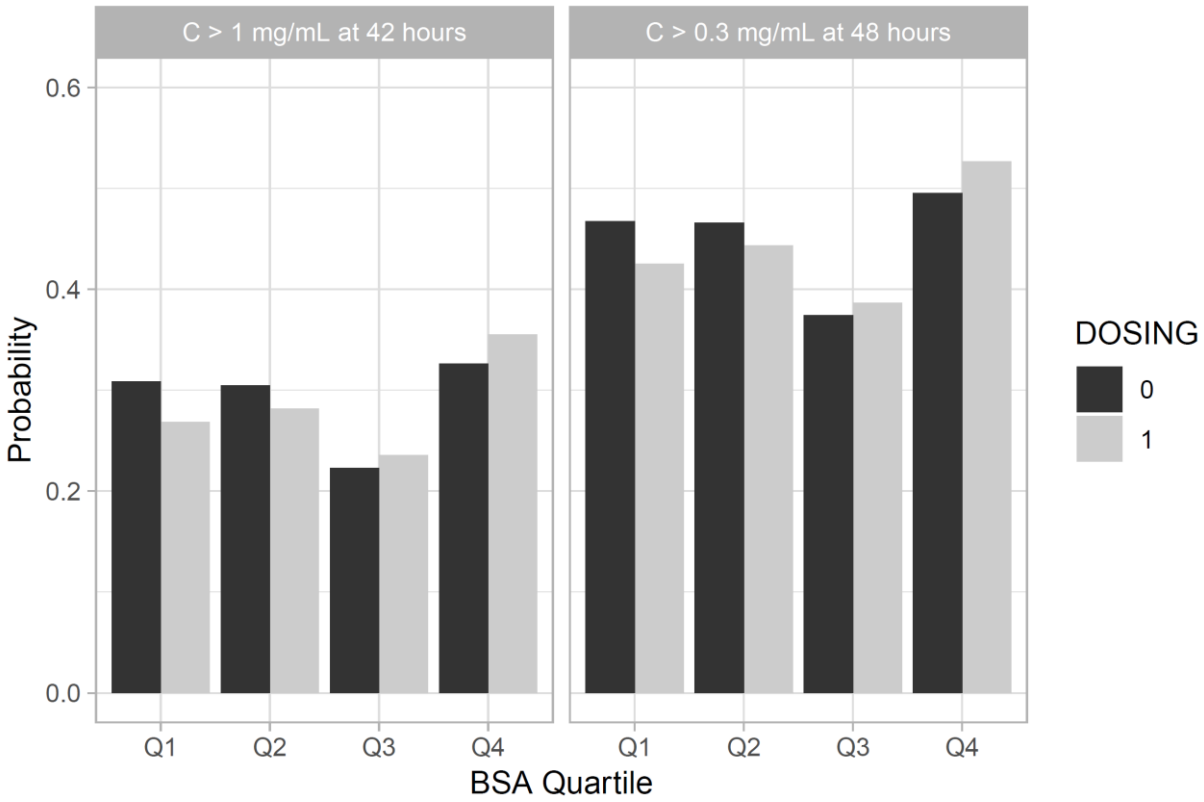

Figure 3: Probability of attaining plasma concentrations > 1 mg/L at 42 hours (left panel), > 0.3 mg/L at 48 hours (right panel) across the observed BSA quartiles with flat and BSA based dosing regimens. Q1: <25%, Q2: >=25% to <50%, Q3: >=50% to <75%, Q4: >75%.

It is evident from the present analysis that flat dosing at least does not appear to enhance the variability in exposure. Keeping in view that fixed dosing regimens avoid the chances of making errors in dose calculation and preparation, it might be advisable to substitute the ongoing clinical practice of methotrexate dose individualization based on BSA.

4. Conclusions

Methotrexate pharmacokinetics were described by a three-compartment model. A lower CL estimated for the female patients needs to be investigated in future studies. Plasma Scr, patient age, and BSA were found additionally as statistically significant covariates on methotrexate CL. Fixed dosing can be a reasonable alternative to BSA guided dosing, as marginal differences in simulated pharmacokinetic exposure between the two dosing strategies were observed in the present analysis.

5. References

1. Goss SL, Klein CE, Jin Z, et al. Methotrexate Dose in Patients With Early Rheumatoid Arthritis Impacts Methotrexate Polyglutamate Pharmacokinetics, Adalimumab Pharmacokinetics, and Efficacy: Pharmacokinetic and Exposure-response Analysis of the CONCERTO Trial. *Clin Ther*. 2018;40(2):309-319. doi:10.1016/j.clinthera.2018.01.002
2. Baram J, Allegra CJ, Fine RL, Chabner BA. Effect of methotrexate on intracellular folate pools in purified myeloid precursor cells from normal human bone marrow. *J Clin Invest*. 1987;79(3):692-697. doi:10.1172/JCI112872
3. Goldman ID, Matherly LH. The cellular pharmacology of methotrexate. *Pharmacol Ther*. 1985;28(1):77-102.
4. Hui KH, Chu HM, Fong PS, Cheng WTF, Lam TN. Population Pharmacokinetic Study and Individual Dose Adjustments of High-Dose Methotrexate in Chinese Pediatric Patients With Acute Lymphoblastic Leukemia or Osteosarcoma. *J Clin Pharmacol*. 2019;59(4):566-577. doi:10.1002/jcph.1349
5. Balis FM, Savitch JL, Bleyer WA, Reaman GH, Poplack DG. Remission induction of meningeal leukemia with high-dose intravenous methotrexate. *J Clin Oncol*. 1985;3(4):485-489. doi:10.1200/JCO.1985.3.4.485
6. Pui C-H, Howard SC. Current management and challenges of malignant disease in the CNS in paediatric leukaemia. *Lancet Oncol*. 2008;9(3):257-268. doi:10.1016/S1470-2045(08)70070-6
7. Delepine N, Delepine G, Cornille H, Brion F, Arnaud P, Desbois JC. Dose escalation with pharmacokinetics monitoring in methotrexate chemotherapy of osteosarcoma. *Anticancer Res*. 15(2):489-494.
8. Schmiegelow K. Advances in individual prediction of methotrexate toxicity: a review. *Br J Haematol*. 2009;146(5):489-503. doi:10.1111/j.1365-2141.2009.07765.x
9. Evans WE, Relling M V, Boyett JM, Pui CH. Does pharmacokinetic variability influence the efficacy of high-dose methotrexate for the treatment of children with acute lymphoblastic leukemia: what can we learn from small studies? *Leuk Res*. 1997;21(5):435-437.
10. Treviño LR, Shimasaki N, Yang W, et al. Germline Genetic Variation in an Organic Anion Transporter Polypeptide Associated With Methotrexate Pharmacokinetics

and Clinical Effects. *J Clin Oncol*. 2009;27(35):5972-5978. doi:10.1200/JCO.2008.20.4156

11. Howard SC, McCormick J, Pui C-H, Buddington RK, Harvey RD. Preventing and Managing Toxicities of High-Dose Methotrexate. *Oncologist*. 2016;21(12):1471-1482. doi:10.1634/theoncologist.2015-0164
12. Seideman P, Beck O, Eksborg S, Wennberg M. The pharmacokinetics of methotrexate and its 7-hydroxy metabolite in patients with rheumatoid arthritis. *Br J Clin Pharmacol*. 1993;35(4):409-412.
13. Chládek J, Grim J, Martínková J, et al. Pharmacokinetics and pharmacodynamics of low-dose methotrexate in the treatment of psoriasis. *Br J Clin Pharmacol*. 2002;54(2):147-156. doi:10.1046/J.1365-2125.2002.01621.X
14. Evans WE, Pratt CB, Taylor RH, Barker LF, Crom WR. Pharmacokinetic monitoring of high-dose methotrexate. Early recognition of high-risk patients. *Cancer Chemother Pharmacol*. 1979;3(3):161-166.
15. de Jonge ME, Huitema ADR, Schellens JHM, Rodenhuis S, Beijnen JH. Individualised Cancer Chemotherapy: Strategies and Performance of Prospective Studies on Therapeutic Drug Monitoring with Dose Adaptation. *Clin Pharmacokinet*. 2005;44(2):147-173. doi:10.2165/00003088-200544020-00002
16. Monjanel-Mouterde S, Lejeune C, Ciccolini J, et al. Bayesian population model of methotrexate to guide dosage adjustments for folate rescue in patients with breast cancer. *J Clin Pharm Ther*. 2002;27(3):189-195.
17. Joerger M. Covariate Pharmacokinetic Model Building in Oncology and its Potential Clinical Relevance. *AAPS J*. 2012;14(1):119-132. doi:10.1208/s12248-012-9320-2
18. Mould DR, Upton RN. Basic Concepts in Population Modeling, Simulation, and Model-Based Drug Development—Part 2: Introduction to Pharmacokinetic Modeling Methods. *CPT Pharmacometrics Syst Pharmacol*. 2013;2(4):e38. doi:10.1038/psp.2013.14
19. Wickham H. tidyverse: Easily Install and Load the 'Tidyverse. 2017. https://cran.r-project.org/package=tidyverse.
20. Lindbom L, Ribbing J, Jonsson EN. Perl-speaks-NONMEM (PsN)—a Perl module for NONMEM related programming. *Comput Methods Programs Biomed*. 2004;75(2):85-94. doi:10.1016/j.cmpb.2003.11.003

21. Keizer RJ, van Benten M, Beijnen JH, Schellens JHM, Huitema ADR. Piraña and PCluster: A modeling environment and cluster infrastructure for NONMEM. *Comput Methods Programs Biomed*. 2011;101(1):72-79. doi:10.1016/j.cmpb.2010.04.018
22. Jonsson EN, Karlsson MO. Xpose--an S-PLUS based population pharmacokinetic/pharmacodynamic model building aid for NONMEM. *Comput Methods Programs Biomed*. 1999;58(1):51-64.
23. Karlsson MO, Sheiner LB. The importance of modeling interoccasion variability in population pharmacokinetic analyses. *J Pharmacokinet Biopharm*. 1993;21(6):735-750.
24. Johansson ÅM, Hill N, Perisoglou M, Whelan J, Karlsson MO, Standing JF. A population pharmacokinetic/pharmacodynamic model of methotrexate and mucositis scores in osteosarcoma. *Ther Drug Monit*. 2011;33(6):711-718. doi:10.1097/FTD.0b013e31823615e1
25. Piard C, Bressolle F, Fakhoury M, et al. A limited sampling strategy to estimate individual pharmacokinetic parameters of methotrexate in children with acute lymphoblastic leukemia. *Cancer Chemother Pharmacol*. 2007;60(4):609-620. doi:10.1007/s00280-006-0394-3
26. Fukuhara K, Ikawa K, Morikawa N, Kumagai K. Population pharmacokinetics of high-dose methotrexate in Japanese adult patients with malignancies: a concurrent analysis of the serum and urine concentration data. *J Clin Pharm Ther*. 2008;33(6):677-684. doi:10.1111/j.1365-2710.2008.00966.x
27. Mei S, Li X, Jiang X, Yu K, Lin S, Zhao Z. Population Pharmacokinetics of High-Dose Methotrexate in Patients With Primary Central Nervous System Lymphoma. *J Pharm Sci*. 2018;107(5):1454-1460. doi:10.1016/j.xphs.2018.01.004
28. Godfrey C, Sweeney K, Miller K, Hamilton R, Kremer J. The population pharmacokinetics of long-term methotrexate in rheumatoid arthritis. *Br J Clin Pharmacol*. 1998;46(4):369-376. doi:10.1046/J.1365-2125.1998.T01-1-00790.X
29. Zhang W, Zhang Q, Tian X, et al. Population pharmacokinetics of high-dose methotrexate after intravenous administration in Chinese osteosarcoma patients from a single institution. *Chin Med J (Engl)*. 2015;128(1):111-118. doi:10.4103/0366-6999.147829
30. Colom H, Farré R, Soy D, et al. Population Pharmacokinetics of High-Dose

Methotrexate After Intravenous Administration in Pediatric Patients With Osteosarcoma. *Ther Drug Monit*. 2009;31(1):76-85. doi:10.1097/FTD.0b013e3181945624

31. Aumente D, Santos Buelga D, Lukas JC, Gomez P, Torres A, Garc??a MJ. Population Pharmacokinetics of High-Dose Methotrexate in Children with Acute Lymphoblastic Leukaemia. *Clin Pharmacokinet*. 2006;45(12):1227-1238. doi:10.2165/00003088-200645120-00007
32. Faltaos DW, Hulot JS, Urien S, et al. Population pharmacokinetic study of methotrexate in patients with lymphoid malignancy. *Cancer Chemother Pharmacol*. 2006;58(5):626-633. doi:10.1007/s00280-006-0202-0
33. Odoul F, Le Guellec C, Lamagnère JP, et al. Prediction of methotrexate elimination after high dose infusion in children with acute lymphoblastic leukaemia using a population pharmacokinetic approach. *Fundam Clin Pharmacol*. 1999;13(5):595-604.
34. Min Y, Qiang F, Peng L, Zhu Z. High dose methotrexate population pharmacokinetics and Bayesian estimation in patients with lymphoid malignancy. *Biopharm Drug Dispos*. 2009;30(8):437-447. doi:10.1002/bdd.678
35. Donelli MG, Zucchetti M, Robatto A, et al. Pharmacokinetics of HD-MTX in infants, children, and adolescents with non-B acute lymphoblastic leukemia. *Med Pediatr Oncol*. 1995;24(3):154-159.
36. Graf N, Winkler K, Betlemovic M, Fuchs N, Bode U. Methotrexate pharmacokinetics and prognosis in osteosarcoma. *J Clin Oncol*. 1994;12(7):1443-1451. doi:10.1200/JCO.1994.12.7.1443
37. Rousseau A, Sabot C, Delepine N, et al. Bayesian Estimation of Methotrexate Pharmacokinetic Parameters and Area Under the Curve in Children and Young Adults with Localised Osteosarcoma. *Clin Pharmacokinet*. 2002;41(13):1095-1104. doi:10.2165/00003088-200241130-00006
38. Jönsson P, Skärby T, Heldrup J, Schrøder H, Höglund P. High dose methotrexate treatment in children with acute lymphoblastic leukaemia may be optimised by a weight-based dose calculation. *Pediatr Blood Cancer*. 2011;57(1):41-46. doi:10.1002/pbc.22999
39. Nader A, Zahran N, Alshammaa A, Altaweel H, Kassem N, Wilby KJ. Population Pharmacokinetics of Intravenous Methotrexate in Patients with Hematological

Malignancies: Utilization of Routine Clinical Monitoring Parameters. *Eur J Drug Metab Pharmacokinet*. 2017;42(2):221-228. doi:10.1007/s13318-016-0338-1

40. Desoky ES EL, Ghazal MH, Singh RP, Abdelhamid ON, Derendorf H. Population Pharmacokinetics of Methotrexate in Egyptian Children with Lymphoblastic Leukemia. *Pharmacol & Pharm*. 2013;4(2):139-145. doi:10.4236/pp.2013.42020
41. Skärby T, Jönsson P, Hjorth L, et al. High-dose methotrexate: on the relationship of methotrexate elimination time vs renal function and serum methotrexate levels in 1164 courses in 264 Swedish children with acute lymphoblastic leukaemia (ALL). *Cancer Chemother Pharmacol*. 2003;51(4):311-320. doi:10.1007/s00280-002-0552-1
42. Bressolle F, Bologna C, Kinowski JM, Sany J, Combe B. Effects of moderate renal insufficiency on pharmacokinetics of methotrexate in rheumatoid arthritis patients. *Ann Rheum Dis*. 1998;57(2):110-113.
43. Dupuis C, Mercier C, Yang C, et al. High-dose methotrexate in adults with osteosarcoma: a population pharmacokinetics study and validation of a new limited sampling strategy. *Anticancer Drugs*. 2008;19(3):267-273. doi:10.1097/CAD.0b013e3282f21376
44. Ribbing J, Niclas Jonsson E. Power, Selection Bias and Predictive Performance of the Population Pharmacokinetic Covariate Model. *J Pharmacokinet Pharmacodyn*. 2004;31(2):109-134. doi:10.1023/B:JOPA.0000034404.86036.72
45. Mathijssen RHJ, de Jong FA, Loos WJ, van der Bol JM, Verweij J, Sparreboom A. Flat-Fixed Dosing Versus Body Surface Area Based Dosing of Anticancer Drugs in Adults: Does It Make a Difference? *Oncologist*. 2007;12(8):913-923. doi:10.1634/theoncologist.12-8-913
46. Ekhart C, de Jonge ME, Huitema ADR, Schellens JHM, Rodenhuis S, Beijnen JH. Flat Dosing of Carboplatin Is Justified in Adult Patients with Normal Renal Function. *Clin Cancer Res*. 2006;12(21):6502-6508. doi:10.1158/1078-0432.CCR-05-1076
47. Schott AF, Rae JM, Griffith KA, Hayes DF, Sterns V, Baker LH. Combination vinorelbine and capecitabine for metastatic breast cancer using a non-body surface area dosing scheme. *Cancer Chemother Pharmacol*. 2006;58(1):129-135. doi:10.1007/s00280-005-0132-2
48. Wallin JE, Friberg LE, Karlsson MO. Model-Based Neutrophil-Guided Dose

Adaptation in Chemotherapy: Evaluation of Predicted Outcome with Different Types and Amounts of Information. *Basic Clin Pharmacol Toxicol*. 2010;106(3):234-242. doi:10.1111/j.1742-7843.2009.00520.x

49. Abrantes JA, Jönsson S, Karlsson MO, Nielsen EI. Handling interoccasion variability in model-based dose individualization using therapeutic drug monitoring data. *Br J Clin Pharmacol*. 2019. doi:10.1111/bcp.13901

Supplementary Table: Bootstrap population pharmacokinetic parameter estimates of nonlinear model obtained from bootstrap analysis

	Mean	% RSE	95% CI
Pharmacokinetic parameters			
LCL (L h^{-1})	4.77	14.1	3.28 - 6.02
Vmax (uM h^{-1})	2.46	31.6	0.96 - 4.19
Km (uM L^{-1})	1.02	31.9	0.56 - 1.80
V_1 (L)	1.12	32.5	0.42 - 1.67
V_2 (L)	3.87	24.5	2.03 - 5.86
V_3 (L)	5.08	30.2	2.12 - 7.70
Q_1 (L h^{-1})	0.52	26.7	0.27 - 0.83
Q_2 (L/h)	0.04	24.1	0.02 - 0.06
Covariate effects on CL			
SCr (mg^{-1} dL)	-0.91	-12.0	-1.11 - -0.68
Age ($year^{-1}$)	-0.23	-37.0	-0.39 - -0.05
Gender (fractional decrease in females)	-0.28	-21.9	-0.39 - -0.14
BSA (m^{-2})	-	-	-
IIV (ω^2)			
LCL	0.07	28.9	0.034 - 0.11
V_1	2.127	58.8	0.46 - 4.43
COV(LCL, V_1)	0.10	79.2	0.002 - 0.28
IOV (ω^2)			
LCL	0.07	28.9	0.034 - 0.11
V_1	2.13	58.8	0.46 - 4.43
Vmax	0.10	79.2	0.002 - 0.28
RUV (σ^2)			
Additive error	0.02	19.3	0.01 - 0.03
Exponential error	0.22	9.67	0.18 - 0.26

RSE = relative standard error, CI = confidence interval, RSE = relative standard error, CL = clearance, LCL = linear fraction of clearance, V_1 = central volume of distribution, V_2 & V_3 = peripheral volumes of distribution, Q_1 and Q_2 = inter-compartmental clearances, AUC = Area under the curve, SCr = Serum creatinine, IIV = inter-individual variability, IOV = inter-occasion variability, RUV = residual unexplained variability.

Chapter 7

Summary and conclusions

Summary and conclusions

Part of this thesis is focused towards the development of VPCs for an improved evaluation of mixture models which have the ability to empirically classify the studied population into subgroups. We mainly aimed to develop NLME models for chemotherapeutic agents used for the treatment of various types of malignancies. Research work presented in this thesis comprises of several objectives mentioned in chapter 2. Major findings and conclusions are described below.

VPCs for mixture models was successfully designed and implemented. The developed approach demonstrated an ability to overcome existing limitations regarding evaluation of mixture models. We were able to perform graphical and statistical assessment of both the observed and the predicted data taking into account the multimodalities associated with pharmacokinetic parameter distributions. Segregation of data between respective subpopulations was evaluated with an objective to avoid allocation bias. It was concluded that randomization of individuals across subpopulations based on the individual probability estimates is a superior strategy (with lower allocation bias) compared to empirical assignment to subpopulations. The magnitude of allocation bias was observed to increase with the decrease in differences in pharmacokinetic parameter estimates between subgroups. An illustrative example using the irinotecan pharmacokinetic mixture model displayed a better power of evaluation with the implementation of mixture VPCs. The recent approach was useful to capture misspecifications in an irinotecan model with a UGT1A1 genotype effect (incorporated as a bimodal mixture) on CL of the metabolite (SN-38), which were otherwise not evident using the previous (classical) approach.

An enzyme autoinduction model for mitotane was developed. Concentration dependent metabolic enzyme induction leading to change in mitotane clearance over time was taken into account. BMI was identified as statistically significant covariate, but the major fraction of IIV was unexplained, therefore clinically relevant decisions could not be based on individual differences in BMI. The model demonstrated adequate predictive ability of plasma concentration data and was further used for the comparative assessment of two dosing regimens used in current clinical practice, namely high dose and low dose regimens. Based on simulation results, use of the high dose regimen with a

first TDM on day 16 of treatment was suggested. A considerably greater lag time to achieve concentrations above the therapeutic threshold was associated with the use of the low dose regimen. The developed model is a significant progress towards personalized dose selection and can be useful for the establishment of TDM protocols in case of mitotane therapy.

A semi-mechanistic PKPD model of 5FU was developed. Individual differences in BSA partly explained the IIV in 5FU CL. Patient *MTHFR* genotype mutation was found to be significantly related to 5FU CL. However, this genotype effect was excluded from the final PKPD model due to the lack of mechanistic plausibility. The present analysis is of significant importance being the first attempt to develop a link between 5FU exposure and myelotoxicity in the same population of cancer patients. A pharmacodynamic interaction of 5FU with cisplatin was taken into account by the model where an aggravated toxicity was observed with the combination regimen compared to 5FU monotherapy. The developed PKPD model was further used to predict the contribution of 5FU to the time course of progression of leukocytes under frequently employed clinical regimens. Significant differences in toxicity were predicted, where a greater contribution to toxicity was associated with the FOLFIRINOX regimen compared to de Gramont regimen. Predictions based on the developed PKPD model can be helpful to identify patients at considerable risk of developing infections, while prediction of the time required for the reestablishment of total leukocyte count can be useful for decision making with regard to dosing cycles.

A PopPK model of methotrexate continuous infusion was developed, where patient gender, age, BSA and Scr were found statistically related to methotrexate CL. Covariate inclusion resulted in an improved model fit but did not provide any significant reduction in IIV (% CV). A 16% difference in CL was observed for the two genders, but the effect size was clinically irrelevant because considerable variability was yet unexplained for methotrexate CL. BSA based methotrexate dosing was not found superior to flat dosing, as marginal differences in plasma drug exposure between the two dosing strategies were evident from model simulations. The present analysis does not support BSA guided methotrexate dosing, considering that fixed dosing regimens may avoid dose calculation/preparation errors.

To conclude, the current research work made contributions to the field of pharmacometrics in both methodological and clinical aspects. Novel methodologies for evaluation of NLME models with mixture components were developed. We were able to develop NLME models for the antineoplastic compounds. The current research work utilized plasma concentration data as well as adverse event data of prospective and retrospective nature to better understand the PK/PD profiles of the investigated drugs. The findings of present analyses were further used to assist the adjustment of doses / dosing schedules in oncology drug treatment. The developed approaches were found adequate to predict drug exposure and toxicity.

Acknowledgements

Acknowledgements

I would first like to thank my family for the support, care, affection and prayers that supported me throughout my academic career and accompanied me through thick and thin. The support of my parents from the very first day of school to the capstone of this thesis is highly acknowledged.

Foremost, I would thank my research supervisor Prof. Dr. Uwe Fuhr, who steered me in the right direction whenever I sought his guidance. The door to Prof. Fuhr's office was always open whenever I ran into difficulties or had questions regarding my research work. I am grateful for the facilitation and support provided by Prof. Dr. Ulrich Jaehde. My utmost gratitude goes to Prof. Dr. Mats O. Karlsson for allowing me to join his research group. Their expertise, kindness, and most of all their support was a major factor behind the successful completion of my PhD studies. I am further thankful to Prof. Dr. Charlotte Kloft and Prof. Dr. Wilhelm Huisinga, for providing me with the opportunity to become a member of the graduate program PharmetrX.

I would like to extend my heartfelt gratitude to my colleagues at University of Cologne and Uppsala University for their help, laughter, fun, and all those shared moments that made my PhD life enjoyable and unforgettable.

All of my achievements are due to the blessings of ALLAH Almighty. This is only as a result of His powers that worked within me and enabled me to accomplish this research work.

Usman Arshad

Appendices

Appendix I: List of Abbreviations

5FU	5-fluorouracil
5FUH2	5-fluoro-5,6-dihydrouracil
ACC	Adrenocortical carcinoma
ALT	Alanine aminotransferase
AST	Aspartate aminotransferase
AUC	Area under the curve
BQL	Below quantitation limit
BMI	Body mass index
BSA	Body surface area
CL	Clearance
CI	Confidence interval
CrCL	Creatinine clearance
CWRES	Conditional weighted residuals
DV	Dependent variable
DPD	Dihydropyrimidine dehydrogenase
EFPIA	European Federation of Pharmaceutical Industries and Associations
EMA	European Medicines Agency
ENSAT	European Network for the Study of Adrenal Tumors
F	Bioavailability
FDA	U.S. Food and Drug Administration
FO	First-order method
FOCE	First-order conditional estimation method
FOCE-I	First-order conditional estimation with interaction

GOF	Goodness of fit
HPLC	High performace liquid chromatogryphy
IIV	Inter-individual variability
IOV	Inter-occasion variability
IPRED	Individual predictions
LLOQ	Lower limit of quantification
LCMS	Liquid chromatography mass spectrometry
MLE	Maximum likelihood estimation
MID3	Model informed drug development and discovery
MTHFR	Methylene tetrahydrofolate reductase
MTT	Mean transit time
NLME	Non-linear mixed effects
NONMEM	Non-linear mixed effects modeling
OFV	Objective function value
o,p'-DDA	o,p′-dichlorodiphenyl- acetate
o,p'-DDE	o,p′-dichlorodiphenyl-ethene
PCR	Polymerase chain reaction
PD	Pharmacodynamics
PK	Pharmacokinetics
PRED	Population predictions
PsN	Perl speaks NONMEM
PXR	pregnane X receptor
Q	Intercompartmental clearance
RUV	Residual unexplained variability
SCr	Serum creatinine

TDM	Therapeutic drug monitoring
TS	Thymidine synthetase
VPC	Visual predictive check
γ-GT	γ-glutamyltransferase

Appendix II: NONMEM control streams/ R codes

NONMEM control stream for mitotane enzyme autoinduction model

```
$PROBLEM        popPK Mitotane
$INPUT          ID TIME AMT ADDL II EVID CMT BMI DV
$DATA           Sim_data_NONMEM.csv IGNORE=@
;-------------------------------------------------------------------
$SUBROUTINES    ADVAN13 TOL=6
;-------------------------------------------------------------------
$MODEL
COMP=(DEPOT)
COMP=(CENTRAL)
COMP=(ENZYME)
;-------------------------------------------------------------------
$PK
KA      = THETA(1)              ; Absorption rate constant
F1      = THETA(2)              ; Bioavailability
VC      = THETA(3)*EXP(ETA(1))  ; Central volume of distribution
KOUT    = THETA(4)              ; Rate of enzyme degradation
SLOPE   = THETA(5)*EXP(ETA(2))

KIN        = KOUT
E0         = KIN/KOUT           ; Steady state enzyme levels
A_0(3)     = E0
;-------------------------------------------------------------------
$DES
DADT(1) = - KA*A(1)
DADT(2) = KA*A(1) - A(3)/VC*A(2)
CP      = A(2)/VC
DADT(3) = KIN*(1 + DELTA_KIN*CP) - KOUT*A(3)
;-------------------------------------------------------------------
$ERROR
IPRED= A(2)/VC
IRES  = DV - IPRED
W     = SQRT(THETA(6)**2*IPRED**2+THETA(7)**2)
Y     = IPRED+ERR(1)*W
IWRES= IRES/W
;-------------------------------------------------------------------
$THETA
(0, 49.9)  FIX        ; KA
(0, 0.35)  FIX        ; F1
(0, 5810)             ; VC
(0, 0.23)             ; KOUT
(0, 4.04)             ; SLOPE
(0, 0.249)            ; EPS1
(0, 2.2)              ; EPS2
;-------------------------------------------------------------------
$OMEGA
0.664                 ; ETA_VC
0.621 FIX             ;   ETA_SLOPE
;-------------------------------------------------------------------
$SIGMA
 1 FIX  ;       EPS1
 1 FIX  ;       EPS2
```

```
;-------------------------------------------------------------------
$EST       METHOD=1 INTERACTION MAXEVAL=9999 NOABORT PRINT=1 SIG=3
;-------------------------------------------------------------------
;$SIM      (12345) (54321) ONLYSIM
;-------------------------------------------------------------------
$TABLE     ID TIME EVID DV Y IRES CWRES PRED IPRED FILE=sdtab17
           NOPRINT NOAPPEND ONEHEADER
$TABLE     ID TIME EVID DV VC DELTA_KIN CL K HL FILE=patab17 NOPRINT
           NOAPPEND ONEHEADER
$TABLE     ID TIME ETA(1) ETA(2) SEX AGE HEIGHT WEIGHT BN TG CHN HDL
           LDL GGT ALB CRN BMI CRCL LBW FILE=cotab17 NOPRINT
           NOAPPEND ONEHEADER
;-------------------------------------------------------------------
;$TABLE    ID TIME DV CMT IPRED ONEHEADER FILE=SIMTAB17
;-------------------------------------------------------------------
```

NONMEM control stream for 5FU PKPD model

```
$PROBLEM    5FU PKPD
$INPUT      ID TIME AMT RATE CMT EVID DV SE AG BS TS MR GE GT AL AS
           CO WEIGHT HEIGHT BSA BMI
$DATA       5FU.csv IGNORE=@
;-----------------------------------------------------------------------
$SUBROUTINE ADVAN13 TOL=6
;-----------------------------------------------------------------------
$MODEL
NCOM = 8
COMP = (CENT DEFDOSE NOOFF)     ; Central 5FU
COMP = (PERIP)                  ; Peripheral 5FU
COMP = (METAB NOOFF)            ; 5FUH2
COMP = (CIRC DEFOBS)            ; Circulating cells
COMP = (PROLIF)                 ; Proliferative cells
COMP = (TRANSIT1)               ; Transit compartment 1
COMP = (TRANSIT2)               ; Transit compartment 2
COMP = (TRANSIT3)               ; Transit compartment 3
;-----------------------------------------------------------------------
$PK

CL5FU   = THETA(1)*(1+(BSA-1.95)*THETA(8))*EXP(ETA(1))
VC5FU   = THETA(2)*EXP(ETA(2))
VP5FU   = THETA(3)
FM      = THETA(4)
CL5FU_0 = CL5FU*FM         ; CL via conversion to 5FUH2
CL5FU_1 = CL5FU*(1-FM)     ; CL of fraction not converted to 5FUH2
CL5FUH2 = THETA(5)*(1+(BSA-1.95)*THETA(8))*EXP(ETA(3))
V5FHU2  = THETA(6)*EXP(ETA(4))
Q       = THETA(7)
SLOPE   = THETA(9)
IF(CO.EQ.0) SLOPE = THETA(10)
MTT     = THETA(11)
KTR     = 4/MTT
CIRC0   = THETA(12)*EXP(ETA(5))
GAM     = THETA(13)

K12 = Q/VC5FU
K21 = Q/VP5FU
K13 = CL5FU_0/VC5FU
K31 = 0
K10 = CL5FU_1/VC5FU
K30 = CL5FUH2/V5FHU2

S1=VC5FU
S3=V5FUH2

A_0(4) = CIRC0
A_0(5) = CIRC0
A_0(6) = CIRC0
A_0(7) = CIRC0
A_0(8) = CIRC0
;-----------------------------------------------------------------------
$DES
CP  = A(1)/VC5FU
```

```
CM  = A(3)/V5FUH2
EFF = SLOPE*CP
DADT(1) = - K12*A(1) + K21*A(2) - K13*A(1) - K10*A(1)
DADT(2) =   K12*A(1) - K21*A(2)
DADT(3) =   K13*A(1) - K30*A(3)
DADT(4) = - KTR*A(4) + KTR*A(8)
DADT(5) = - KTR*A(5) + KTR*A(5)*(1-EFF)*(CIRC0/A(4))**GAM
DADT(6) = - KTR*A(6) + KTR*A(5)
DADT(7) = - KTR*A(7) + KTR*A(6)
DADT(8) = - KTR*A(8) + KTR*A(7)
;-----------------------------------------------------------------------
$ERROR
CFU  = A(1)/VCFU+0.00001
CFUH = A(3)/V5FUH2
CWBC = A(4)

IF(CMT.EQ.1) THEN
IPRED= CFU
W    = THETA(14)*IPRED
ENDIF
IF (CMT.EQ.3) THEN
IPRED= CFUH
W    = THETA(15)*IPRED
ENDIF
IF(CMT.EQ.4) THEN
IPRED= CWBC
W    = THETA(16)*IPRED
ENDIF

IRES = DV-IPRED
IWRES= IRES/W
Y    = IPRED + EPS(1)*W
;-----------------------------------------------------------------------
$THETA
(1, 278,500)          ; CL5FU
(1, 6.52,50)          ; VCFU
(1, 33.4)             ; VP5FU
(0.85) FIX            ; FM
(10, 120,700)         ; CL5FUH2
(1, 96.7,400)         ; V5FUH2
(0.1, 16.4,100)       ; Q
(-2.63, 0.68,2.12)    ; BSA
(0, 2.95)             ; SLOPE_1
(0, 1.02)             ; SLOPE_2
(0, 269)              ; MTT
(0, 6.8)              ; CIRC0
(0, 0.17) FIX         ; GAM
(0, 0.581)            ; W_CFU
(0, 0.381)            ; W_CFUH
(0, 0.309)            ; W_CWBC
;-----------------------------------------------------------------------
$OMEGA
 0.0265               ; IIV_CL5FU
 1.04                 ; IIV_VCFU
 0.0826               ; IIV_CL5FUH2
 0.257                ; IIV_V5FUH2
```

```
 0.0563              ; IIV_CIRC0
;-----------------------------------------------------------------------
$SIGMA 1 FIX
;-----------------------------------------------------------------------
$ESTIMATION     METHOD=1 INTER PRINT=5 NOABORT MAXEVAL=9999
$COVARIANCE
;-----------------------------------------------------------------------
$TABLE          ID TIME DV EVID CMT PRED IPRED IRES IWRES CWRES MR
                NOPRINT ONEHEADER FILE=sdtab97
;-----------------------------------------------------------------------
```

R codes for Mixture VPCs

VPCs default

```
---
title: "VPC"
output: pdf_document
classoption: landscape
geometry: margin=1.5cm
---

```{r loading_libraries, warning=FALSE, message=FALSE, include =
FALSE}
# get libPaths
source(file.path(rscripts.directory,"common/R_info.R"))
R_info(directory=working.directory,only_libPaths=T)
library(xpose4)
#add R_info to the meta file
R_info(directory=working.directory)
```

```{r vpc_plots, warning=FALSE, message=FALSE,
results='hide',echo=FALSE,fig.width=9,fig.height=6.5,fig.keep="high"
,fig.align="center"}

if (is.tte) {
    #data is in the model directory, go there to read input
    setwd(model.directory)
    xpdb <- xpose.data(xpose.runno)
    plots <- kaplan.plot(object=xpdb, VPC=T)
    #go back to vpc directory
    setwd(working.directory)
} else if (is.categorical) {
    plots <- xpose.VPC.categorical(vpc.info=tool.results.file,
vpctab=vpctab)
} else if (have.loq.data | have.censored) {
    plots <- xpose.VPC.both(vpc.info=tool.results.file,
vpctab=vpctab)
} else {
    plots <- xpose.VPC(vpc.info=tool.results.file, vpctab=vpctab)
}
print(plots)

if (exists('mix')) {       # A mixture model is a special case
    if (require("vpc")) {
        source(paste0(rscripts.directory, "/vpc/vpc_mixtures.R"))
        observations_tablefile <- paste0(working.directory,
'/m1/vpc_original.npctab.dta')
        simulations_tablefile <- paste0(working.directory,
'/m1/vpc_simulation.1.npctab.dta')

        obs <- vpc::read_table_nm(observations_tablefile)
        sim <- vpc::read_table_nm(simulations_tablefile)
        plots_plain <- vpc_mixtures(obs=obs, sim=sim,
numsims=samples, mixcol=mix, dv=dv, bins=bin_boundaries)
```
```

```
        plots_phm <- vpc_mixtures(obs=obs, sim=sim, numsims=samples,
mixcol=mix, dv=dv, phm_obs=phm_obs_file, phm_sim=phm_sim_file,
bins=bin_boundaries)

        for (p in plots_plain) {
            print(p)
        }
        for (p in plots_phm) {
            print(p)
        }
    }
}
#add R_info to the meta file
R_info(directory=working.directory)
```

VPCs mixtures

```
suppressMessages(library(vpc))
suppressMessages(library(dplyr))
library(ggplot2)
library(xpose)

vpc_mixtures <- function(obs, sim, numsims, mixcol="MIXNUM",
dv="DV", phm_obs, phm_sim, bins) {
    # Put in replicate numbers in sim table
    sim$sim <- rep(1:numsims, each=nrow(sim) / numsims)

    if (!missing(phm_sim)) {
        phm_table <- subpopulations_from_nonmem_phm(phm_sim,
numsims)
        sim <- dplyr::full_join(sim, phm_table)
        phm_table_obs <- subpopulations_from_nonmem_phm(phm_obs, 1)
        obs <- dplyr::full_join(obs, phm_table_obs)
        mixcol <- 'SUBPOP'
        method <- 'Randomized Mixture'
    } else {
        method <- 'MIXEST Mixture'
    }

    num_ids <- length(unique(obs$ID))

    unique_subpops <- sort(unique(c(obs[[mixcol]], sim[[mixcol]])))

    table_list <- list()

    for (i in unique_subpops) {
        subobs <- filter_(obs, paste0(mixcol, "==", i))
        subsim <- filter_(sim, paste0(mixcol, "==", i))
        if (nrow(subsim) == 0) {
            next
        }
        if (missing(bins)) {
            vpc <- vpc::vpc(obs=subobs, sim=subsim,
obs_cols=list(dv=dv), sim_cols=list(dv=dv))
        } else {
```

```
            vpc <- vpc::vpc(obs=subobs, sim=subsim,
obs_cols=list(dv=dv), sim_cols=list(dv=dv), bins=bins)
        }

        obs_ids <- length(unique(subobs$ID))
        perc_obs_ids <- (obs_ids / num_ids) * 100

        ids_per_sim <- subsim %>% group_by(sim) %>%
summarise(count=length(unique(ID)))
        ids_per_sim <- ids_per_sim$count
        lower_quantile <- (quantile(ids_per_sim, probs=0.05) /
num_ids) * 100
        upper_quantile <- (quantile(ids_per_sim, probs=0.95) /
num_ids) * 100

        title <- sprintf("%s SUBPOP=%d\nORIGID=%.1f%% SIMID=[%.0f%%,
%.0f%%] (5%%, 95%% percentiles)",
                         method, i, perc_obs_ids, lower_quantile,
upper_quantile)
        vpc <- vpc + ggtitle(title)
        table_list[[i]] <- vpc
    }

    return(table_list)
}


# Takes a NONMEM phm file as input and outputs a data.frame with ID
and SUBPOP columns
# The SUBPOP is a random sample given the PMIX probabilities nrep is
the number of replicates
# phm can either be a file name of a phm file or a data.frame

subpopulations_from_nonmem_phm <- function(phm, nrep) {
    if (is.character(phm)) {
        phm_table <- xpose::read_nm_files(file=phm)
    } else {
        phm_table <- phm
    }

    ind_table <- dplyr::bind_rows(phm_table[['data']])   # One table
for all replicates
    ind_table <- data.frame(ID=ind_table$ID,
SUBPOP=ind_table$SUBPOP, PMIX=ind_table$PMIX)

# Keep only interesting columns

    ind_table$sim <- rep(1:nrep, each=nrow(ind_table) / nrep) #
number the replicates

    result <- data.frame(ind_table %>% group_by(sim, ID) %>%
summarize(SUBPOP=sample(SUBPOP, size=1, prob=PMIX)))

    return(result)
}
```

Appendix III: List of Publications (from PhD thesis)

1. **Arshad U,** Chaselloup E, Nordgren R and Karlsson MO. Development of visual predictive checks accounting for multimodal parameter distributions in mixture models. Journal of Pharmacokinetics and Pharmacodynamics 2019. 46(3):241-250 doi: 10.1007/s10928-019-09632-9

   Contributions: I contributed toward the development of methodology and its implementation. I further tested the developed methodology using simulated and real datasets, and finally wrote the manuscript. The publication, presented in Chapter 3 of my thesis, is not used or will not be used for any other dissertation.

2. **Arshad U***, Taubert M*, Kurlbaum M, Frechen S, Herterich S, Megerle F, Hamacher S, Fassnacht M, Fuhr U and Kroiss M. Enzyme autoinduction by mitotane supported by population pharmacokinetic modeling in a large cohort of adrenocortical carcinoma patients. European Journal of Endocrinology 2018. 179(5):287–297. doi: 10.1530/EJE-18-0342. *shared first authorship

   Contributions: I prepared a tidy dataset using R from the database files provided by University Hospital Würzburg. I analyzed plasma concentration and covariate data of mitotane to develop pharmacokinetic models incorporating the autoinduction of its metabolism due to the effect of the drug on hepatic CYP3A4. I further evaluated the attainment of therapeutic mitotane concentrations for both the low and the high dose regimen. Max Taubert shared this publication as a co-first author due to his contributions towards model development, model evaluation and simulation development. I finally prepared the manuscript draft. The publication, presented in Chapter 4 of my thesis, is not used or intended to be used for any other thesis.

3. **Arshad U***, Ploylearmsaeng S*, Karlsson MO, Doroshyenko O, Frank D, Schömig E, Kunze S, Güner SA, Skripnichenko R, Ullah S, Jaehde U, Fuhr U, Jetter A and Taubert M. Prediction of exposure-driven myelotoxicity of 5-fluorouracil by a semi-physiological pharmacokinetic-pharmacodynamic model in gastrointestinal cancer patients. Cancer Chemotherapy and Pharmacology 2020. [In press]. *shared first authorship

Contributions: I analyzed the plasma concentration (PK) and total WBC count (PD) data simultaneously, and developed a semi-mechanistic PKPD model using plasma concentration data of 5-fluorouracil, its metabolite, total WBC counts over time and covariate data. I further designed simulations for the comparative evaluation of toxicity attributed to the clinically applied dosing regimens, and finally wrote the manuscript. Su-arpa Ploylearmsaeng, who was supervised by the same supervisors, shared the publication as a co-first author. Her dissertation with the topic **"**A Pilot Study to Identify Sources of Variability in 5-Fluorouracil Pharmacokinetics and Toxicity" was awarded with the degree of a "doctor rerum naturalium" of the Faculty of Mathematics and Natural Sciences of the Rheinische Friedrich-Wilhelms-Universität Bonn (2007) and made use of the plasma concentration data to develop a PK model. However, at the time of her thesis, Dr. Ploylearmsaeng was not able to develop a joint PKPD model to describe the PD data. I successfully developed the simultaneous PKPD model and wrote the manuscript afterwards. The publication, presented in Chapter 5 of my thesis, is not used or intended to be used for any further dissertation.

4. **Arshad U***, Taubert M*, Seeger-Nukpezah T, Fuhr U, Vehreschild JJ and Jakob C. Population pharmacokinetic model of methotrexate continuous infusion in a large cohort of cancer patients. [manuscript under revision by co-authors]

   Contributions: Max Taubert (shared co-first author) prepared an initial dataset using R. I further validated and expanded the dataset incorporating data obtained from additional patients. Max Taubert and I analyzed plasma concentration and covariate data to develop a pharmacokinetic model of methotrexate and designed simulations for comparative evaluation of BSA based and flat dosing regimens. I finally wrote the manuscript, presented in Chapter 6, which is not used or aimed to be used for any other dissertation. *shared first authorship